FORCeS

Constrained aerosol forcing for improved climate projections – GA 821205

Final scientific summary report (D9.5)

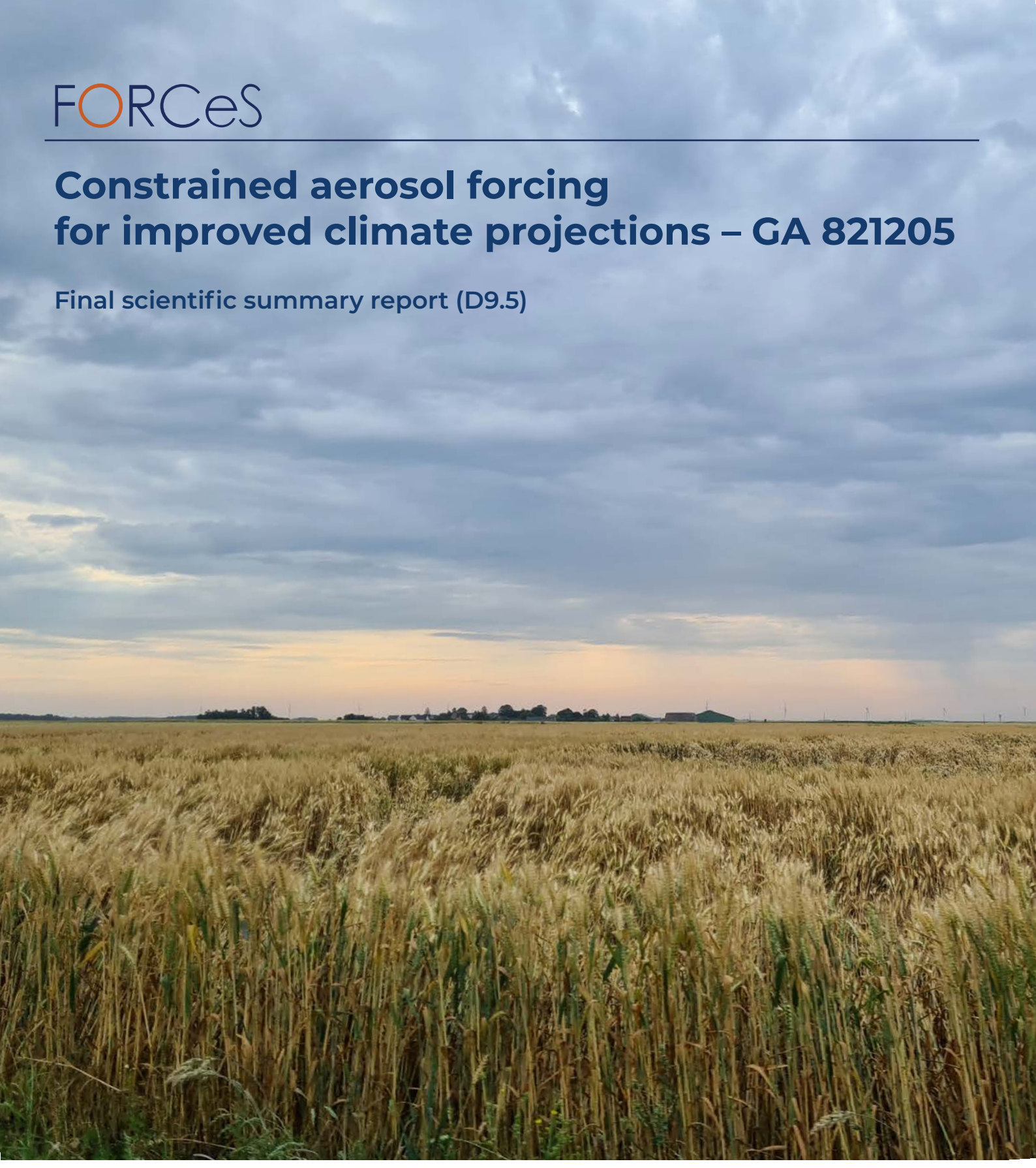

The ultimate aim of the FORCeS project is to understand and reduce the long-standing uncertainty in anthropogenic aerosol radiative forcing. This is crucial if we are to increase confidence in climate projections.

This project has received funding from the European Union's Horizon 2020 research and innovation programme under grant agreement No 821205.

Contents

1. Summary . . . 3
2. Dissemination uptake . . . 3
3. Background and FORCeS objectives . . . 3
4. Approach and methods used within FORCeS science . . . 4
5. Scientific outcomes and progress within the FORCeS WPs . . . 5
   - 5.1 Progress within WP1 “Critical aerosol forcing processes and factors” . . . 5
   - 5.2 Progress within WP2 “Understanding of cloud processes and aerosol-cloud interactions” . . . 11
   - 5.3 Progress within WP3 “Role of aerosol and cloud changes for aerosol radiative forcing between 1950 and 2050” . . . 20
   - 5.4 Progress within WP4 “Novel constraints on aerosol radiative effects” . . . 24
   - 5.5 Progress within WP5 “Climate response and feedbacks within ESMs” . . . 31
   - 5.6 Progress within WP6 “Constraining climate sensitivity and near-term climate response” . . . 34
   - 5.7 Scientific progress contributing to the FORCeS objectives and outcomes achieved . . . 42
6. Summary . . . 43

References . . . 43

FORCeS contact information . . . 52

Document information

Project title: FORCeS – Constrained aerosol forcing for improved climate projections
Grant Agreement 821205
Project start date: 01.10.2019
Duration of the project: 54 months
Coordinator: Stockholm University (SU)
Coordinators: Ilona Riipinen (SU) and Annica Ekman (SU)
Document title: Deliverable 9.5 – Final scientific summary report
Work package: WP9 – Scientific management
Contributing partners: All Partners
Lead authors: Ilona Riipinen (SU) and Annica Ekman (SU)
Contributing authors: FORCeS work package leaders
Dissemination level: Public
Due date: 30.03.2024
Submission date: 22.03.2024

1. Summary

This document summarizes the scientific progress of the European Union (EU) Horizon 2020 project FORCeS ("Constrained aerosol forcing for improved climate projections"). It is based on the original peer-reviewed literature associated with the work conducted within the project, covering more than 190 articles in international scientific journals and in addition some conference presentations. Overall, FORCeS progressed according to the original plan, and has reached its objectives and goal, as specified in this report. For further information on the project, please see *forces-project.eu*.

2. Dissemination uptake

This report is aimed at scientists, policymakers and the general interested public. However, it is in the form of a scientific report, so some scientific literacy and knowledge of the basic concepts within atmospheric and climate science is needed. It is based on the body of peer-reviewed literature, and just briefly highlights the topics covered and key results obtained within the more than 190 scientific articles published within the project. Detailed descriptions of the studies conducted, the methodologies used, the results obtained and the conclusions drawn can be found in these articles – the grand majority of which are freely and openly available online (see the References section). While this report covers some of the work done in the first half of the project and therefore repeats some of the findings covered in the mid-term report (D9.4), the primary focus is on the second half of the project. For more details on the first two years of FORCeS, the reader is referred to the mid-term scientific report.

3. Background and FORCeS objectives

The challenge: The Paris Agreement (PA), adopted within the United Nations Framework Convention on Climate Change (UNFCCC) in December 2015, requires the majority of the world's countries to limit global warming from anthropogenic activities within 2°C above pre-industrial levels. The actions needed to reach this goal, and the urgency and effectiveness of their implementation, rely crucially on accurately predicting the time evolution of radiative forcing and the resulting climate response. Uncertainty in simulating the components of the atmosphere, especially those related to aerosol, clouds and their interactions severely hampers our ability to understand the past and project future climate change. This is because anthropogenic aerosols exert a net cooling impact on climate that offsets – but with large uncertainty – part of the warming effect from greenhouse gas emissions. As a result, the time left for achieving the necessary greenhouse gas reductions to achieve the PA target, and our understanding of the expected regional impacts of climate change, are hampered by the inability to robustly quantify the anthropogenic climate forcing associated with aerosols. In particular, the anticipated large reductions in aerosol emissions in the coming decades will result in a warming effect that is currently very poorly quantified. It is therefore crucial to establish the extent to which aerosol changes, whether due to anthropogenic emissions or as a feedback induced by warming, offset greenhouse gas warming.

The goal of FORCeS was to resolve the above challenge and, in support of the Intergovernmental Panel on Climate Change (IPCC), substantially increase the confidence in estimates of aerosol radiative forcing and its impact on transient climate response. FORCeS did this by bridging crucial gaps that existed between knowledge on the process scale and model application on the climate scale upon the start of the project. FORCeS has identified, observationally constrained and efficiently parameterized some of the most important processes driving aerosol radiative forcing. With this knowledge, FORCeS has produced more robust estimates of the overall aerosol contribution to past climate change, leading to insights on plausible climate sensitivity, and more accurate projections of the near-term climate change. Observations, computational models and theoretical considerations were used to constrain and predict the anthropogenic aerosol impact on climate. Throughout its duration, FORCeS strived for a good balance between an accurate representation of aerosol processes, computational requirements and the need for simplification of climate models. FORCeS has operated on a continuum of temporal and spatial scales, included several metrics and produced outcomes with direct relevance for policy and ultimately society. Based on the scientific knowledge gained, FORCeS has informed decision and policymakers about the effect of aerosol emission changes on regional and global climate evolution and on emission pathways to meet the targets of the PA. The results from FORCeS further highlight 1)

the need for urgent reduction of greenhouse gas (GHG) emissions and adaptation measures; 2) the important role of aerosols in past and future warming; 3) the need for continued further development and revision of the standard methodologies used for quantifying aerosol-cloud-climate interactions.

To reach its goal, FORCeS

- *Worked systematically towards identifying the most important cloud and aerosol processes or components controlling radiative forcing and transient climate response, and made a number of targeted improvements of the corresponding parameterizations for a set of leading European climate models, to obtain more reliable transient climate simulations. (**OBJECTIVE 1**)*
- *Exploited models, statistical methods, data mining and the recent wealth of observations to reduce the uncertainty in anthropogenic radiative forcing from more than ±100% to closer to ±50%. (**OBJECTIVE 2**)*
- *Made efforts to quantify the near-term climate impact and associated uncertainty ranges for a set of plausible combinations of near-term greenhouse gas and aerosol emission pathways, in support of the Paris Agreement. (**OBJECTIVE 3**)*

In the following Sections, we will describe the approach and methods used to reach these Objectives, as well as the corresponding scientific outcomes of the project.

4. Approach and methods used within FORCeS science

The key scientific bottlenecks that FORCeS targeted, the scientific objectives (see Sect. 3) and the expected outcomes of FORCeS are schematically outlined in Fig. 1. FORCeS has dealt with a large breadth of processes and scales – all the way from building fundamental understanding on molecular-scale phenomena (nanometer scale) to understanding their implications on regional and global scales (scales from tens to several hundreds of kilometers). Therefore, the associated time scales also range from less than seconds up to centuries.

The key for successfully addressing the challenge of bridging over spatial and temporal scales is the smart combination and connection of the relevant theoretical and experimental techniques applied within and outside the field of atmospheric and climate science (see Fig. 2). To succeed with the overall goals of the project (see Sect. 3), the process-level investigations within FORCeS were guided by and conducted with the ultimate aim of improving the climate models used within FORCeS. The overall concept was based on the following three pillars, where particularly pillars I and II are relevant for this report (for pillar III, see report on FORCeS communication activities, D8.10):

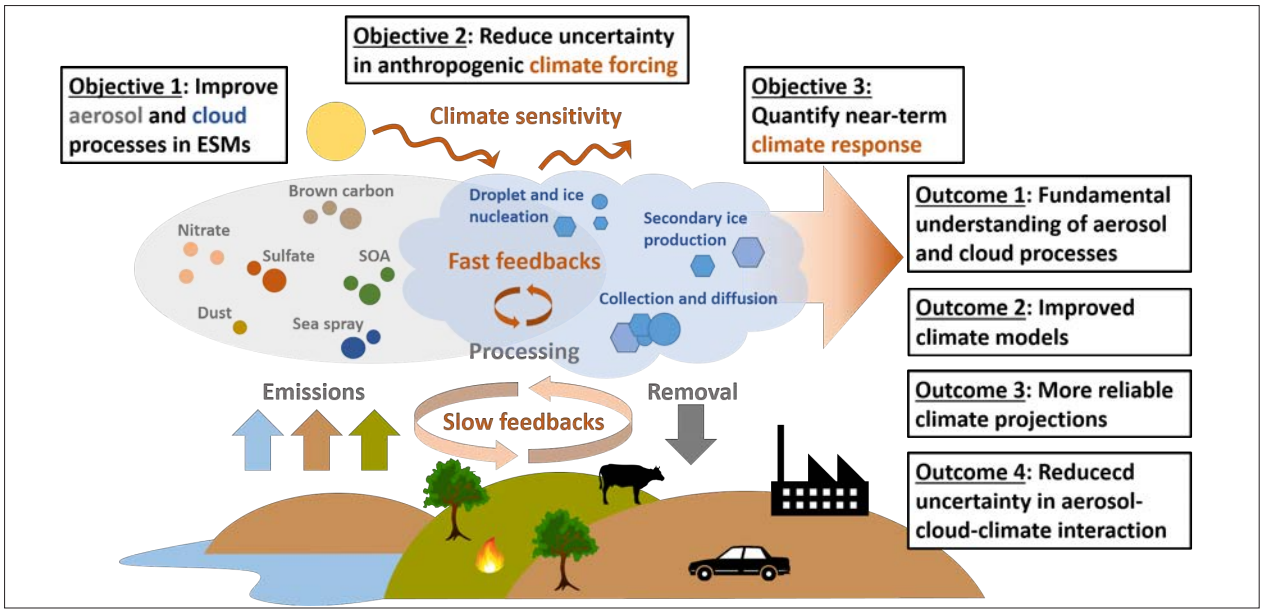

Figure 1. The knowledge gaps addressed in FORCeS, expected outcomes, and contribution to objectives. Figure by Tinja Olenius

Pillar I: Quantifying aerosol loadings and aerosol climate forcing through combining "bottom-up" process knowledge with "top-down" constraints;

Pillar II: Targeted investigation of fundamental phenomena, their systematic up-scaling and climate model improvement using novel techniques such as machine learning;

Pillar III: Active communication using metrics and approaches relevant for climate assessment groups and stakeholders.

The practical implementation of the work within FORCeS was structured in nine interlinked Work Packages (WPs, see Fig. 3). The scientific activities are primarily conducted within WPs 1–6, and hence the description of the scientific progress below has been structured according to these WPs and the Tasks within them.

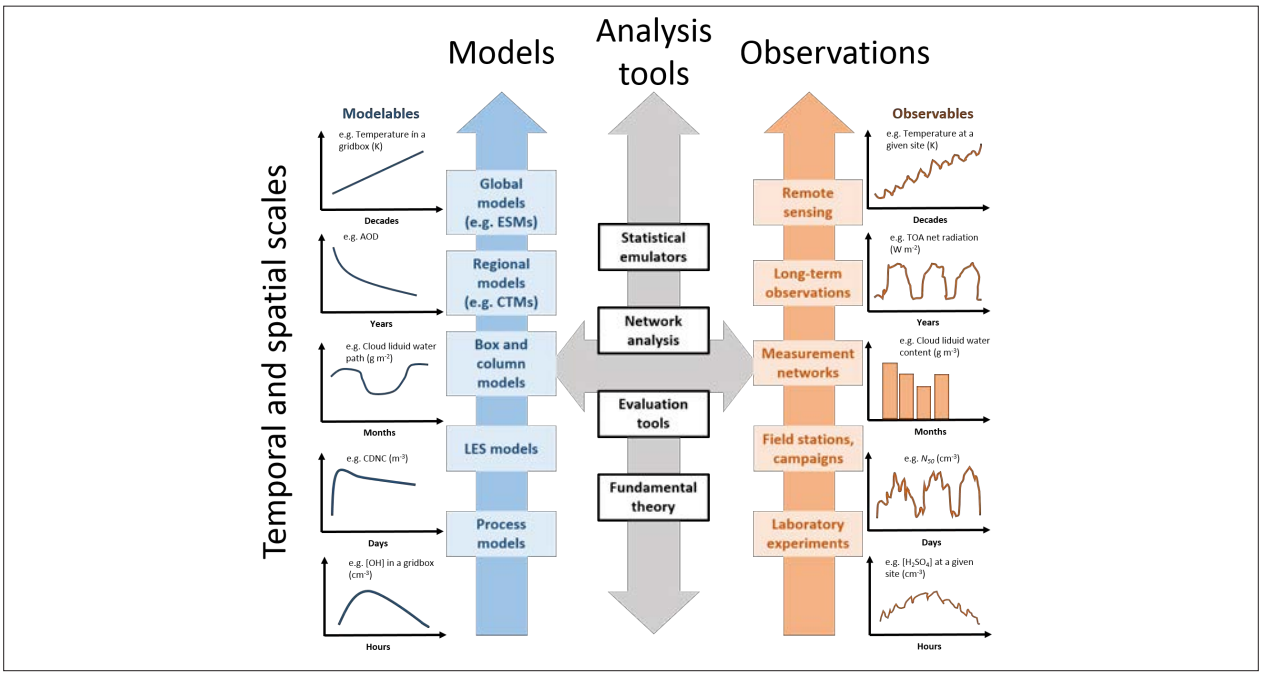

Figure 2. The relevant scales and methods applied in FORCeS for moving between them, along with examples of time series of key variables needed for quantifying the effective radiative forcing caused by aerosol particles and aerosol-cloud interactions ($ERF_{ari+aci}$). Figure by Tinja Olenius

5. Scientific outcomes and progress within the FORCeS WPs

Overall, the work carried out in FORCeS proceeded according to the plan within each of the scientific WPs 1–6 (see Fig. 3). The scientific progress within WPs 1–6 is elaborated in detail below and the scientific progress towards the FORCeS objectives is summarized at the end of this Section.

5.1 Progress within WP1 "Critical aerosol forcing processes and factors"

The main objective of WP1 was the improvement of the representation of aerosol processes in the Earth System Models (ESMs) used within FORCeS in an effort to increase the accuracy, and reduce the uncertainty, of the simulated aerosol effective radiative forcing (ERF). Based on recommendations of previous EU projects in this research area (particularly EUCAARI, PEGASOS, BACCHUS and ECLIPSE), and a series of dedicated FORCeS meetings, four key aerosol species and processes were selected for a deeper analysis: organic aerosol (OA), nitrate aerosol, absorbing aerosol and ultrafine aerosols.

The work in WP1 has progressed according to the Description of Action (DoA) and focused on the development and testing of the parameterizations related to the four key aerosol processes and components. The parameterizations developed in WP1 were provided to WP3 and WP5 where they were included and tested in the FORCeS atmospheric general circulation models (AGCMs) and ESMs.

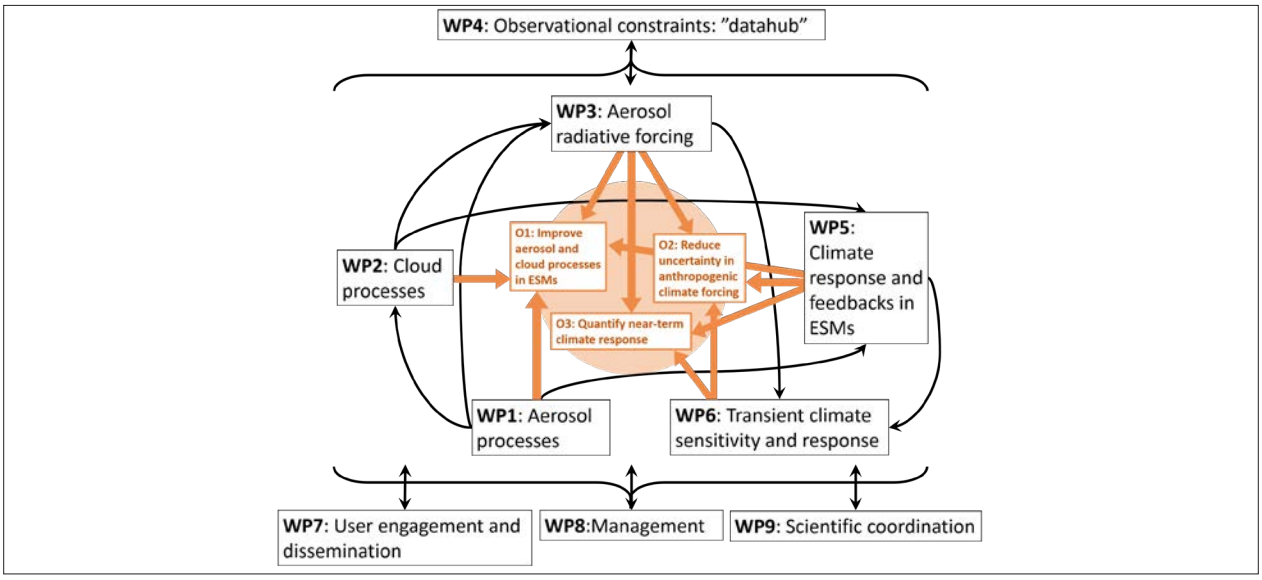

Figure 3. Graphical representation of FORCeS Work Package structure, their interactions (black arrows) and contribution to the overall objectives (see Sect. 3). Figure by Tinja Olenius

Task 1.1: Organic aerosol formation and chemical evolution

FORCeS has developed a reduced-form version of the comprehensive ORACLE module (Tsimpidi et al., 2014), called ORACLE-lite (Tsimpidi et al., 2024 *manuscript to be submitted to Geoscientific Model Development*), which was first implemented to the climate model EMAC and is still in the process of being implemented in the other FORCeS ESMs. The ORACLE module is based on the volatility basis set (VBS) framework proposed by Donahue et al. (2006). It uses fixed logarithmically-spaced saturation concentration bins to describe the OA volatility distribution and assumes formation of pseudo-ideal solutions in the OA phase. This framework blurs the distinction between the traditional primary (POA) and secondary organic aerosol (SOA), providing a more realistic picture of the behavior of atmospheric OA (see also Theodoritsi et al., 2021 for an application of the VBS scheme). The module simulates the gas-phase photochemical reactions of SOA precursors, and distributes the OA in the size modes used by the ESM. The parameters in this module can be easily updated by the latest laboratory findings regarding the formation of SOA, including detailed studies on the molecular evolution and volatility distributions of OA that are ongoing in the SAPHIR chamber (see e.g. (Wu et al., 2021b; Shen et al., 2022; Tsiligiannis et al., 2022; Luo et al., 2023) and the field observations collected and analysed within the framework of FORCeS. Furthermore, regional-scale modeling work has been conducted to evaluate the performance of the current approaches in reproducing OA concentrations (Dinkelacker et al., 2024), improving the description of Intermediate Volatility Organic Compounds (IVOCs, see Manavi and Pandis, 2022), Extremely Low Volatility Compounds (ELVOCs, see Patoulias and Pandis, 2022) and understanding the role of organic water in Particulate Matter (PM) loadings (Kakavas et al., 2023). These efforts further guide the work towards parameterization and simplification of the complex organic aerosol system. To avoid the computational cost associated with adding several OA tracers, some of the FORCeS ESMs have chosen to focus on two lumped species, namely semi-volatile and extremely low-volatile organic species (SVOCs and ELVOCs), still resulting in generally improved predictions of aerosol number and optical depth (Bergman et al., 2022).

The laboratory studies on OA formation have targeted particularly the SOA formation pathways where knowledge gaps remain. These include the oxidation of various biogenic precursors by the NO_3 radical (Wu et al., 2021b, 2021a; Bell et al., 2022; Guo et al., 2022; Tsiligiannis et al., 2022; Carlsson et al., 2023; Graham et al., 2023) limonene + OH (Luo et al., 2023), as well as dark-ozonolysis of α-humulene (Sippial et al., 2023), all the way to identifying previously overlooked reaction pathways of the well-studied α-pinene system (Shen et al., 2022; Graham et al., 2023) and effects on nitrogen oxides on the Cloud Condensation Nuclei (CCN) activity of monoterpene-driven SOA (Zhang et al., 2023). These laboratory studies have, for instance, quantified the yields, molecular composition and volatility distributions (see also Hyttinen et al., 2022 for the evaluation of the common methodologies for obtaining volatilities) of the formed aerosol (see Fig. 4 for an example from Graham et al., 2023).

Various field observations have been utilized in FORCeS to yield new inisghts of OA, and a few highlight are given here. Applying the FIGAERO-CIMS setup for analysing samples collected in the Arctic for the first time (Siegel et al., 2021) reveals a potentially significant signal from organic and sulfur-containing compounds in the aerosol particles. These signals are indicative of marine aerosol sources, with a wide range of carbon numbers and O:C ratios – including a clear secondary component. Several of the sulfur-containing compounds were oxidation products of dimethyl sulfide (DMS), a gas released by phytoplankton and ice algae (see also Mansour et al., 2022, 2023). These results highlight the importance of understanding the marine organics and DMS as a source of CCN in this vulnerable region (see also Schmale et al., 2021 and references therein). In their analysis of cloud residual data from the NASCENT campaign, Gramlich et al. (2023) found the overall chemical composition of the organic aerosol particles to be before, during, and after the cloud – indicating that the particles had already undergone one or several cycles of cloud processing before being measured at the Zeppelin station. Yli-Juuti et al. (2021), Petäjä et al. (2022) (see also Räty et al., 2023) and Blichner et al. (2024) focused on the feedbacks between forests, aerosol populations, clouds and climate (see Sect. 5.4 for more details), using long-term in-situ data from boreal and tropical forest environments. Tsiligiannis et al. (2022), on the other hand, used in-situ observations as a comparison to their laboratory study to confirm the important role of four-carbon organonitrate as a significant product of secondary isoprene chemistry.

Another aspect of organic aerosol evolution and fate that received special attention within FORCeS is the wet removal of OA and its precursors by clouds and precipitation (see also Sect. 5.2 and e.g. Isokääntä et al., 2022), given its important role in the overall OA budgets (see e.g. Holopainen et al., 2020). To investigate this process, Bardakov et al. (2020) used a framework coupling trajectories from a Large Eddy Simulation (LES) model MIMICA and a box model to investigate the uptake of isoprene and its oxidation products onto the hydrometeors within convective clouds in the tropical atmosphere (see Sect. 5.2 for more details).

FORCeS has also contributed to three broad and topical reviews with relevance for our understanding of atmospheric OA: Artaxo et al. (2022) who reviewed the similarities and differences of tropical and boreal forests, with a particular focus on atmospheric chemistry and biogeochemical cycles; Stolzenburg et al. (2023) who reviewed the current knowledge of atmospheric nanoparticle growth and Decesari et al. (2024) whose review focused on the application of the Nuclear Magnetic Resonance (NMR) technique in atmospheric organic analysis.

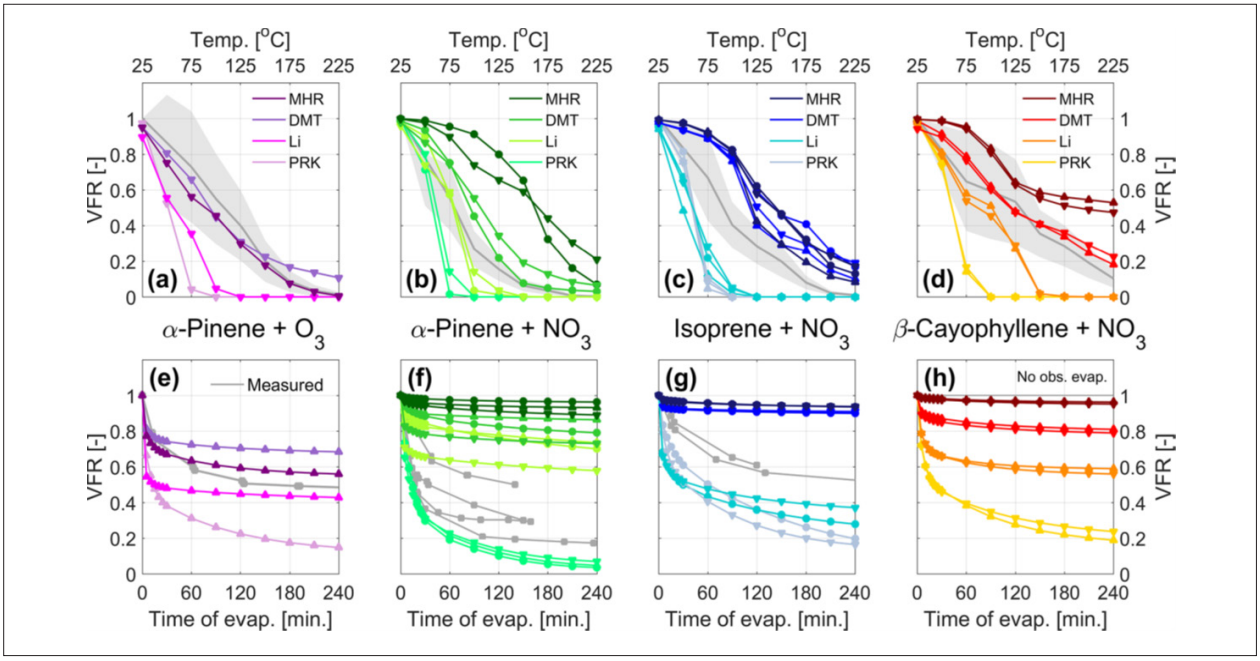

Figure 4. Figure from Graham et al. (2023) comparing the evaporation of SOA in a thermodenuder TD (a–d) and isothermal evaporation chamber (e–h) predicted by a kinetic model using different volatility assumptions as input for α-pinene ozonolysis and nitrate oxidation of α-pinene, isoprene, and β-caryophyllene. The symbols (▲ ● ▼) mark the experiments in chronological order, during which the VBS data were collected. For comparison, the experimental volume fraction remaining (VFR) data are displayed in gray, with the shaded areas displaying the uncertainty of the measurement. Reproduced under the Creative Commons 4.0 (CC 4.0) license.

Task 1.2: Nitrates in fine and coarse particles

Even if our understanding of the formation of inorganic nitrate salts has advanced and the corresponding processes are reasonably well simulated in regional chemical transport models (CTMs), the computational cost has seriously limited, and in most cases prohibited, the simulation of this aerosol component in ESMs. Besides influencing the radiative effect caused by the aerosol particles, it is a key player in the atmospheric acid-base chemistry, which has important implications also for air quality and deposition of nutrients as demonstrated by a series of FORCeS-publications (Baker et al., 2021; Kakavas and Pandis, 2021; Karydis et al., 2021; Nenes et al., 2021; Paglione et al., 2021).

Given the importance of simulating aerosol nitrate and acid-base chemistry accurately, we have in FORCeS explored ways to reduce the computational cost of the simulation of the formation and evaporation of ammonium nitrate, reactions of nitric acid with coarse sea-salt and dust particles, and the competition of fine and coarse particles for the available nitric acid. This has resulted in the development of ISORROPIA-lite, which is a simplified and computationally more efficient version of the thermodynamic model ISORROPIA-II (Fountoukis and Nenes, 2007) that can be used by ESMs to simulate aerosol nitrates with a small additional computational cost. This is a very timely contribution, as the simulation of aerosol nitrate is still at a development stage in the FORCeS ESMs. The study by Kakavas et al. (2022) evaluated ISORROPIA-lite, and in general the results show good agreement with ISORROPIA-II, but with a significantly reduced computational cost (see Fig. 5).

Minerals present in dust, such as calcite, influence aerosol pH and thus the distribution of nitrate between the gas and particulate phases (see e.g. Karydis et al., 2021). ESMs typically assume a globally uniform dust composition. Within FORCeS, a new climatology of dust has been developed and used by the FORCeS ESMs, allowing them to characterize regional changes in dust composition and its potential impact on aerosol pH and nitrate (see e.g. Myriokefalitakis et al., 2022; Gonçalves Ageitos et al., 2023).

In terms of laboratory and field studies involving nitrate, the work within FORCeS has focused in particular on organic nitrates, outlined in the previous section (e.g. Tsiligiannis et al., 2022; Graham et al., 2023).

Task 1.3: Improved parameterizations of aerosol absorption

When it comes to absorbing aerosol, the scientific work within FORCeS focused particularly on how to further improve the estimates of dust (see e.g. Kakavas and Pandis, 2021; Kok et al., 2021b, 2021a) and BrC sources (related to e.g. biomass burning, see e.g. Theodoritsi et al., 2020), although some work on the absorptive properties (Kelesidis et al., 2022), trends (Heslin-Rees et al., 2024) and impacts of atmospheric BC (Slater et al., 2022) have also been conducted. To underline the importance of getting the absorbing aerosol right in global models, Williams et al. (2022) report on the important effect that the spatial distribution of absorbing aerosol components has on the overall effective radiative forcing by aerosols.

Three major types of aerosols have absorbing properties: black carbon (BC), brown carbon (BrC) and dust aerosols. BC is the type of aerosol that has the largest potential to warm the climate and it is currently considered in most climate models, including ESMs. Dust aerosol is partially absorbing. This is translated into dust aerosol having an imaginary part in its refractive index used in climate models. Dust aerosol is a mixture of different minerals, whose relative abundances, particle size distribution, shape, surface topography and mixing state influence their effect on climate. However, ESMs typically assume that dust is a homogeneous aerosol species, neglecting the known regional variations in the mineralogical composition of the sources. As described above (Task 1.2), a climatology considering the regional variation in the mineralogical composition of dust has been developed within FORCeS (Klose et al., 2021; Kok et al., 2021a, 2021b; Li et al., 2021; Gonçalves Ageitos et al., 2023). The work by Li et al. (2021) highlighted particularly the need for an improved description of iron oxides (such as hematite and goethite) for capturing the radiative effects of dust. Gonçalves Ageitos et al. (2023) investigated the sensitivity of dust composition and climate impacts on the soil mineralogy atlases and found feldspars and calcites to be particularly sensitive to the soil mineralogy dataset used (see Fig. 6, see also Sect. 5.5). For the least abundant or more difficult-to-determine minerals, such as iron oxides, uncertainties in soil mineralogy the differences in annual mean aerosol mass fractions could be as much as about 100 %. In terms of the climate impacts, particularly single-scattering albedo and iron deposition were found to be sensitive to the assumed mineralogy map. The review by Kok et al. (2023) identified the work still needed to constrain the radiative effects of dust on climate and to improve the representation of dust in climate models. Bergas-Massó et al. (2023) highlighted the importance of dust for capturing soluble iron cycling, and concluded that further studies are needed to constrain human-induced changes on both dust and wildfire emissions.

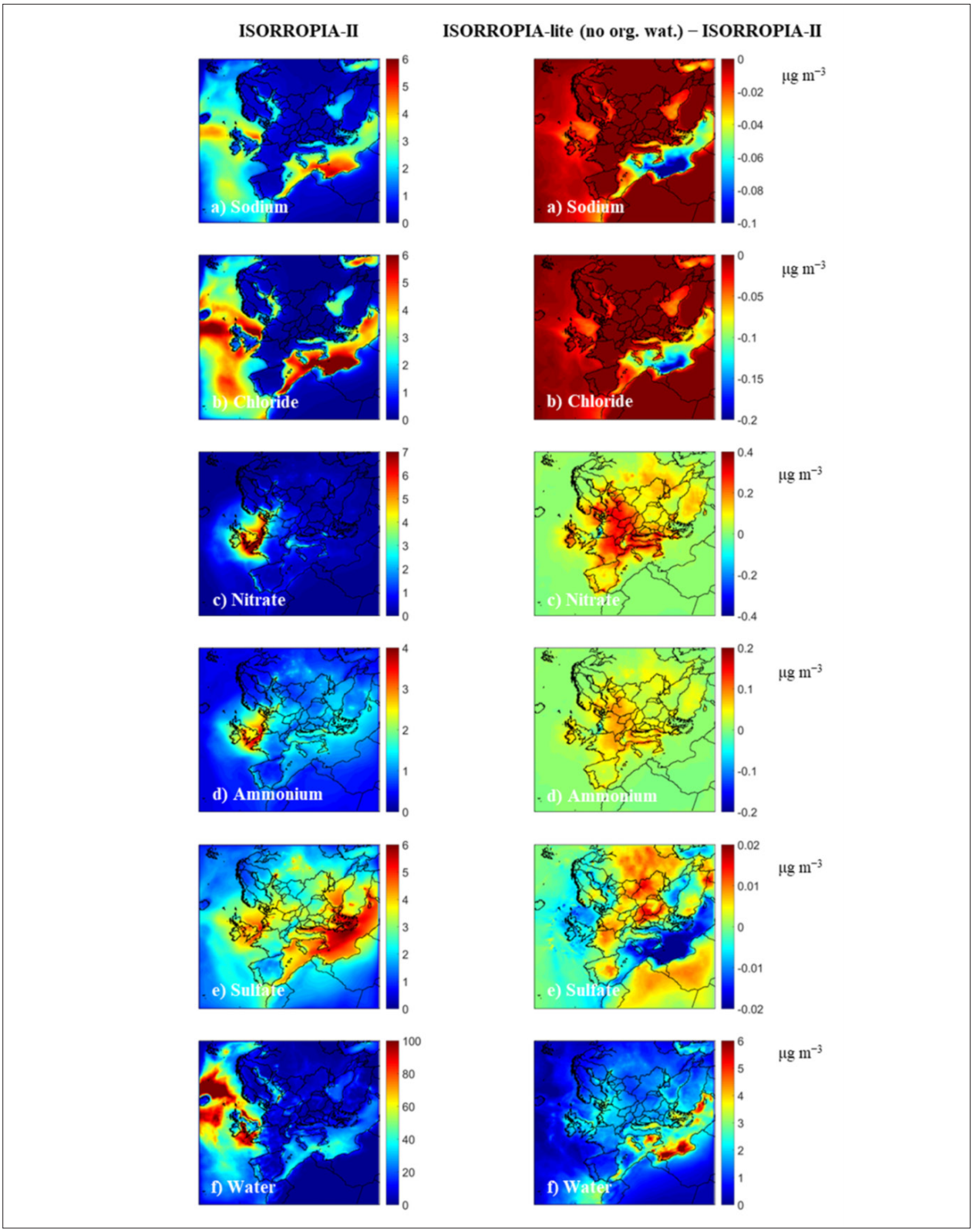

Figure 5. Figure from Kakavas et al. (2022) comparing the main aerosol components between ISORROPIA-lite and ISORROPIA II. Average ground-level PM10 concentrations (in µg m^{-3}) of a) sodium, b) chloride, c) nitrate, d) ammonium, e) sulfate, and f) water using ISORROPIA-II in stable mode with online calculation of binary activity coefficients and ISORROPIA-lite without organic water during May 2008. Reproduced under the Creative Commons 4.0 (CC 4.0) license.

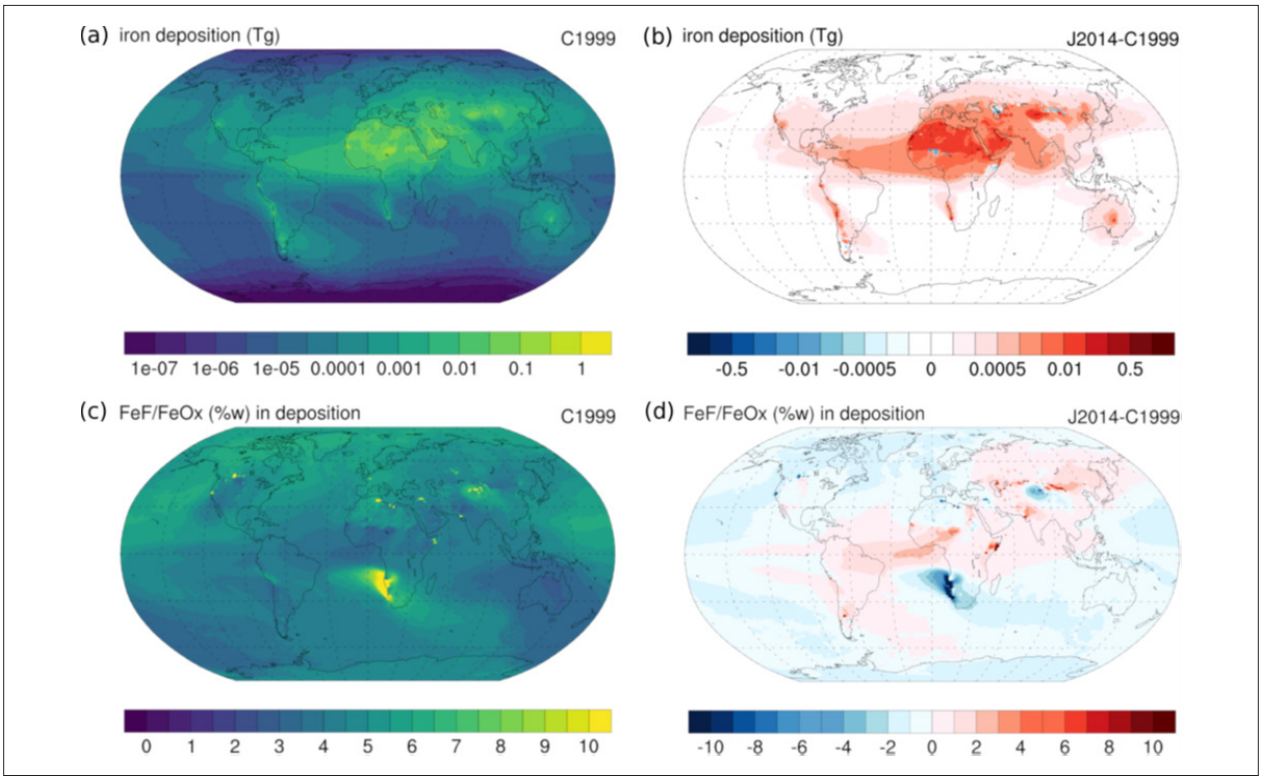

Figure 6. Figure from Gonçalves Ageitos et al. (2023). Comparison of the two soil mineralogy databases (denoted C1999 and J2014) in terms of iron deposition. Total iron deposition and ratio of ferrihydrite and nano-iron oxides (FeF) over pure crystalline iron oxides (FeOx) according to C1999 (a, c, respectively). Differences compared to J2014 (b, d, respectively). Reproduced under the Creative Commons 4.0 (CC 4.0) license.

While BC and dust are explicitly treated in most ESMs, BrC, which is the absorbing fraction of OA, is still disregarded by most climate models. This is despite its known impact on the effective radiative forcing due to aerosol-radiation-interactions (ERFari) and its potential impact on the snow albedo which may accelerate the melting of polar and glacial ice, similar to BC. Only recently has BrC attracted enough attention to start being incorporated in global climate models. Current climate models generally underestimate the absorbing properties of atmospheric aerosol although they reasonably estimate BC. As part of the AeroCom Phase III intercomparison of absorbing aerosol, Sand et al. (2021) evaluated the fraction of absorbing aerosol optical depth due to BC, dust, and organic aerosol and found it to be 57%, 30 and 10%, respectively.

Task 1.4: Ultrafine aerosol formation and growth

The work within FORCeS for improving the description of ultrafine particles and the corresponding aerosol number size distributions in ESMs has focused particularly on the improvement of the simulation of the new particle formation (NPF)/growth processes based on both laboratory and field observations as well as on the treatment of number emissions. The objective was once more to improve accuracy with a small computational cost for the ESMs. As already mentioned under Task 1.1, an important component in this has been the improvement of the description of OA, part of which is highly relevant for the formation and growth of nanoparticles (e.g. Bergman et al., 2022). Systematic work has also been conducted for unraveling the mechanisms of nanoparticle growth (Kontkanen et al., 2022; Stolzenburg et al., 2023) and NPF (Wang et al., 2022; Jorga et al., 2023), as well as developing methodologies for accurate interpretation of field observations of ultrafine aerosol microphysics (Hakala et al., 2022, 2023).

In their regional-scale modeling study, Patoulias et al. (2024) show that – unlike many previous studies have assumed – the formation of new nanoparticles can in fact reduce the concentrations of CCN. This effect is due to a similar effect as the underlying mechanisms of the Twomey effect: the condensable vapors being distributed to a larger number of (smaller) particles, and therefore limiting the growth of the Aitken mode particles to sizes where they can activate as CCN (see Fig. 7).

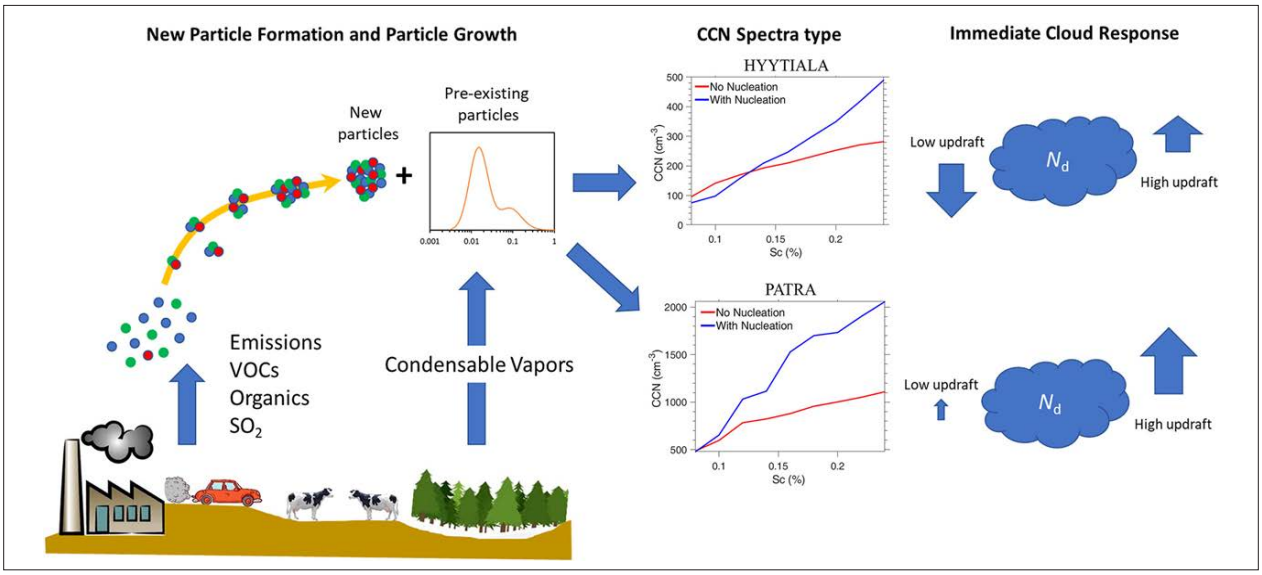

Figure 7. Figure from Patoulias et al. (2024). Sketch representing the impacts of NPF on aerosol size distribution, CCN and droplet number. Depending on the pre-existing particles, the number of particles forming, and the available condensable vapor mass for aerosol growth and vertical velocity (i.e., cloud type), the aerosol may experience a reduction in CCN and droplet number at lower supersaturations (top graphs), or an increase in CCN and droplet number for all cloud-relevant supersaturations (bottom graphs). Blue lines indicate aerosol with the effects of NPF, and red without NPF effects. Reproduced under the Creative Commons Attribution-Non-Commercial license.

Task 1.5: Identification of microphysical processes related to aerosols that can be simplified

The goal of this Task was to identify microphysics processes related to aerosols to which the global models are less sensitive. The work focused particularly on microphysical processes related to aerosol formation and growth, and ice hydrometeors. Proske et al. (2022) explored the potential to simplify through a sensitivity analysis of an emulated perturbed parameter ensemble (PPE) of ECHAM-HAM to illuminate the impact of selected cloud ice processes on model output (see Fig. 8). They found the autoconversion of ice crystals to be the dominant microphysical process influencing key variables such as the ice water path and cloud radiative effects in their model, while riming of cloud droplets on snow had the most influence on the liquid phase. Accretion of ice and snow and self-collection of ice crystals had a negligible influence on the model results and were therefore identified as suitable candidates for future simplifications. In turn, the dominating role of autoconversion suggests that this process has the greatest need to be represented correctly. The simulations by Proske et al. (2022) were conducted for ECHAM-HAM, but show a general method for model simplification that can be applied on other climate models.

While the studies by Proske et al. (2022, 2023) were the only ones within FORCeS that focused on systematically exploring potential model simplifications, many other of the FORCeS studies also included elements of testing and simplifying models to the degree possible. An example of such studies were the articles by Bardakov et al. (2021, 2022) and Wang et al. (2022) that employed an appropriate simplified version of the convective updraft + chemistry model following up the work by Murphy et al. (2015) allowing for acquiring a better understanding of the system with less computation cost. The work with the ISORROPIA-lite (Kakavas et al., 2022; Milousis et al., 2024) is of course also an example of such well-documented and justified simplications.

5.2 Progress within WP2 “Understanding of cloud processes and aerosol-cloud interactions”

The work within WP2 aimed at an improvement of cloud-, precipitation and aerosol processes within ESMs, targeting particularly the processes governing the effective radiative forcing caused by aerosol-cloud interactions (ERFaci). WP2 focused on aerosol-cloud interactions and cloud microphysics and interacted closely with WPs 3 and 5 through providing input and recommendations for the ESMs used within these WPs, and complementing the aerosol process-focused WP1. Overall, the work within WP2 progressed as outlined within the DoA. Many of the Tasks within WP2 are highly interlinked (see below for detailed descriptions).

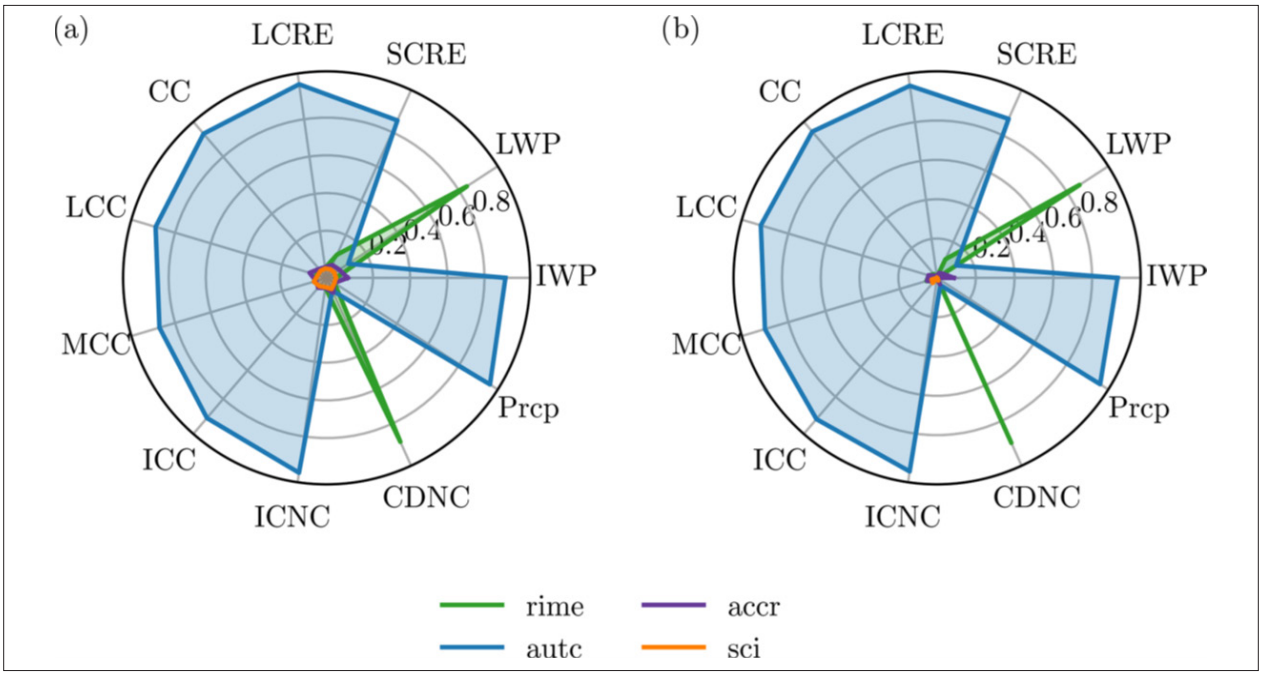

Figure 8. Figure from Proske et al. (2022). First-order (a) and total effect (b) sensitivity indices for the emulated response surface of global annual mean cloud cover (CC), liquid cloud cover (LCC, T >0 C), mixed-phase cloud cover (MCC, 0 C<T <−35 C), ice cloud cover (ICC, T <−35 C), longwave cloud radiative effect (LCRE), shortwave cloud radiative effect (SCRE), liquid water path (LWP), ice water path (IWP), and total precipitation. The indices are always between 0 and 1, and high values signal an important variable. Since the climate model is non-additive, the terms do not add up to 1 as interactions have to be taken into account. Reproduced under the Creative Commons 4.0 (CC 4.0) license.

Three major campaigns, one at Ny Ålesund station in the Arctic (NASCENT campaign coordinated by Stockholm University, from fall 2020 onwards, see Pasquier et al., 2022a), one at Puijo SMEAR IV station at the semiurban environment (coordinated by the University of Eastern Finland, during fall 2021, see e.g. (Väisänen et al., 2020; Ruuskanen et al., 2021; Kommula et al., 2024) and one at the San Pietro Capofiume in Italy (coordinated by the National Research Council, Institute of Atmospheric Sciences and Climate (CNR-ISAC, see e.g. Paglione et al., 2021; Neuberger et al., *in review*) were planned and organized within this WP.

Task 2.1: Droplet activation

Results from the first half of FORCeS investigating links between aerosols and cloud microphysics from satellite data have demonstrated that the simple approaches typically used to derive the relationship between Cloud Droplet Number Concentration (CDNC) and aerosol particles from observations of Aerosol Optical Depth (AOD) or Aerosol Index (AI) strongly underestimate the sensitivity, and that more elaborate ways to quantify the CCN concentration are required (Hasekamp et al., 2019). Furthermore, a review with inputs from several FORCeS partners on the options to constrain the droplet activation from satellite retrievals (Quaas et al., 2020) pointed out the general need to improve satellite-based methods to derive aerosol-cloud relationships. It emphasized the need to use LES to better assess the data requirements for CCN, updraft and cloud drop number (Nd) observations, and to analyse the impact of spatial aggregation scales. These findings have been thoroughly followed up upon during the last years of the project by e.g. Foskinis et al., (2022); Jia et al., (2022); Jia and Quaas, (2023) (see also (Manshausen et al., 2022; Watson-Parris et al., 2022a), described below. Also a study combining satellite and in-situ data sets on the susceptibility of cloud microphysics to aerosol perturbations is currently in preparation and will be submitted after the formal end of the project (Virtanen et al., *manuscript in preparation*).

As it was highlighed as one of the major methodological needs for improving our understanding on aerosol-cloud interactions, FORCeS conducted LES studies that coupled cloud activation to the other relevant processes that simultaneously take place when a cloud is formed. As an example, studies on the factors controlling Arctic cloud sustenance reveal the importance of meteorological conditions (Bulatovic et al., 2023) but also the

important role of Aitken mode particles in cloud droplet activation and CDNC. This result shows the need for understanding the sources and sinks of these nanoscale particles in the Arctic (Bulatovic et al., 2021; Maahn et al., 2021; Schmale et al., 2021; Siegel et al., 2021). The work by Calderón et al. (2022) demonstrated the power of LES modeling and present activation theories in the case of the FORCeS Puijo 2020 campaign, where a closure study of aerosol–cloud interactions during stratocumulus formation using UCLALES–SALSA (University of California Los Angeles large eddy simulation model–sectional aerosol module for large applications) was carried out. The unique observational setup allowed for a detailed look into the aerosol size–composition dependence of droplet activation and droplet growth in turbulent boundary layer driven by surface forcing and radiative cooling. The model successfully reproduced the probability distribution of updraft velocities and consequently the size dependency of aerosol activation into cloud droplets, recreating the size distributions for both interstitial aerosol and cloud droplets (see Fig. 9). This was the first time such a detailed closure was achieved not only accounting for activation of cloud droplets in different updrafts, but also accounting for processes like evaporating droplets and drizzle production through coagulation–coalescence. Further methodological developments with relevance to cloud droplet activation include the e.g. parameterization of updraft by Ahola et al. (2022) and the implementation of an embedded LES model in to General Circulation Model (GCM) modeling framework described by Nordling et al. (2024). Che et al. (2022), in their part, developed a new framework for the source attribution of cloud condensation nuclei and their impact on stratocumulus clouds and radiation within a climate model setting. Schwarz et al. (*in review*) pointed out an issue that bulk microphysics models may encounter at high aerosol concentrations or low updraft velocities as they do not explicitly account for water vapor competition effects.

On the detailed process level, the work conducted within FORCeS includes e.g. CCN activation of BC (Laaksonen et al., 2020; Lohmann et al., 2020), which has traditionally been considered non-hygroscopic and does not participate in CCN activation in many global models. Laaksonen et al. (2020) present a theory describing heterogeneous nucleation on soot particles with adsorption nucleation theory, and conclude that soot particles can activate as CCN, and any treatment (including chemical ageing) that increases the number of adsorption sites will respectively increase their CCN activity. Lohmann et al. (2020), used ECHAM-HAM to conduct global simulations of past and future climate effects of both ozone-aged soot particles acting as cloud condensation nuclei and sulfuric acid-aged soot particles acting as ice-nucleating particles, and analysed the effects on structure and radiative effects of clouds. Under pre-industrial conditions, soot aging led to an increase in thick, low-level clouds that reduced negative shortwave effective radiative forcing by 0.2 to 0.3 $W m^{-2}$. In the simulations of a future, warmer climate under double pre-industrial atmospheric carbon dioxide concentrations, soot aging and compensating cloud adjustments led to a reduction in low-level clouds and enhanced high-altitude cirrus cloud thickness, which influenced the longwave radiative balance and exacerbated the global mean surface warming by 0.4 to 0.5 K. These findings suggest that reducing emissions of soot particles is beneficial for future climate, in addition to air quality and human health. Other, more recent, process-level investigations include e.g. the laboratory on the impact of nitrogen oxides on monoterpene-derived CCN (Zhang et al., 2023) and field studies on the size distribution (Karlsson et al., 2022) and chemical composition (Gramlich et al., 2023) of cloud residuals during the NASCENT campaign in the Arctic (see also Sect. 5.1).

Task 2.2: Condensational and coagulation growth of cloud particles, precipitation sink

The response of cloud liquid water path (LWP) and cloud fraction (CF) to altered CDNC is among the most important and most uncertain adjustment mechanisms for aerosol-cloud interactions (see e.g. Maahn et al., 2021). These responses depend on the details of the cloud microphysics, particularly condensation and coagulation (and coalescence) of the cloud droplets, which are typically heavily parameterized in global models but also subject to large uncertainties in the process level. FORCeS used in particular LES modeling, field observations and satellite data to understand these processes and improve their descriptions in ESMs (see e.g. Kim et al., 2020; Gryspeerdt et al., 2021; Spill et al., 2021; Zhang et al., 2021). Many of the first published studies have dealt with improving the methodologies used in using and interpreting satellite data (alone or in combination with other data sets). Gryspeerdt et al., 2021 used reanalysis wind fields and ship emission information matched to observations of ship tracks to measure the timescales of cloud responses to aerosol in instantaneous (or "snapshot") images taken by polar-orbiting satellites. Besides highlighting the importance of the meteorological environment, this work demonstrated the importance of accounting for the time evolution of the cloud response and the aerosol source, especially in the case of an isolated aerosol source where there is no replenishment of the particle loadings. Kim et al. (2020), on the other hand, developed a novel machine-learning-based retrieval technique for obtaining LWP from satellite observations. In the second half

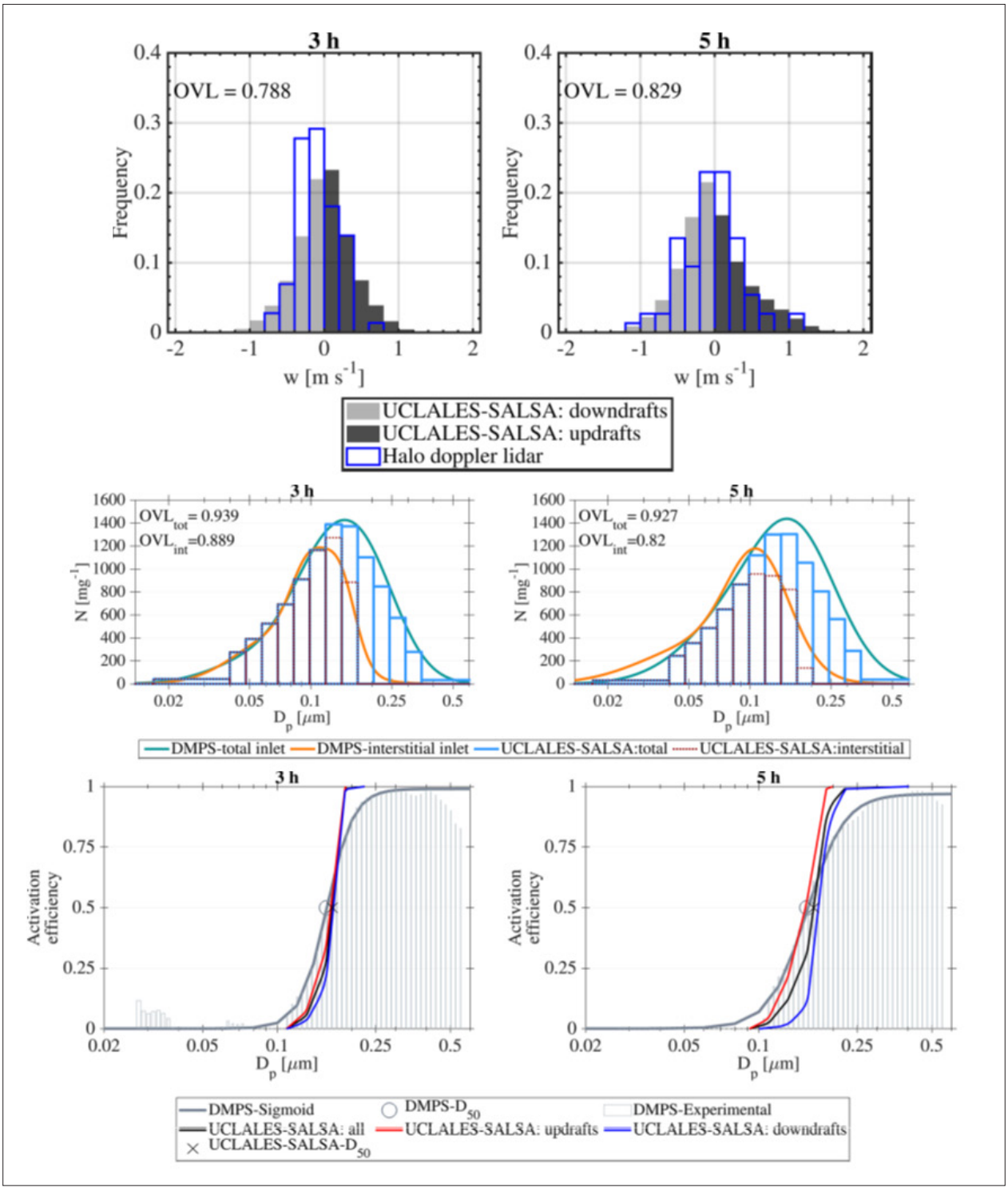

Figure 9. Figure from Calderón et al. (2022). Top row: Comparison of model-based distributions of vertical wind at cloud base during 24 September 2020 to those retrieved from Doppler lidar observations. Each panel shows the overlapping index value (OVL) as an indicator of agreement between distributions. Middle row: Comparison of aerosol size distributions calculated with UCLALES–SALSA at Puijo altitude of 225 m and measured by the twin-inlet DMPS system during 24 September 2020. Bottom-row: Comparison of activation efficiency curves calculated with UCLALES–SALSA at Puijo altitude of 225 m and retrieved from aerosol number concentrations measured by the twin-inlet DMPS system during 24 September 2020. Reproduced under the Creative Commons 4.0 (CC 4.0) license.

of FORCeS, a series of studies on the potential aerosol effects on LWP (Andersen et al., 2022, 2023; Arola et al., 2022; Christensen et al., 2022; Jia et al., 2022; Sudhakar et al., 2022; Zipfel et al., 2022) has been conducted to follow up on the earlier work.

The LES studies conducted within FORCeS (e.g. Boutle et al., 2022; Calderón et al., 2022; Prank et al., 2022; Raatikainen et al., 2022; Bulatovic et al., 2023; Nordling et al., 2024), Schwartz et al. *in review*) naturally also contribute importantly to our improved understanding on cloud microphysics during the evolution of a cloud beyond the initial activation process. Figure 10 shows the LWP predictions by the models assessed by Boutle et al. (2022) who conducted an intercomparison between 10 single-column (SCM) and 5 LES models for a radiation fog case study loosely based on the Local and Non-local Fog Experiment (LANFEX) field campaign in the UK. The LES model results were found to be of variable quality, particularly under high aerosol or CDNC conditions. The main SCM bias was reported to be toward the overdevelopment of fog. Unsurprisingly, the ability of the model to simulate the fog development was determined by its ability to capture the water vapor budget and the interactions between surface and atmosphere. It was also found that some of the models lacked some of the key processes required to accurately simulate the fog (e.g. droplet sedimentation) therefore calling for future process improvements. The results also indicated that the modeled fog development is sensitive to the shape of the cloud droplet size distribution. In this regard, some work on the fundamental observational techniques for constraining hydrometeor size distributions has also been conducted within FORCeS (Tiitta et al., 2022). Needless to say, these methodological developments should naturally continue beyond the lifetime of the project.

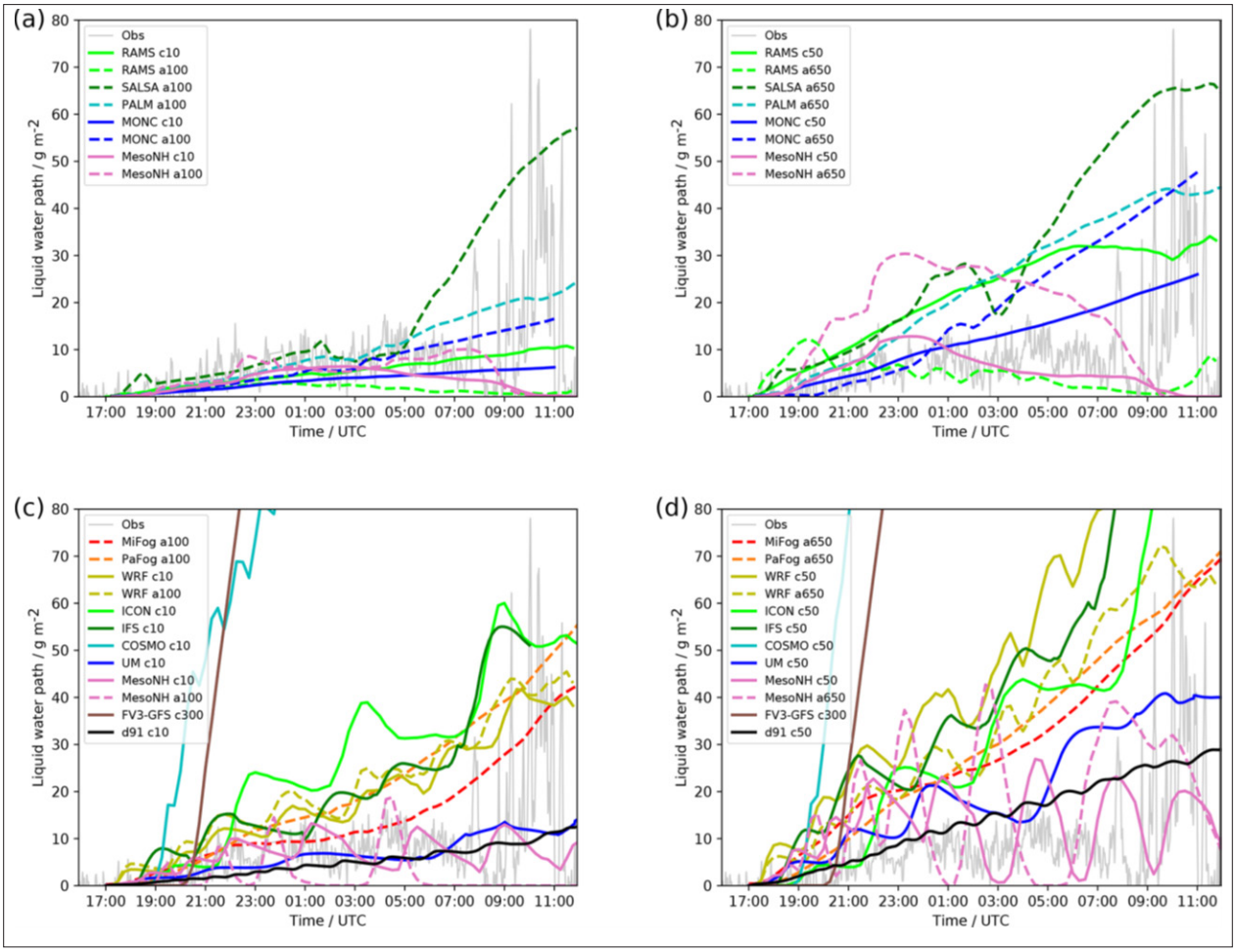

Figure 10. Figure from Boutle et al. (2022). Liquid water path observed and modelled by (a) low aerosol/CDNC LES, (b) high aerosol/CDNC LES, (c) low aerosol/CDNC SCMs, and (d) high aerosol/CDNC SCMs. Reproduced under the Creative Commons 4.0 (CC 4.0) license.

Task 2.3: Ice nucleation, secondary ice and freezing

Ice nucleation, secondary ice and freezing have been some of the key topics explored within the NASCENT campaign in the Arctic (Schmale et al., 2021; Li et al., 2022; Pasquier et al., 2022a, 2022b). Rinaldi et al. (2021) discussed implications for ice nuclei origin from local terrestrial (dust), marine and distant (Artic haze pollution), also noting that the majority of the ice-nucleating particles (INP) on the site were fine particles, although the coarse INP contribution increased somewhat during the summer. Pereira Freitas et al. (2023) contributed to the discussion of Arctic INP sources through utilizing single-particle fluorescence spectroscopy to identify and quantify primary biogenic aerosol particles (PBAP) at an Arctic mountain site, with transmission electronic microscopy analysis supporting the presence of PBAP. Their results suggested that the terrestrial Arctic biosphere is an important regional source of PBAP, given the high correlation between air temperature, surface albedo, surface vegetation and PBAP tracers. PBAP clearly also correlated with high-temperature ice nucleating particles (INP) (>−15 °C), of which a high a fraction (>90%) were proteinaceous in summer, implying biological origin. On the larger scale, Papakonstantinou-Presvelou et al. (2022) found strong contrasts between ocean and sea ice in satellite-retrieve ice crystal numbers, finding more ice crystals over the open ocean. This finding was against previous expectation and warrants further studies of the macro- and microphysics driving the formation of Arctic ice and mixed-phase clouds (Fig. 11).

One of the key focal points of this Task was Secondary Ice Production (SIP) (see e.g. Hoose, 2022). Sotiropoulou et al. (2021a) discussed the importance of secondary ice processes as a source of ice crystals in Antarctic clouds and highlighted the need to understand this process better. Sotiropoulou et al. (2021b) used LES simulations to investigate the potential of ice multiplication from breakup upon ice–ice collisions could account for the observed cloud ice in a stratocumulus cloud observed during the Arctic Summer Cloud Ocean Study (ASCOS) campaign. The results from this work suggested that the overall efficiency of this process in these conditions is weak; increases in fragment generation were compensated for by subsequent enhancement of precipitation and sub-cloud sublimation. The largest uncertainty in the simulations stems from the correction factor for ice enhancement due to sublimation included in the breakup parameterization. These results indicate that the lack of a detailed treatment of ice habit and rimed fraction in most bulk microphysics schemes is perhaps not detrimental for the description of the collisional breakup process in the examined conditions as long as cloud-ice-to-snow autoconversion is considered. These results were corroborated by the findings of the NASCENT campaign (Pasquier et al., 2022a, 2022b, 2023) and have led to the parameterization of SIP which is described by (Sotiropoulou et al., 2021a, 2021b) and Georgakaki and Nenes (*manuscript in review*).

In addition to the Arctic-focused studies mentioned above, Proske et al. (2021) have demonstrated a mechanism of natural cloud seeding of lower-level clouds by ice clouds over Switzerland, while Villanueva et al. (2021) have taken a global view and used satellite observations of the hemispheric and seasonal contrast in cloud top phase to assess the dust-driven droplet freezing in the ECHAM-HAM model (see also Chatziparaschos et al., 2023). Quaas et al. (2021) investigated the impact of the COVID-19 recovery plans for aviation-induced cirrus clouds. As described in Sect. 5.1 above and Sect. 5.5 below, Proske et al. (2022, 2023) have further investigated the potential of the complex ice cloud processes to be simplified.

To investigate the fundamental ice properties on the molecular scale, molecular dynamics and kinetic model studies of ice crystal growth, interactions between ice and organic molecules, and the dynamics of the Wegener-Bergerron-Findeisen (WBF) process have been conducted (Schlesinger et al., 2020). This study targeted particularly the accommodation of water molecules arriving from the gas phase to the crystal structure, and concluded the order parameter (instead of energy) to be the main factor differentiating the ice surface from the bulk crystal. These fundamental molecular scale studies have been continued also during the second half of the project in the form of e.g. investigations of the molecular mechanism of deposition ice nucleation on silver iodide – a compound commonly used for cloud seeding (Roudsari et al., 2024).

Task 2.4: Entrainment and mixing as cloud sink

Much of the work conducted within Task 2.4 is directly linked to work done for Tasks 2.1 and 2.2 – since LES simulations, satellite observations, and large-scale model evaluation typically give an integrated view on the cloud responses to aerosol perturbations. Entrainment and mixing are among the key processes playing into explaining cloud responses to various types of aerosol perturbations (Gryspeerdt et al., 2021; Maahn et al., 2021; Zhang et al., 2021; Christensen et al., 2022) as well as long-term trends (Cherian and Quaas, 2020).

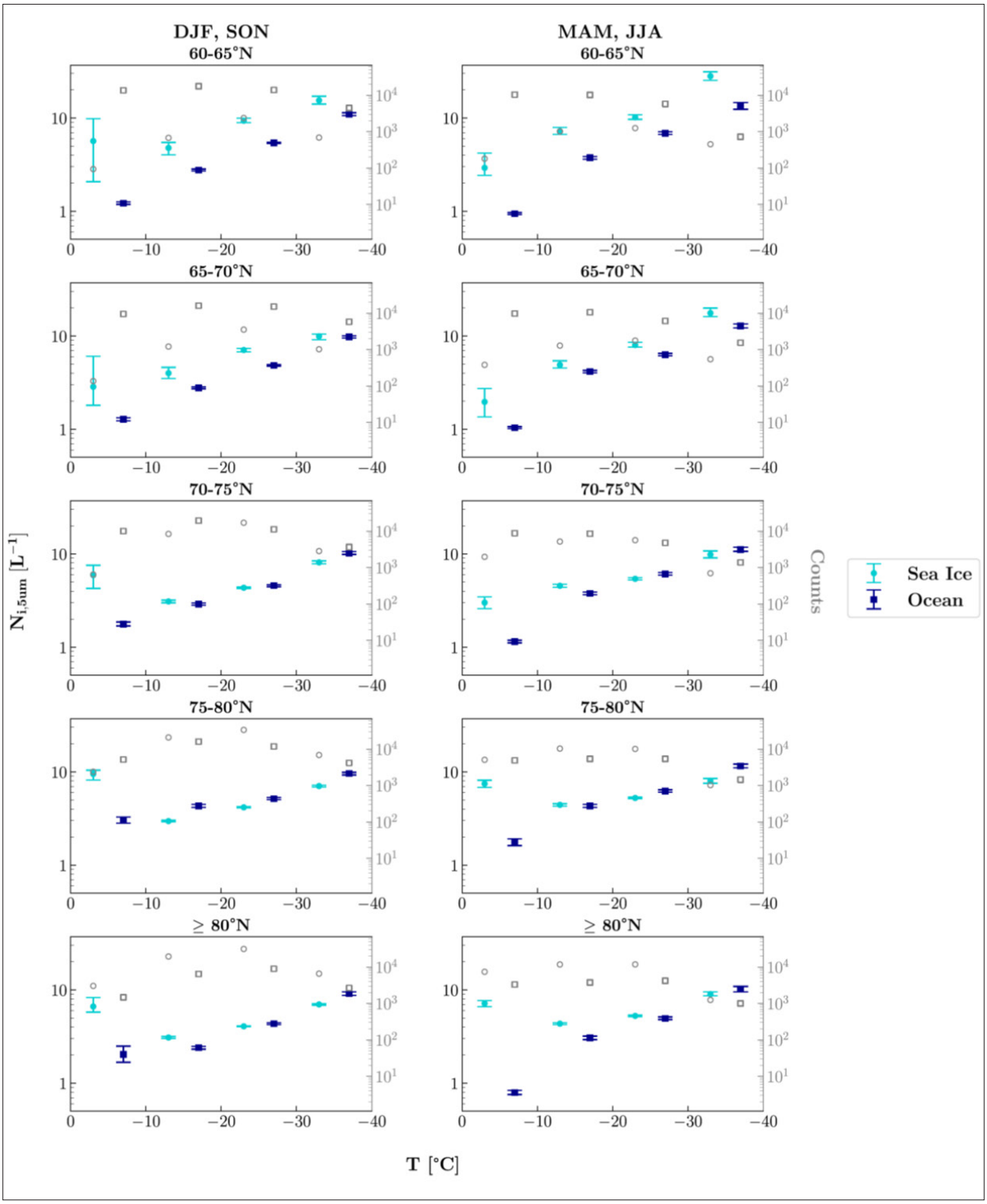

Figure 11. Figure from Papakonstantinou-Presvelou et al. (2022). Medians of distributions of daily number concentrations of ice crystals that are larger than 5 μm (in L −1; left y-axis) as a function of temperature for the time period 2006–2016. The temperature scale (x-axis) is not continuous; it comprises distinct temperature bins of 10°C each. The temperature offset between each consecutive point is artificial and introduced only for readability of the plot. Different colors indicate the surfaces over which these clouds exist; sea ice (in turquoise) and open ocean (in blue). Two different seasons are presented (cold: DJF, SON and warm: MAM, JJA) and five geographical regions (latitude belts). The 95% confidence intervals are displayed as the error bars. The numbers of samples used to calculate the medians are shown in gray (right y-axis. Reproduced under the Creative Commons 4.0 (CC 4.0) license.

Task 2.5: Aerosol processing and scavenging

A key aspect related to the NASCENT, Puijo and FAIRARI campaigns was the investigation of aerosol and vapour processing by clouds. Long-term observations on cloud scavenging of absorbing aerosol components at the Puijo station were analysed (Ruuskanen et al., 2021). These observations provided an estimate on the partitioning of black carbon on different sized aerosol particles, and how efficiently those were scavenged by cloud droplets. The results from Puijo were complemented with the findings of e.g. Isokääntä et al. (2022) and Heslin-Rees et al. (2024), the former of which found BC to be efficiently scavenged by clouds and precipitation at the boreal forest site in Hyytiälä, Finland, and the latter showed wet scavenging to be one of the key drivers of long-term BC trends at the Arctic Zeppelin station. In terms of organic species, Graham et al. (2020) found that while the scavenging of aerosol particles was clearly visible in the aerosol size distribution observations, no indication of significant chemical processing in the form of e.g. aqueous-phase SOA formation was observed in the Åre site in central Sweden. These results were corroborated by the study by Isokääntä et al. (2022), who also found no statisticaly significant impact of clouds and precipitation on the OA concentration in airmasses arriving at Hyytiälä (see Fig. 12). Signal of aqueous-phase production of sulphate in clouds was, however, observed as expected.

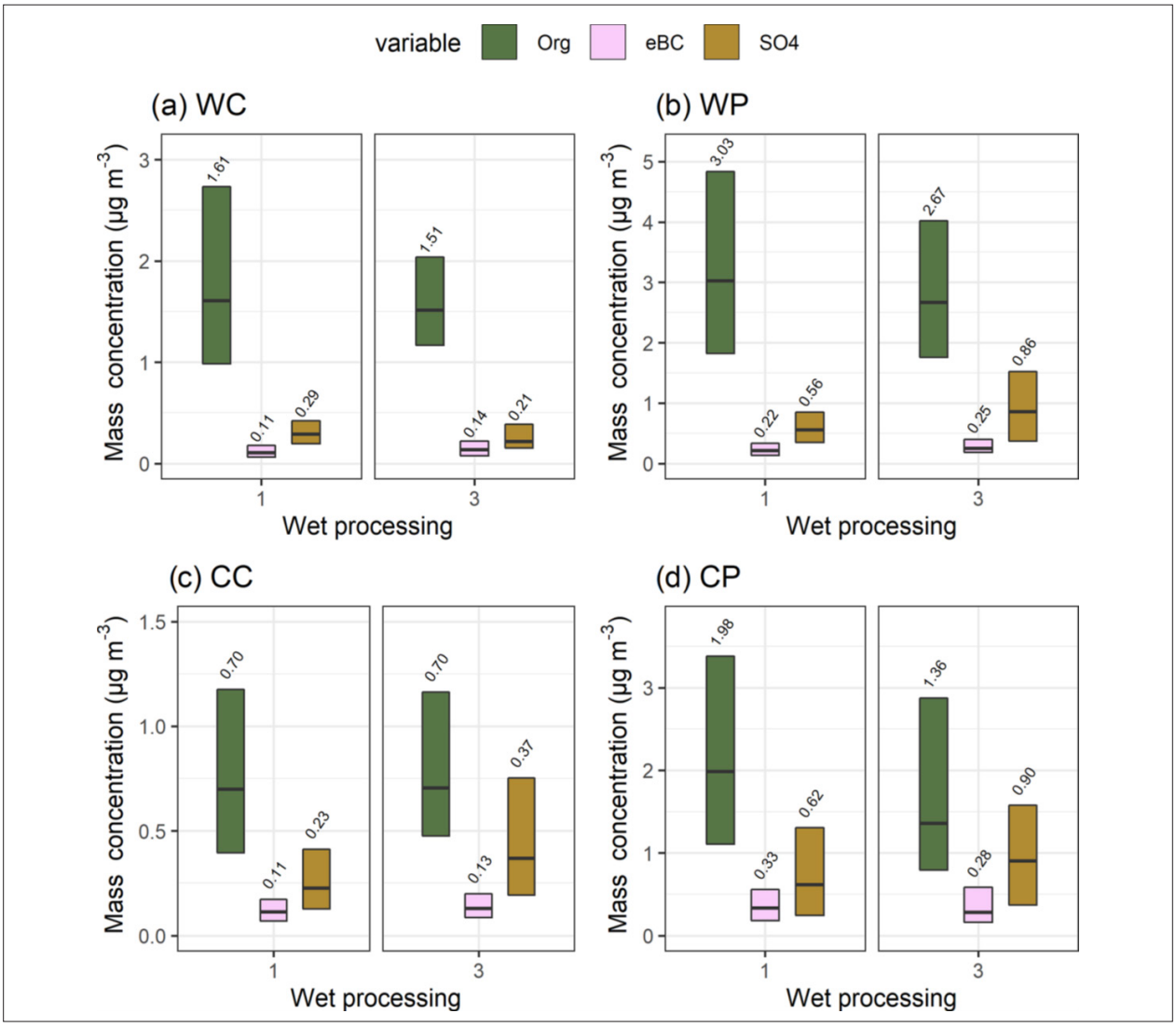

Figure 12. Figure from Isokääntä et al. (2022). Median (black horizontal lines and numerical values) particle mass concentration with 25th–75th percentiles (boxes) for Org, eBC, and SO4 for wet processing groups 1 (no precipitation or high humidity experienced by the airmass) and 3 (high humidity but no precipitation experienced by the airmass) as described in Table 1. Subplots show the air mass sectors (clean and polluted) with the seasonal (warm and cold) division: (a) warm and clean, (b) warm and polluted, (c) cold and clean, and (d) cold and polluted. The figure is based on simultaneous observations of these three species between March 2012 and August 2019. Note the different y-axis limits in each subplot. Reproduced under the Creative Commons 4.0 (CC 4.0) license.

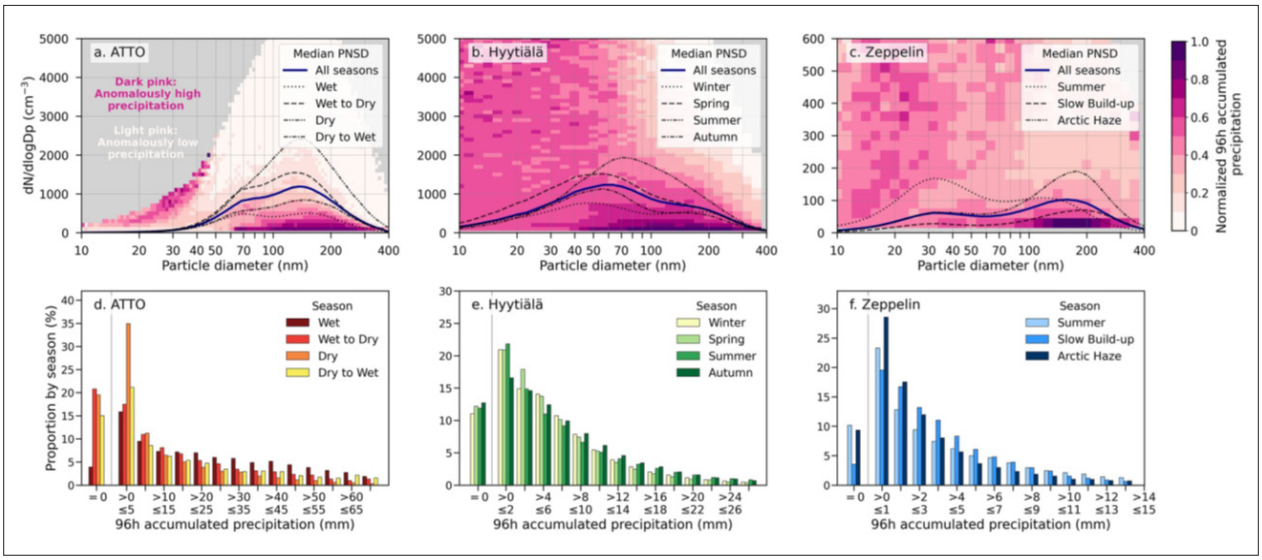

Figure 13. Figure from Khadir et al. (2022). The relationship between aerosol particle number size distribution and 96 hr accumulated precipitation (a–c), and the distribution of 96 hr accumulated precipitation values for trajectories (d–f) arriving at each of the measurement sites (ATTO, HYY, ZEP). The blue solid lines represent the median size distributions over the whole year, the dotted, dashed and dash-dotted lines represent the different seasons (see legends for details). The median accumulated precipitation values during the last 96 hr for a given size distribution value are depicted using the color scale, normalized to the maximum of each site. Note the different x-axis ranges for the sites, indicative of the unique precipitation regimes in these regions. Reproduced under the Creative Commons 4.0 (CC 4.0) license.

The results of Isokääntä et al. (2022) highlight the importance of uptake and processing of atmospheric constituents by clouds. The important role of nucleation scavening when investigating the impact of precipitation history on aerosol number size distributions in boreal, tropical and Arctic environments (Khadir et al., 2023). Figure 13 shows anomalously low concentrations of >40–100 nm particles in airmasses that had experienced precipitation – quantitatively in line with the expected threshold diameter for CCN cloud droplet activation in supersaturations relevant for the three environments (see also Calderón et al., 2022).

We have also investigated the processes that affect gas transport within deep convective clouds (Bardakov et al., 2020, 2021). Using LES, we have produced individual parcel trajectories within a simulated deep convective cloud. A box model has then been coupled to these trajectories to calculate e.g. gas condensation on hydrometeors, gas-phase chemical reactions, gas scavenging by hydrometeors and turbulent dilution. We found that the trace gas transport approximately follows one out of three scenarios, determined by a combination of the equilibrium vapor pressure (containing information about water-solubility and pure component saturation vapor pressure) and the enthalpy of vaporization. In one extreme, the trace gas will eventually be completely removed by precipitation. In the other extreme, there is almost no vapour condensation on hydrometeors and most of the gas is transported to the top of the cloud. The results from Bardakov et al. (2021) on the isoprene system show that gas uptake to anvil ice is an important parameter for regulating the intensity of the isoprene oxidation and associated low volatility organic vapor concentrations in the outflow – a result that is also true for the transport of ammonia critical for NPF in the upper troposphere (Wang et al., 2022).

5.3 Progress within WP3 "Role of aerosol and cloud changes for aerosol radiative forcing between 1950 and 2050"

FORCeS WP3 investigated the temporal development of key aerosol components, their physical characteristics, as well as cloud changes between 1950 and 2050 using different scenarios. The specific objectives of WP3 included:

- Determining transient changes in aerosols and clouds and the corresponding ERF from 1950 to present day,
- Understanding and quantifying the key uncertainties in the aerosol forcing between 1950–2050,
- Providing plausible near-future projections of ERF.

The scientific work in WP3 proceeded generally as described in the DoA.

This WP undertook to determine aerosol-related changes from 1950 to the present day through coordinated FORCeS ESM model simulations. Transient aerosol records were produced using three FORCeS ESMs using aerosol schemes of different levels of complexity and different host climate characteristics. All three models are well documented (Neubauer et al., 2019; Seland et al., 2020; van Noije et al., 2021). Relevant model data for the period 1950-present were assembled and published under CMIP6 ESGF nodes. The three FORCeS ESMs were diagnosed for aerosol composition and radiative property diagnostics based on their AeroCom and CMIP6 simulations (Gliß et al., 2021 and D3.4). The three models, altogether provide a rather representative spread of the wider CMIP6 and AeroCom ensemble. A corresponding comprehensive large observational data set of the aerosol physical properties and composition evolution has been assembled from in-situ data, wet deposition and ice core data and satellite remote sensing since 1979. The trends in models and observations 2000-2014 have been found to be similar to the first order (Mortier et al., 2020). A comparison to incoming surface radiation shows significant and unexplained bias in Asia which may hint at emission uncertainties (Moseid et al., 2020). .

Task 3.1: Determine aerosol and cloud changes 1950–present

Three types of experiments were performed with the FORCeS ESMs which are crucial for the documentation and analysis of the historical aerosol forcing record:

- AeroCom phase III *control and historical* atmospheric simulations nudged to reanalysed meteorology. These simulations have been conducted for the year 2010 and the period 1750–2014 using the same emissions as CMIP6. Note, that the models cover the 1750–2014 period in differing levels of detail.
- CMIP6 coupled ESM historical simulations and perturbations of that using pre-industrial aerosol emissions (*hist-piAer*). These simulations are part of the DECK (Eyring et al., 2016) and AerChemMIP model intercomparisons (Collins et al., 2017).
- CMIP6 AGCM simulations with sea surface temperature fields derived from the historical simulation (*histSST*) and the corresponding perturbed simulation with pre-industrial aerosol (histSST-piAer) are the basis for the calculation of the evolution of the aerosol ERF.

Extensive analysis and discussion on the various aspects of aerosol loadings and cloud changes in recent history based on the available simulations has been published (Allen et al., 2020; Mortier et al., 2020; Moseid et al., 2020, 2022; Turnock et al., 2020; Gliß et al., 2021; Lee et al., 2021; Su et al., 2021; Andersen et al., 2022, 2023; Daskalakis et al., 2022; Quaas et al., 2022; Williams et al., 2022; Kok et al., 2023) and only very brief highlights will be provided here.

Mortier et al. (2020) compared regional AOD trends for different aerosol components from the 11 different AeroCom and CMIP6 models compared to observational data as analysed for the period of 2000–2014. The results reveal that the observations exhibit mostly negative trends of the extensive parameters in the different regions of the world. Significant decreases are found in Europe, North America, South America, North Africa and Asia. In Asia, the aerosol extinction (AE) increases in time and is consistent with increases in AOD_f (f referring to fine) and SO_4, which reflects a regional increase in the anthropogenic aerosols in that region in the overall study period from 2000 to 2014. The models tend to capture observed AOD, AE, SO_4 and PM trends but show larger discrepancies regarding AODc (c referring to coarse). The rather good agreement of the trends across different aerosol parameters between models and observations, when co-locating them in time and space, implies that

global model trends, including those in poorly monitored regions, are likely reasonable – when looking at the overall development of AOD and AE. A comprehensive analysis and more detailed evaluation of various aspects of the aerosol life cycle, budgets and optical properties for the reference year 2010 from 14 different models participating in the AeroCom Phase III Control Experiment was conducted by Gliß et al. (2021). For instance, the analysis of aerosol budgets for sulfate, black carbon, organics, dust, sea salt and nitrate show significant differences in aerosol lifetime between the models, indicating the need to improve the interactions between aerosols, clouds and precipitation.

Moseid et al. (2020), on the other hand, investigated global and regional aerosol radiative effects over the time period 1961–2014 by looking at surface downwelling shortwave radiation (SDSR). They used observations from ground stations as well as multiple experiments from eight ESMs participating in CMIP6. The results showed that this subset of models reproduces the observed transient SDSR well in Europe but poorly in China. The likely explanation for this was associated with missing emissions of sulfur dioxide in China, highlighting the importance of accurate emission inventories for narrowing down uncertainties in aerosol-climate interactions. This study was followed up on the one hand by Julsrud et al. (2022) and on the other hand by Moseid et al. (2022). The former (Julsrud et al. 2022) investigated the contributions of aerosols and clouds of global dimming and brightening trends and largely corroborated the earlier findings in the sense of concluding aerosols having played a major role in influencing these trends, as well as in terms of warranting a more detailed look on the Asian emission. The latter (Moseid et al., 2022) compared long term trends in concentrations of sulfate and black carbon (BC) between 15 ice cores and 11 ESMs over nine regions around the world during the period 1850–2000. For sulfate concentration trends, the model results were found to generally agree with ice core records, whereas modeled BC concentration trends differed from the records (Fig. 14).

Task 3.2: Provide transient ERFari+aci records 1950-present from the available FORCeS atmospheric global models constrained by observational data

Comparisons made against observed radiative properties by e.g. Gliß et al. (2021), Mortier et al. (2020), and Moseid et al (2020) suggest that the ERFari effect might be underestimated in the FORCeS models – similarly to the majority of the other models analysed. Both optical depth and surface aerosol scattering are underestimated significantly (Gliß et al., 2021). These results are also qualitatively in line with the analysis by Julsrud et al. (2022), which indicate models to generally underestimate the dimming and brightening trends, most likely due to issues related to aerosols (see Fig. 15).

Fiedler et al. (2023) used the simulations conducted within The Radiative Forcing Model Intercomparison Project (RFMIP) allows estimates of ERF in CMIP6. They analysed the RFMIP output, including the new experiments from models that use the same parameterization for anthropogenic aerosols (RFMIP-SpAer), to characterize and better understand model differences in aerosol ERF. They found little changes in the aerosol ERF for 1970–2014 in the CMIP6 multi-model mean, which implies greenhouse gases primarily explain the positive trend in the total anthropogenic ERF. Cloud-mediated effects dominate the present-day aerosol ERF in most models. The results highlight a regional increase in marine cloudiness due to aerosols, despite suppressed cloud lifetime effects in that RFMIP-SpAer experiment. Negative cloud-mediated effects mask positive direct effects in many models, which arise from strong anthropogenic aerosol absorption (see also (Watson-Parris et al., 2021, Williams et al., 2022). The findings suggest opportunities to better constrain simulated ERF by revisiting the optical properties and long-range transport of aerosols.

Task 3.3: Determine the main contributions to model uncertainty to the simulated transient ERF (1950–2050) using perturbed physics ensembles and emulators

The work towards this Task was conducted using an emulator setup (Watson-Parris et al., 2021) and the results are summarized within Regayre et al. (2023), who sampled the uncertainty in 37 model parameters related to aerosols, clouds, and radiation in a PPE of the UK Earth System Model and evaluated 1 million model variants (different parameter settings from Gaussian process emulators) against satellite-derived observations over several cloudy regions. Figure 16 shows the contributions of different model processes to the aerosol radiative forcing (see Regayre et al., 2023 for the description of the abbreviated processes). The analysis of a very large set of model variants exposes model internal inconsistencies that would not be apparent in a small set of model simulations, of an order that may be evaluated during model tuning efforts. The analysis showed that, by neglecting variables associated with these inconsistencies, it was possible to reduce the parametric uncertainty

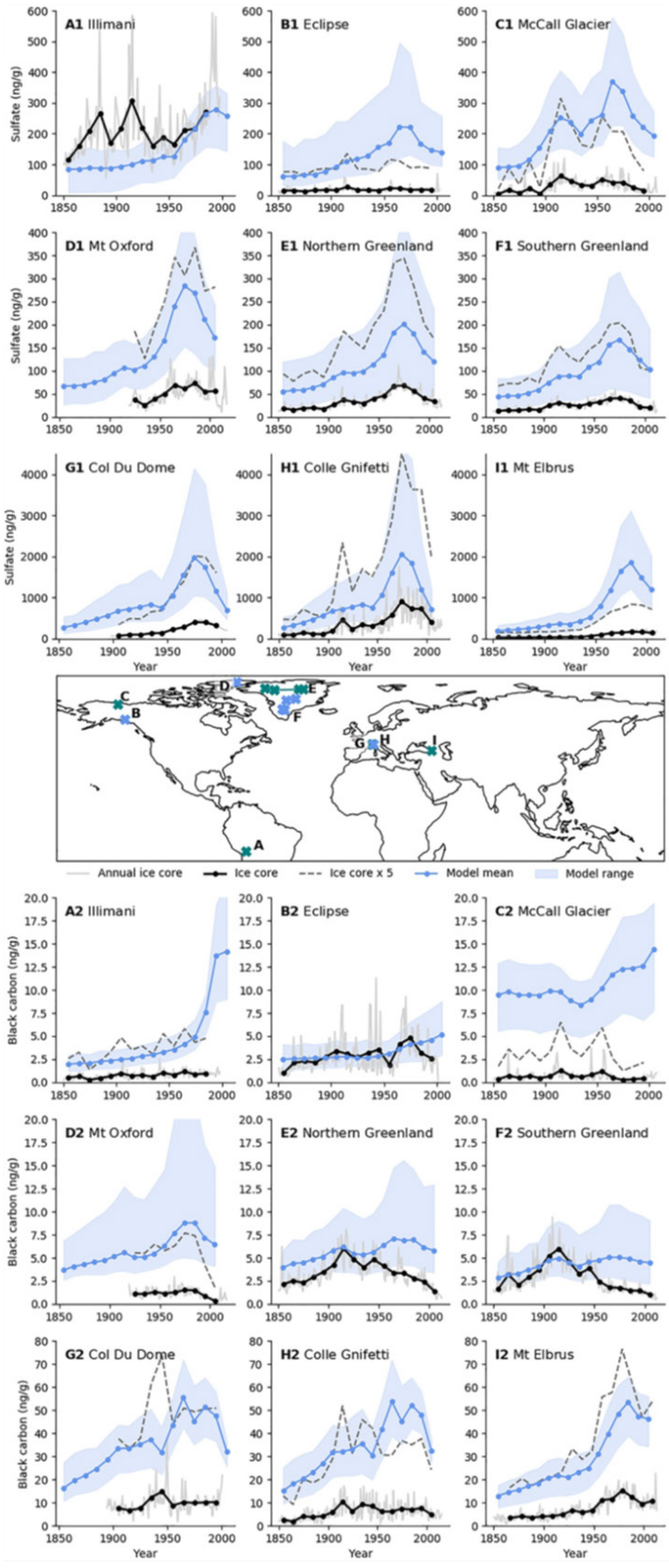

Figure 14. Figure from Moseid et al. (2022). Decadal sulfate (a1–i1) and black carbon (a2–i2) concentrations [ng/g] in ice cores (black) and model mean of 11 models (blue), decadally averaged. The shading shows the maximum/minimum decadal average of the 11 models. The light gray solid line shows the annual ice core concentration. The stippled dark gray line shows the respective decadal ice core concentrations multiplied by a factor of 5. Reproduced under the Creative Commons 4.0 (CC 4.0) license.

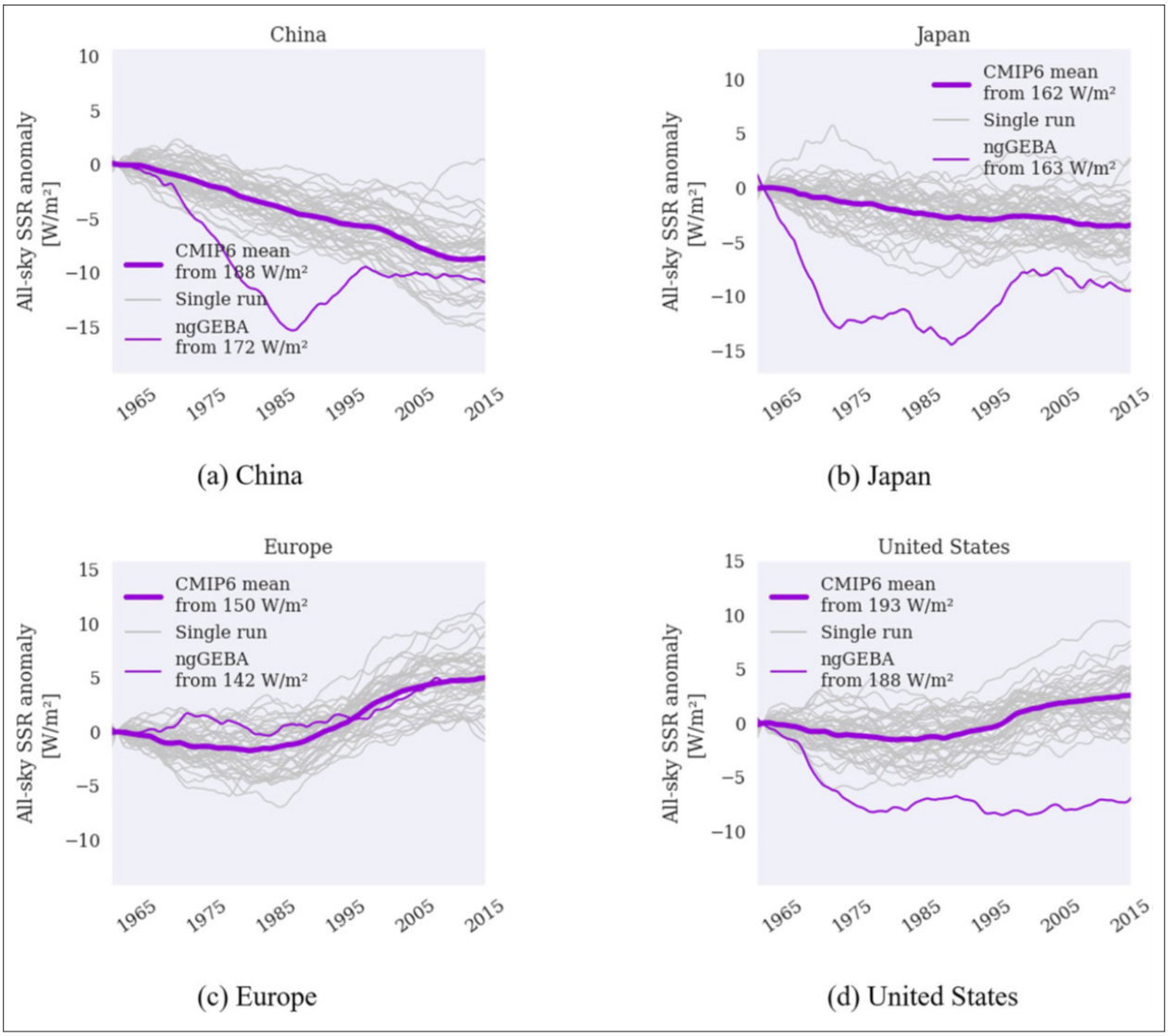

Figure 15. Figure from Julsrud et al. (2022). Decadal running means of mean simulated (CMIP6) and observed (ngGEBA) all-sky SSR anomalies between 1961 and 2014 averaged over ngGEBA stations in four regions: Multi-model mean CMIP6 in boldface and ngGEBA in lightface. Gray lines are decadal running means of each model run included. The anomalies are computed by averaging the initial 5 years of the running mean timeseries (this average is printed after "from" in the legend items), and subtracting this mean value from each subsequent time step. Included in the computation is a CMIP6 historical all-forcing simulation (r1i1f1p1) from each of the 42 models studied. Reproduced under the Creative Commons 4.0 (CC 4.0) license.

in global mean aerosol forcing by more than 50 %, constraining it to a range (around −1.3 to −0.1Wm^2) in this model. Structural model developments targeted at the identified inconsistencies would enable a larger set of observations to be used for constraint, which would then very likely narrow the uncertainty further and possibly alter the central estimate.

Another study applying the concept of the PPE in the context of this Task is the work by Peace et al. (2022) who studied the links between aerosols and tropical precipitation shifts. The results suggested that projections of tropical precipitation shifts will be improved by reducing aerosol radiative forcing uncertainty, but predictive gains may be offset by temporary shifts in tropical precipitation caused by future major volcanic eruptions.

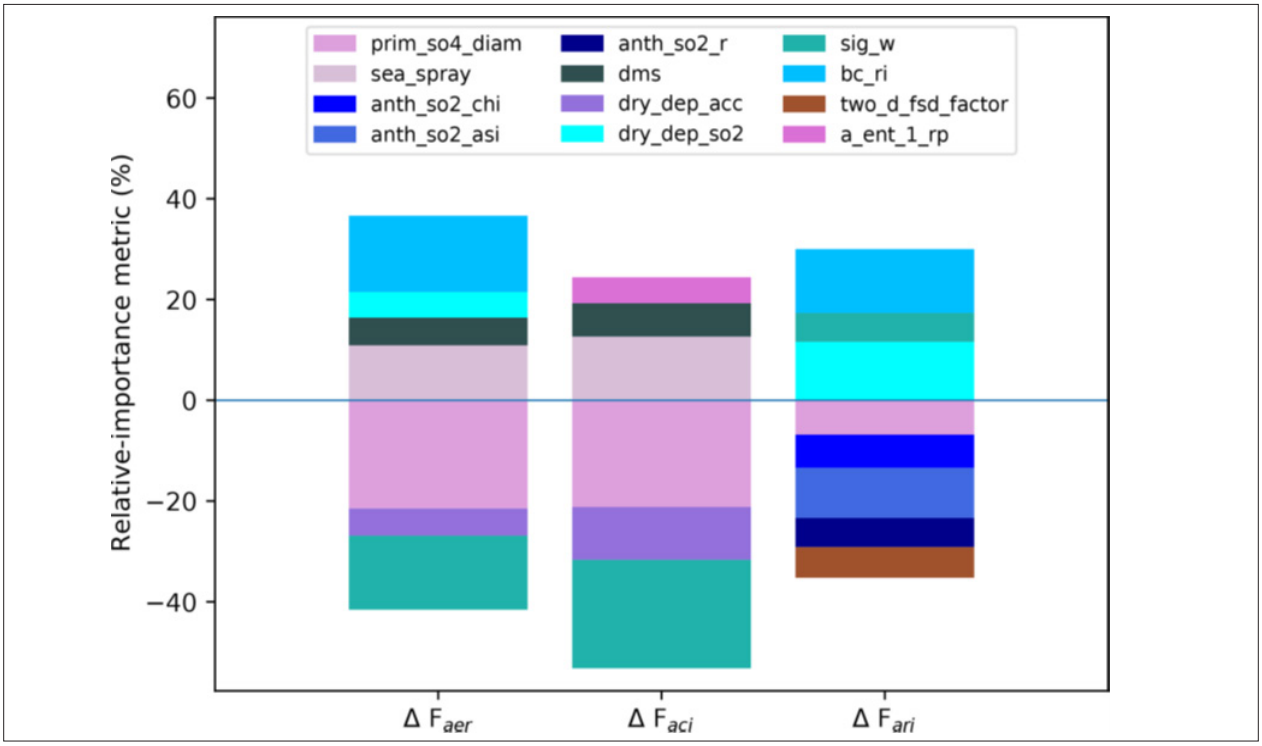

Figure 16. Figure from Regayre et al. (2023). Relative importance of model parameters as causes of uncertainty in global mean ΔFaer and its components ΔFaci and ΔFari. Only parameters with a relative importance of 5% or larger are shown. Positive values correspond to parameters where increasing the parameter value causes median values of ΔFaer, ΔFaci, or ΔFari to become weaker (less negative) across the set of 1 million model variants. Reproduced under the Creative Commons 4.0 (CC 4.0) license.

Task 3.4: Provide several likely near future (until 2050) aerosol composition and ERFari+aci trends

This Task encompasses contributions from e.g. Allen et al. (2020), Turnock et al. (2020), Fiedler et al. (2021), Watson-Parris et al. (2022a), Jenkins et al. (2023b), Jia and Quaas (2023) and Lapere et al. (2023), who all have worked on slightly different aspect of potential future aerosol and radiative forcing trends. As an example, Lapere et al. (2023) focused specifically on sea spray aerosols in past, present and future, and found that future climate scenarios SSP126 and SSP585, SSaer concentrations increase at both poles at the end of the 21st century, with more than two times mid-20th century values in the Arctic (see Fig. 17).

5.4 Progress within WP4 “Novel constraints on aerosol radiative effects”

Four of the WP4 tasks were targeted towards developing and applying novel ways of constraining models: process scale-chains, natural analogues, long-term transient constraints and perturbed parameter ensembles (see Tasks 4.2–4.5 below). Another role of WP4 was to act as a “data-hub” for the project (see Task 4.1 below). Overall, the work within WP4 progressed according to the plan laid out in the DoA.

Task 4.1: Synthesis of in-situ and remote sensing observations

WP4 conducted scoping work of the data used and produced within FORCeS, which includes data from laboratory studies, field observations, remote sensing and various kinds of model output datasets (see for example Kim et al., 2020; Väisänen et al., 2020; Gliß et al., 2021; Gryspeerdt et al., 2021; Herbert et al., 2021; Paglione et al., 2021; Ruuskanen et al., 2021; Wu et al., 2021b; Leinonen et al., 2022; Pasquier et al., 2022a; Sudhakar et al., 2022; Fiedler et al., 2023; Graham et al., 2023; Pereira Freitas et al., 2023; Blichner et al., 2024); Neuberger et al. *in review* to name a few). The data from these studies are made openly availble in various databases, depending on the type of data and the most suitable dissemination channel.

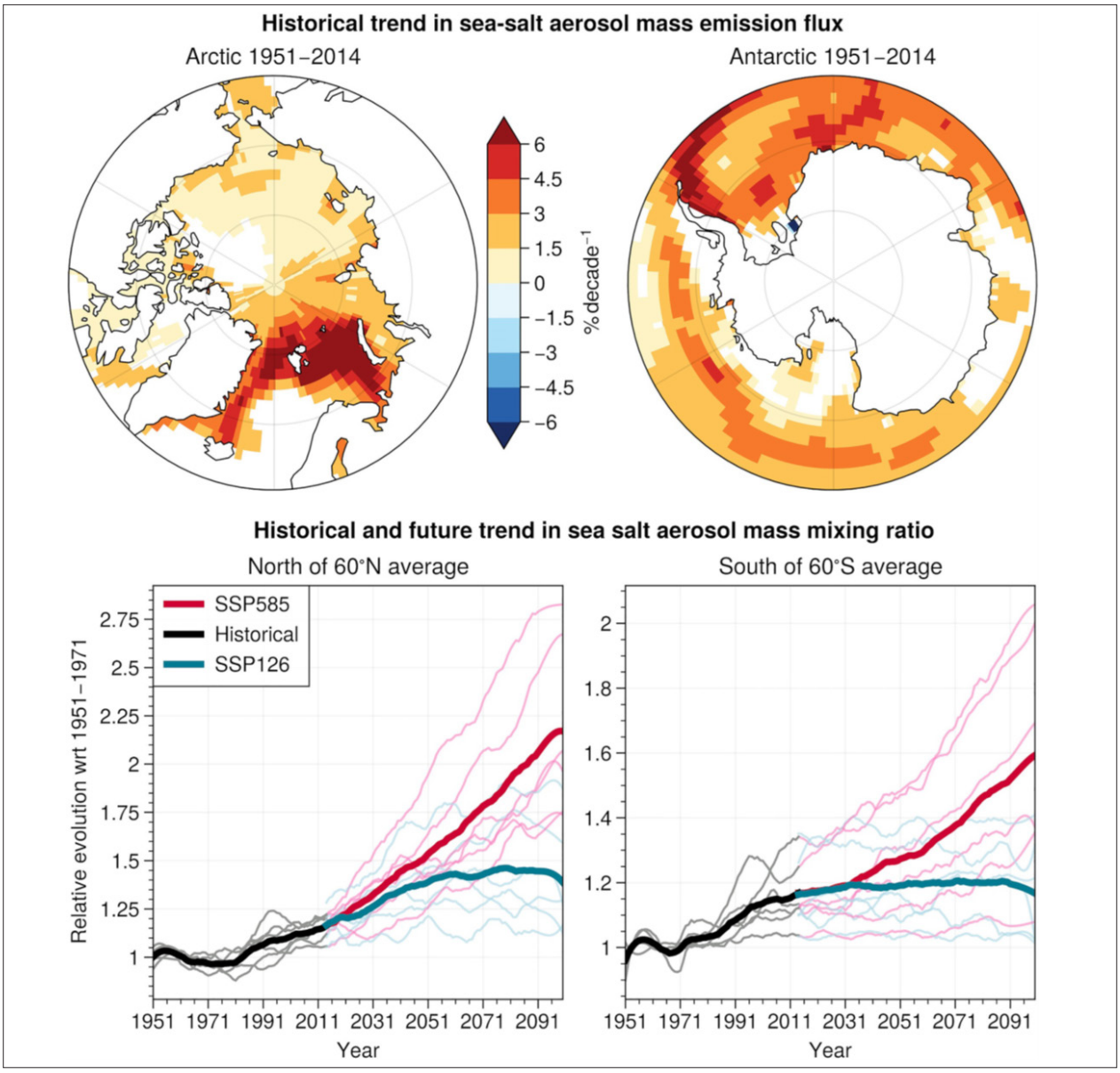

Figure 17. Figure from Lapere et al. (2023). Top: trends in sea salt aerosol mass emissions in the ensemble mean for the period 1951–2014. The mass emission is normalized by the 1951–2014 average to obtain %/decade. Bottom: historical and future (relative to the 1951–1971 mean) yearly time series (1951–2099) of average sea salt surface mass mixing ratio north of 60°N (left) and south of 60°S (right), including ocean and land. Mixing ratios are weighted by grid cell area for spatial averaging. Time series are smoothed using a Savitzky-Golay filter with a window length of 19 years and a polynomial order 3. Ensemble means are shown as thicker lines (black for the historical period, blue for SSP126, red for SSP585). Individual members use the same color code but with thinner lines. Included models are: GISS, HadGEM, MIROC-ES2L, MRI-ESM, NorESM and UKESM. The smallest (largest, respectively) trend in SSP585 corresponds to NorESM (UKESM, respectively). Reproduced under the Creative Commons 4.0 (CC 4.0) license.

Task 4.2: Observational constraints along the scale chain

The compilation and collection of data sets used and produced by FORCeS allows for the design of novel observational constraints that propagate over different scales – from process-level understanding to regional and global scale impacts. In addition, significant progress was made on the development of metrics and methodologies for observational constraints along the scale chain, including, but not limited to novel approaches to understand aerosol-cloud interactions and feedbacks in a regime-based context. In the following, we will give some highlights on the scientific work conducted so far within FORCeS that includes an element of moving over scale boundaries.

A study by Yli-Juuti et al. (2021) combined long-term in-situ observations of meteorological parameters, aerosol size distribution and chemical composition to collated remote sensing observations on cloud and aerosol properties, in order to study and quantify the feedback between temperature, aerosol loadings and cloud properties in the boreal region. Summertime OA loadings showed a clear increase with temperature (see also e.g. Heikkinen et al., 2021), with a simultaneous increase in CCN concentration in a boreal forest environment. Remote sensing observations revealed a change in cloud properties with an increase in cloud reflectivity in concert with increasing OA loadings in the area. The results provide direct observational evidence of the significance of this negative climate feedback mechanism. The study by Yli-Juuti et al. (2021) was followed up by Blichner et al. (2024) who combined the observational data from the boreal zone (SMEAR-II station) to corresponding data from the ATTO tower representing the atmosphere over a tropical forest environment, and satellite observations. Blichner et al. (2024) used these data to evaluate four of the ESMs used within FORCeS, and found substantial differences in how the models represent the key processes contributing to the biogenic VOC feedback cycle (see Fig. 18 for the response of aerosol particle number size distribution to OA).

When comparing the magnitude of this feedback between the different models, it was concluded that the weakest modelled feedback estimates can likely be excluded. However, the study also highlights that compensating errors make it difficult to draw firm conclusions regarding the strongest estimates. Overall, the method of evaluating along process chains shows promise in pin-pointing sources of uncertainty and constraining modelled aerosol feedbacks.

A new framework for the definition of dynamical regimes for cloud forcing and feedback studies has been developed (Douglas and Stier, 2021). This method is based on the analysis of global satellite datasets, objectively clustering cloud (parameter) controlling envi-ronmental factors derived from gradient boost regression and neural network machine learning models to determine the dominant combination of cloud controlling factors for each region. This approach provides a new way to control for confounding factors in the causal attribution of aerosol climate effects and feedback studies as well as a new way to evaluate the representation of clouds in ESMs. A complementary approach, attributing model-simulated ERF_{aci} to objectively clustered cloud regimes (based on k-means clustering in cloud-top-height/cloud optical depth space) has been developed and applied to the model UKESM (Langton et al., 2021).

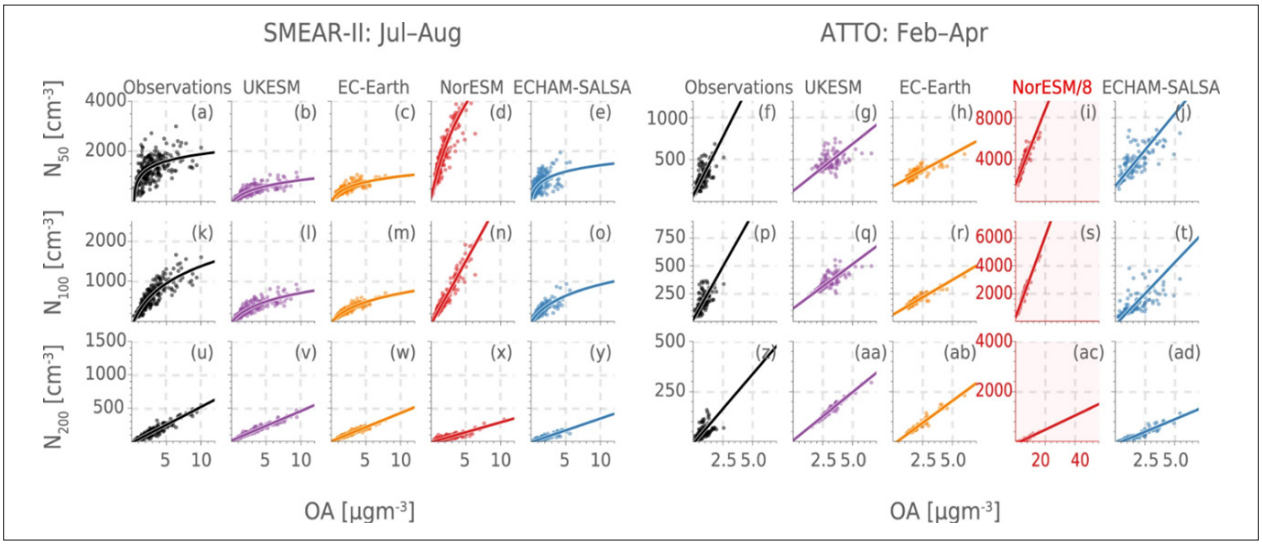

Figure 18. Figure from Blichner et al. (2024). The Station for Measuring Ecosystem-Atmosphere Relationships (SMEAR-II) in July–August is shown in the left panel in a–e (N50), k–o (N100) and u–y(N200) and the Amazon Tall Tower Observatory (ATTO) in February–April is shown in the right panels in f–j (N50), p–t (N100) and z–ad(N200). For ATTO, the size distribution measurements only go up to 500 nm, so we use the same intervals for the models. The lines show the least-square regression to a logarithmic function for N50 and N100 at SMEAR-II and the orthogonal distance regression to a linear function for all the others (ax + b) (see Methods for details). The regressions and their properties are summed up in Tables S1–S2 and the residuals for the regressions are shown in Figs. S21, S23, S25–S28. The equivalent figure, but with all regression lines linear is shown in Fig. S17 with residuals in Figs. S22 and S24. NB: For ATTO, the axis limits for NorESM are eight times those of the other plots (indicated by the red axis and background colour of the plot). Also note that for N100 at SMEAR-II, NorESM is shown with a linear fit because the regression did not converge for the logarithmic function. Reproduced under the Creative Commons 4.0 (CC 4.0) license.

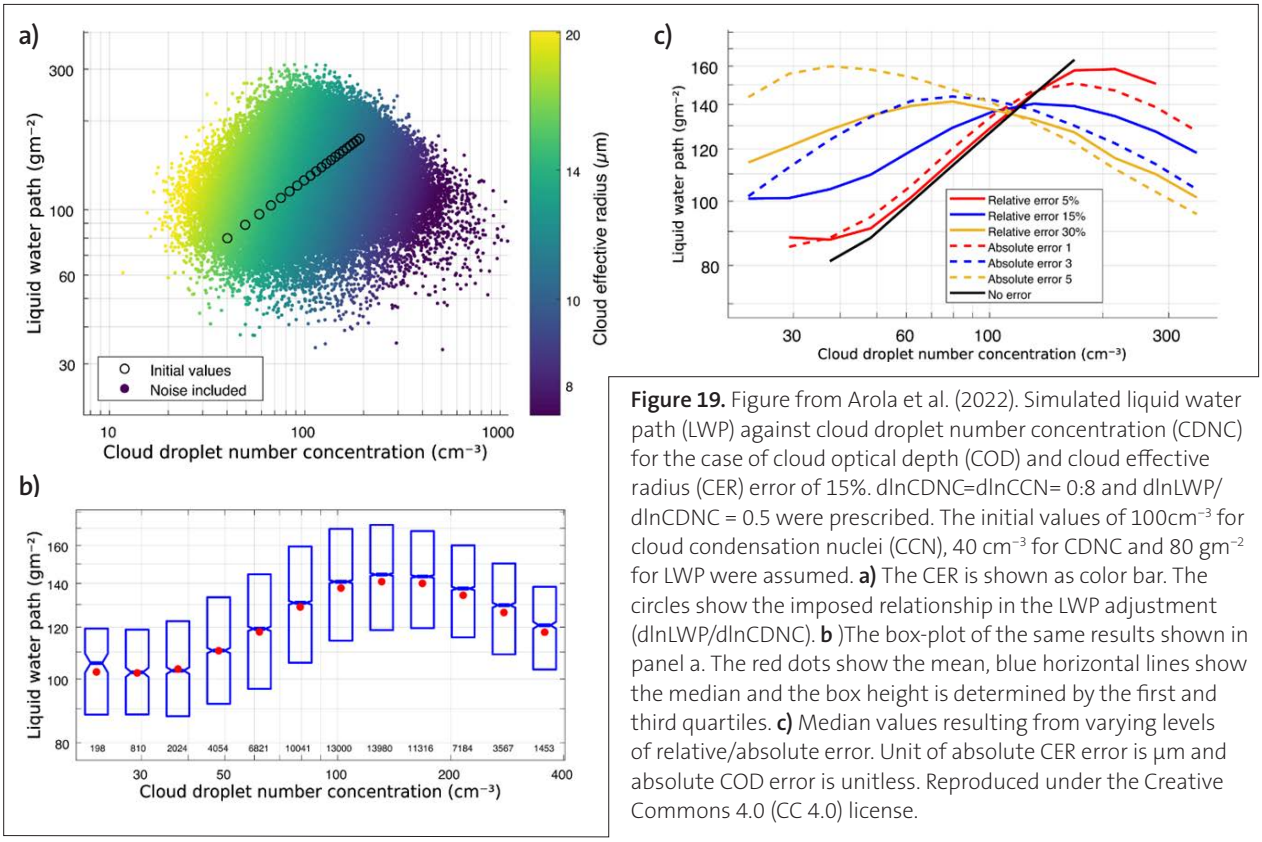

Figure 19. Figure from Arola et al. (2022). Simulated liquid water path (LWP) against cloud droplet number concentration (CDNC) for the case of cloud optical depth (COD) and cloud effective radius (CER) error of 15%. dlnCDNC=dlnCCN= 0:8 and dlnLWP/dlnCDNC = 0.5 were prescribed. The initial values of 100cm^{-3} for cloud condensation nuclei (CCN), 40 cm^{-3} for CDNC and 80 gm^{-2} for LWP were assumed. **a)** The CER is shown as color bar. The circles show the imposed relationship in the LWP adjustment (dlnLWP/dlnCDNC). **b**)The box-plot of the same results shown in panel a. The red dots show the mean, blue horizontal lines show the median and the box height is determined by the first and third quartiles. **c)** Median values resulting from varying levels of relative/absolute error. Unit of absolute CER error is μm and absolute COD error is unitless. Reproduced under the Creative Commons 4.0 (CC 4.0) license.

A review of our current understanding of observational constraints on the Twomey effect from satellite observations has been conducted (Quaas et al., 2020), highlighting underlying uncertainties in the quantification of (i) the cloud-active aerosol – the CCN concentrations at or above cloud base, (ii) cloud droplet number concentrations, (iii) the statistical approach for inferring the sensitivity of Nd to aerosol particles from the satellite data and (iv) uncertainty in the anthropogenic perturbation to CCN concentrations, which is not easily accessible from observational data. Arola et al. (2022), on the other hand, focused on the responses of LWP to aerosol and CDNC perturbations, and noted the importance of the propagation of natural spatial variability and errors in satellite retrievals of cloud optical depth and cloud effective radius to estimates of CDNC and LWP. To this end, Arola et al. (2022) used satellite and simulated measu-rements to demonstrate that, because of this propagation, even a positive LWP adjustment is likely to be misinterpreted as negative (see Fig. 19). This biasing effect would likely result in an underestimate of the aerosol-cloud-climate cooling. To follow up on this work, a study on the susceptibility of clouds to aerosol perturbations – utilizing the combination of in-situ and remote sensing techniques – is currently in preparation, but its' publication will unfortunately need to wait until the end of the formal project duration of FORCeS (Virtanen et al., *manuscript in preparation*)

Task 4.3: Natural and anthropogenic analogues of aerosol-cloud interactions

This task strived to establish a set of observations representative of different natural and anthropogenic analogues from satellite and in-situ data.

The work by Maahn et al. (2021), Gryspeerdt et al. (2021) and Herbert et al. (2021) focused on analysing cloud responses to well-constrained aerosol perturbations in different types of environments: industrial emissions to the clean Arctic atmosphere, emissions from ships to the marine boundary layer and biomass burning plumes in the Amazon (see also Sect. 5.2). As an example, Maahn et al., (2021) used anthropogenic emissions at the North Slope of Alaska as a natural laboratory to study relationships between aerosols and Arctic liquid-containing clouds. Averaging 14 years of MODIS satellite observations, a reduction in temporally averaged cloud effective radius (r_e) of up to 1.0 μm related to localized pollution was observed, with potentially significant implications for radiative forcing. Due to the frequent occurrence of liquid-containing clouds, this implies that enhanced local emissions in Arctic regions can impact climate processes.

Christensen et al. (2022) reviewed available satellite datasets and field campaigns to place these opportunistic experiments of aerosol influence on cloud microphysics. They found that based on the satellite data, cloud albedo perturbations were strongly sensitive to background meteorological conditions and LWP increases due to aerosol perturbations could generally not be concluded upon based on the data (in line with Arola et al., 2022). While they found these opportunistic experiments to have significantly improved process-level understanding of ACI, they also concluded that it remains unclear how reliably the relationships found can be scaled to the global level. Manshausen et al. (2022), on the other hand, took a closer look at ship tracks, leveraging from the fact that only a small fraction of the clouds polluted by shipping show ship tracks in satellite images. They showed aerosols emissions to lead to substantial changes in cloud properties even when no ship tracks were visible in satellite images (see Fig. 20). The study by Manshausen et al. (2022) indicated selection biases in previous studies of ship tracks, and found a strong LWP response to clouds to aerosols perturbations – which is its turn potentially indicates a higher climate sensitivity than observed temperature trends would otherwise suggest (see also Watson-Parris et al., 2022b), which discusses the importance of shipping regulations for climate).

Hakala et al. (2022 and 2023) used standard analysis methods of in-situ aerosol size distribution to yield novel insights on NPF and testing the applicability of the methods in varying environments. The former study focused on Beijing, where cumulative airmass exposure to anthropogenic emissions proved to be a useful concept to interpret the observation, and the latter on a site in Western Saudi Arabia and similarly highlighted the need for knowing the airmass history when interpreting field observations of NPF and growth.

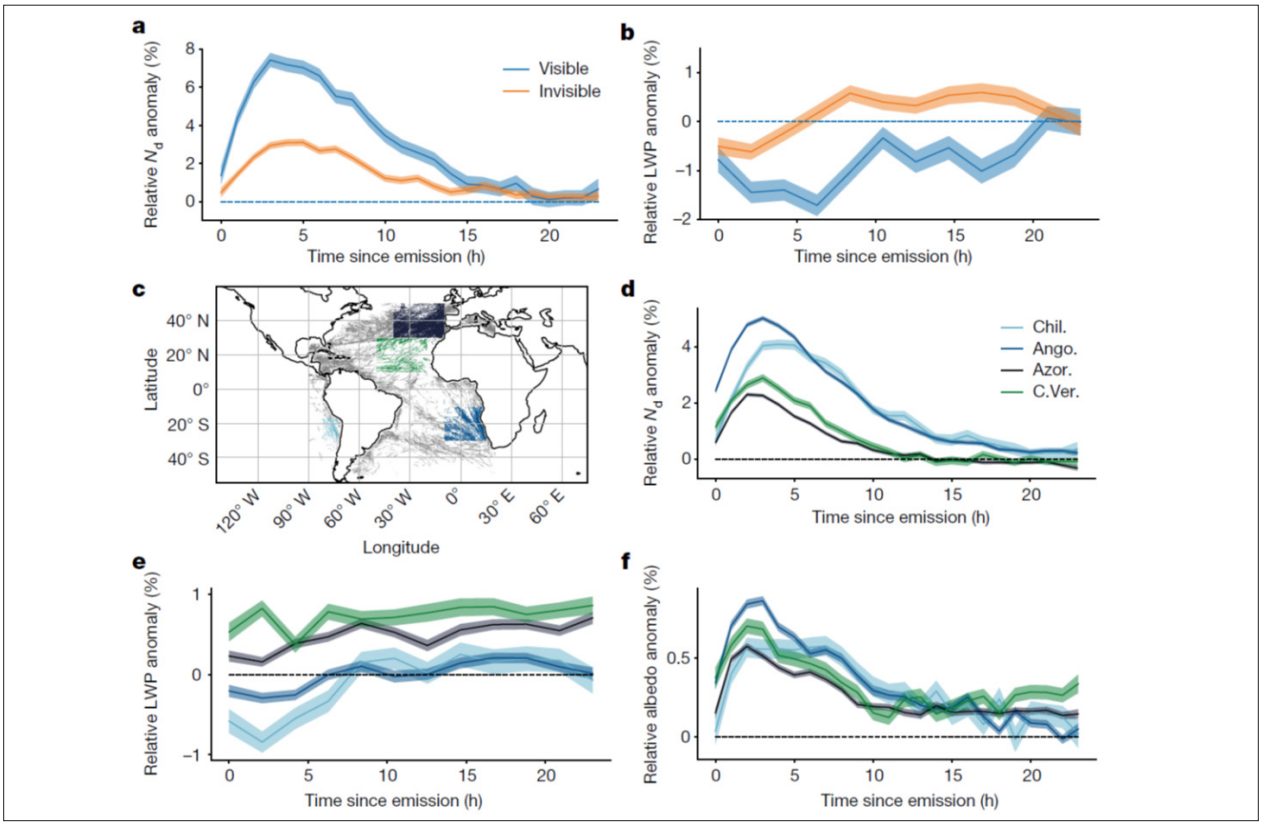

Figure 20. Figure from Manshausen et al. (2022). There are cloud property changes even when there are no visible tracks. a,b, Comparing Nd (a) and LWP (b) in the Chilean Sc between those days when ship tracks are visible (blue) and those when none are visible (orange) in the region. Plotted are ratios of hourly means of in-track and out-of-track properties, so that a value larger than 0% means an enhancement in the track. Shaded areas show standard errors of the means. LWP anomalies are given in 2 h means rather than 1 h because of noisier data. Retrievals from the MODIS-cloud product on Aqua and Terra, all for 2014–2019, 25% of days with visible tracks. Also, there are measurable responses to ship emissions everywhere.c, A plot of a comparison of in-track and out-of-track properties in four regions: the Chilean (Chil., light blue) and Angolan/Namibian (Ango., blue) Sc, and the Cu around the Azores (Azor., navy) and Cabo Verde (C.Ver., green). The regions are shown in different colours representing the ship track location data of around six days. d–f, Plots showing relative Nd (d), LWP (e) and albedo (f) anomalies. Shaded areas show standard errors of the means. Retrievals from the MODIS-cloud product on Aqua and Terra, all for 2014–2019. Reproduced under the Creative Commons 4.0 (CC 4.0) license.

Task 4.4 and 4.5: Observational constraints for the transient aerosol forcing record and decadal changes in aerosols and radiative forcing

These tasks are closely linked to Tasks 3.1–3.3 (see Sect. 5.3), so only highlights of studies with a substantial data dimension in terms of the long-term aerosol forcing record are provided here. The observational constraints applied within the FORCeS studies included both in-situ as well as remote sensing observations of aerosols, clouds and relevant atmospheric variables.

In their emulator study, Regayre et al. (2023) used radiative and physical properties of clouds as observed by the MODIS satellite as their key observational data set to constrain aerosol forcing. Quaas et al. (2022), on the other hand, used multiple lines of evidence in their analysis of the aerosol contribution to radiative forcing trends since the year 2000, including emissions from the Community Emissions Data System (CEDS), aerosol optical depth trends from satellites (MODIS and Metop-A), as well as ground-based sun photometer network AERONET. Andersen et al. (2022 and 2023) also used a combination of satellite products and reanalysis data sets in their investigations of the driving factors behind cloud properties. In Andersen et al. (2023), for example, the sensitivity of Cloud Radiative Effects (CREs) to selected Cloud Controlling Factors (CCFs) was analysed (see Fig. 21 for examples of CRE sensitivities of Sea Surface Temperature, SST).

Julsrud et al. (2022) used observational datasets of surface solar radiation (SSR) data between the mid-20th century and present-day obtained from GEBA (Global Energy Balance Archive) together with CRU TS cloud cover data set to evaluate CMIP6 models in terms of their ability to simulate global dimming and brightening trends (see also Sect. 5.3). Kok et al. (2023) combined 19 dust deposition records, with constraints on the modern-day dust cycle, reconstructing the evolution of global dust mass loading since pre-industrial times to evaluate climate models against (see also Sect. 5.5), and Leinonen et al. (2022) used the long-term in-situ observations of aerosol number size distributions from the ACTRIS network to evaluate the ability of five ESMs to describe aerosol microphysics (see Fig. 22).

As examples of long-term data sets combined and generated as part of FORCeS, one can mention the observations of fog trends and acidity in the Po Valley (Paglione et al., 2021) and the long-term trends in absorbing aerosols in the Arctic Zeppelin station as reported by Heslin-Rees et al. (2024) – both of which also demonstrate the importance of understanding the role of clouds and precipitation in determining aerosol trends.

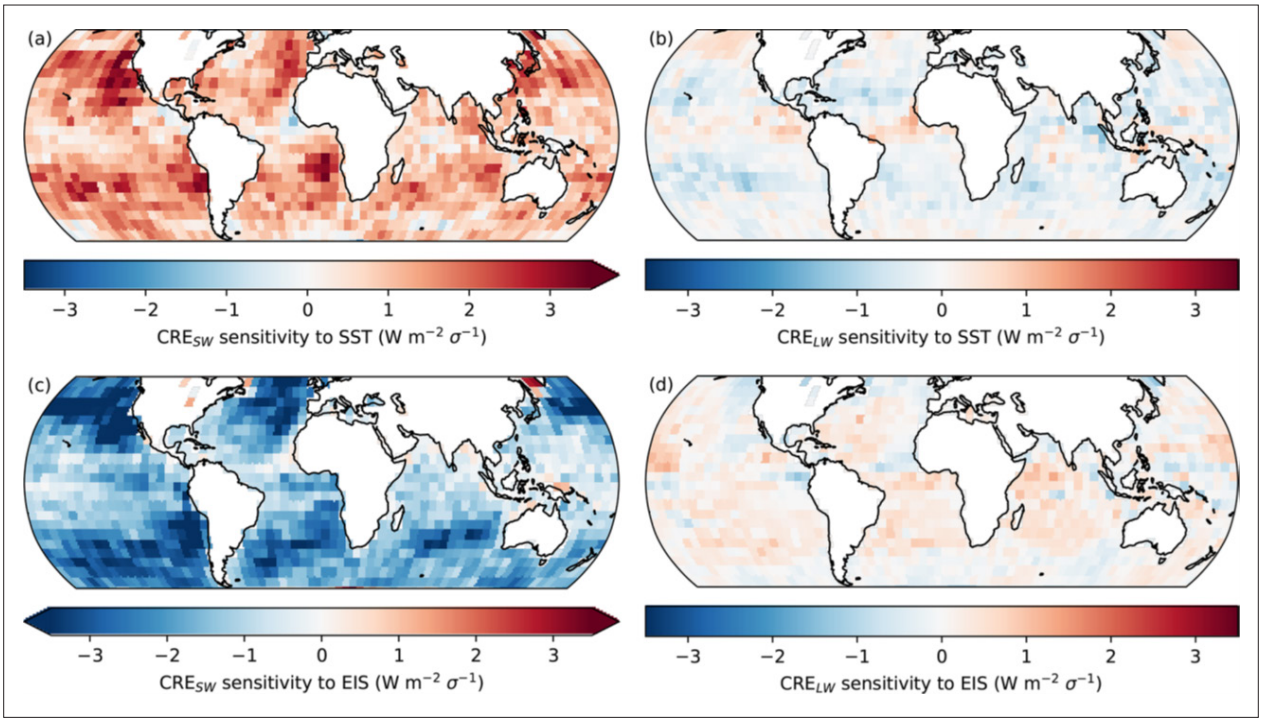

Figure 21. Figure from Andersen et al. (2023). Sensitivity of CRESW (a, c) and CRELW (b, d) to SST (a, b) and EIS (c, d). Reproduced under the Creative Commons 4.0 (CC 4.0) license.

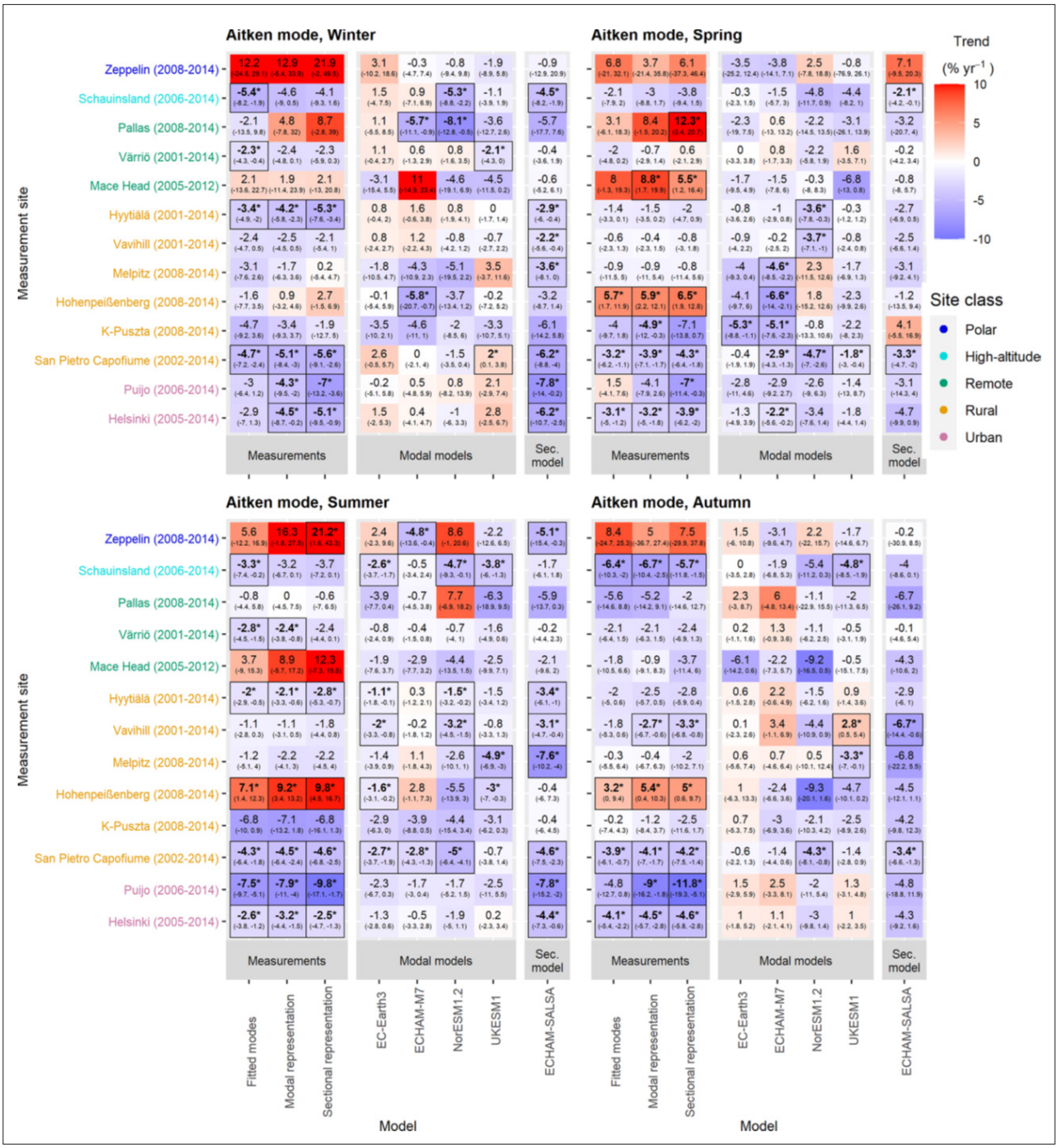

Figure 22. Figure from Leinonen et al. (2022). Seasonal trend estimates for Aitken mode number concentration for four seasons: winter (January, February, December), spring (March, April, May), summer (June, July, August), and autumn (September, October, November). Sites are ordered by site class and within site class most northerly to most southerly. Bold numbers, asterisks, and line borders around the estimate indicate that the trend is statistically significant (95% confidence level). Trends have been calculated using the Sen–Theil estimator and complemented with bootstrap confidence intervals. Reproduced under the Creative Commons 4.0 (CC 4.0) license.

Task 4.6: Community evaluation tools for aerosols and clouds in support of IPCC

In this Task, a new ESM evaluation package was developed and shared with the wider research community. The AeroCom/FORCeS evaluation package is a community tool and consists of two components: a public website, called AeroVal (*https://AeroVal.met.no/evaluation.php?project=FORCeS*) and an open-source python software package called pyaerocom (*https://pyaerocom.readthedocs.io/en/latest*). The AeroVal website allows dynamic insight into the evaluation results of the FORCeS models for expert users. The results comprise a variety of statistics on different spatial and temporal aggregation levels. The pyaerocom software is the backbone of this AeroVal evaluation visualisation and is used for quality assurance and to preprocess data and statistics for AeroVal, so that the web visualisation is reproducible and quick. Pyaerocom can also be used by interested aerosol scientists to retrace the evaluation and eventually produce their own model evaluation. The pyaerocom library is maintained via the open source github platform (*https://github.com/metno/pyaerocom*) and can be installed by anyone and used together with selected datasets, as described in the documentation.

5.5 Progress within WP5 "Climate response and feedbacks within ESMs"

Overall, the work within WP5 progressed according to the plan, and WP5 collaborated closely with WPs3 and 6 (see Sects. 5.3 and 5.6). The specific objectives of WP5 were to analyze simulated climate response, feedbacks and sensitivities to aerosol and cloud forcing in ESMs, quantify the simulated responses to specific key processes and their effects in regional focus areas, and improve the simulation of processes relevant for regional and global sensitivities. The predictions by ESMs before FORCeS, implementation of new parameterizations from WPs 1 and 2, their testing and analysis of the ESM results before making these implementations formed the hard core of this WP.

Task 5.1: Identification of relevant processes for response and feedbacks to aerosol and cloud forcing

The goal of this task was to analyse and better understand the role aerosols play in climate model simulations, in particular the CMIP6 experiments and with a special focus on the three FORCeS ESMs. Throughout the project, there has been substantial progress along these lines in the form of both multimodel studies (e.g. (Cherian and Quaas, 2020; Mortier et al., 2020; Turnock et al., 2020; Wyser et al., 2020; Gliß et al., 2021; Sand et al., 2021; Su et al., 2021; Dagan et al., 2022; Leinonen et al., 2022; Ahsan et al., 2023; Bergas-Massó et al., 2023; Fiedler et al., 2023; Kuma et al., 2023a; Lapere et al., 2023; Blichner et al., 2024), as well as detailed studies focusing on specific models (e.g. Krishnan et al., 2020; Lohmann et al., 2020; Dingley et al., 2021, 2023; Fiedler et al., 2021; Frey et al., 2021; Langton et al., 2021; Spill et al., 2021; Villanueva et al., 2021; Zhang et al., 2021; Braun et al., 2022; Dagan et al., 2022; Li et al., 2022; Myriokefalitakis et al., 2022; Slater et al., 2022; Regayre et al., 2023) – the results from many of which have already been discussed above. In the following, some further highlights from this work conducted so far are presented.

Su et al. (2021) analysed biases in AOD and land surface albedos in the AeroCom models, which manifest themselves in the top-of-atmosphere (TOA) clear-sky reflected shortwave (SW) fluxes. Biases in the SW fluxes from AeroCom models were quantitatively related to biases in AOD and land surface albedo by using their radiative kernels. It was found that over ocean, AOD contributes to about 25% of the 60S–60N mean SW flux bias for the multi-model mean (MMM) result. Over land, AOD and land surface albedo contributed to about 40% and 30%, respectively, of the 60S–60N mean SW flux bias for the MMM result. Su et al. (2021) also compared the AOD trend from three models with the observation-based counterpart. These models reproduce all notable trends in AOD except the decreasing trend over eastern China and the adjacent oceanic regions due to limitations in the emission data set (see also Krishnan et al., 2020, Moseid et al., 2020, 2022 and Section 5.3).

Turnock et al. (2020) analysed the key air pollutants, specifically O_3 and $PM_{2.5}$ predicted for years 2000–2014 and projected for the near-future of years 2015–2100 by 11 models participating in CMIP6. An evaluation of these models against surface observations of O_3 and $PM_{2.5}$ reveals that the CMIP6 models consistently overestimate observed surface O_3 concentrations across most regions and in most seasons by up to 16 ppb, with a large diversity in simulated values over Northern Hemisphere continental regions. Conversely, observed surface $PM_{2.5}$ concentrations are consistently underestimated in CMIP6 models by up to 10 µg m^{-3}, particularly for the Northern Hemisphere winter months, with the largest model diversity near natural emission source regions. When compared to observations of O_3 and $PM_{2.5}$ the biases in CMIP6 models are similar to those found in previous studies. The projection of regional air pollutant concentrations from the latest climate models and ESMs

used within CMIP6 shows that the particular future trajectory of climate and air quality mitigation measures could have important consequences for regional air quality, human health and near-term climate (see also Allen et al., 2020 for a detailed discussion). Differences between individual models emphasize the importance of understanding how future Earth system feedbacks influence natural emission sources, e.g. response of biogenic emissions under climate change. This result is corroborated by the study by Blichner et al. (2024) (see Sect. 5.4).

Wyser et al., (2020) investigated the reasons behind warmer climate projections for the 21st century in CMIP6 than in CMIP5 despite nominally identical instantaneous radiative forcing. The stronger warming in the CMIP6 projections has typically been attributed to the higher climate sensitivity of the new generation of climate models. However, Wyser et al. (2020) demonstrate that changes in the forcing datasets also can play an important role, in particular the prescribed concentrations of greenhouse gases (GHG) that are used to force the models. In the EC-Earth3-Veg model the ERF was reduced by 1.4 W m^{-2} when the GHG concentrations from SSP5-8.5 (used in CMIP6) are replaced by the GHG concentrations from RCP8.5 (used in CMIP5), and similar yet smaller reductions are seen for the SSP2-4.5/RCP4.5 and SSP1-2.6/RCP2.6 scenario pairs. Wyser et al. (2020) also tested whether the additional forcing caused by the changes in GHG concentrations from CMIP5 to CMIP6 is possibly compensated by other changes in the SSP forcing datasets, in particular a stronger cooling from CMIP6 aerosols. There was, however, only a minor impact on the ERF in EC-Earth3-Veg.

Previous work using NorESM1-M has shown that decreases in regional SO_2 emissions lead to three key responses – an enhanced temperature response in the Arctic, a weakening of the Atlantic Meridional overturning circulation (AMOC), and anomalous poleward heat transport from the sub-polar North Atlantic into the Arctic. To better understand the enhanced temperature response, we have analyzed simulations using NorESM1-M in a slab-ocean mode (Krishnan et al., 2020). These simulations showed that the atmosphere plays the primary role in driving Arctic warming in response to European aerosol reductions. A key mediator of the temperature response is a change in sea-ice extent, through modifications of turbulent flux exchanges and surface temperature. A good representation of Arctic sea ice is therefore vital for confident projections of future Arctic climate change. Further, the key to understanding this Arctic response is to constrain the specific atmospheric processes and feedbacks that drive the initial sea-ice melt. Dagan et al. (2020), on the other hand, studied the impact of aerosol forcing on the North Atlantic Warming Hole (NAWH, i.e. the reduced warming, or even cooling, of the North Atlantic during an anthropogenic-driven global warming). A NAWH is predicted by climate models during the 21st century, and its pattern is already emerging in observations. Using output from CMIP6 simulations, Dagan et al. (2020) show that anthropogenic aerosol forcing opposes the formation of the NAWH (by leading to a local warming) and delays its emergence by about 30 years. In agreement with previous studies, they also demonstrated that the relative warming of the North Atlantic under aerosol forcing is due to changes in ocean heat fluxes, rather than air-sea fluxes. These results suggest that the predicted reduction in aerosol forcing during the 21st century may accelerate the formation of the NAWH. Much of the past aerosol forcing has been due to sulfate aerosol, which is among the better-studied anthropogenic aerosol components. Some issues remain, however, even in the description of this core component within state-of-the-art ESMs: Ahsan et al. (2023) analyse the simulations contributing to Emissions-MIP, and, based on their results, articulate the need to ensure that anthropogenic emission injection height and SO_4 emission fraction are accurately and consistently represented in global models.

Several of the studies conducted within the second half of FORCeS highlight the importance of improving the representation of dust (Bergas-Massó et al., 2023; Kok et al., 2023). As an example, Figure 23 shows the comparison between the dust loading reconstruction made based on 19 different data sets and CMIP6 models, illustrating the underestimation of the dust loadings.

Finally, it is evident that simulating aerosol-cloud -interactions (ACI), is still probably the single most important issue when it comes to the ability of ESMs to describe aerosol radiative forcing. Fiedler et al. (2023) investigated the factors driving model differences, concluding that cloud-mediated effects dominate the aerosol ERF in the present day, noting however the compensating effects of absorbing aerosol (see also Williams et al., 2022). They therefore conclude the need to revising also the optical properties and long-range transport of aerosols in ESMs. Several studies within FORCeS have also identified the need to improve the description of convection in global models (e.g. Dingley et al., 2021, 2023; Braun et al., 2022; Dagan et al., 2022). Finally, a key requirement for capturing ACI is a reasonable representation of the aerosol size distribution (Leinonen et al., 2022; Hodzic et al., 2023) – naturally together with the meteorological drivers such as updraft velocities (Andersen et al., 2022, 2023).

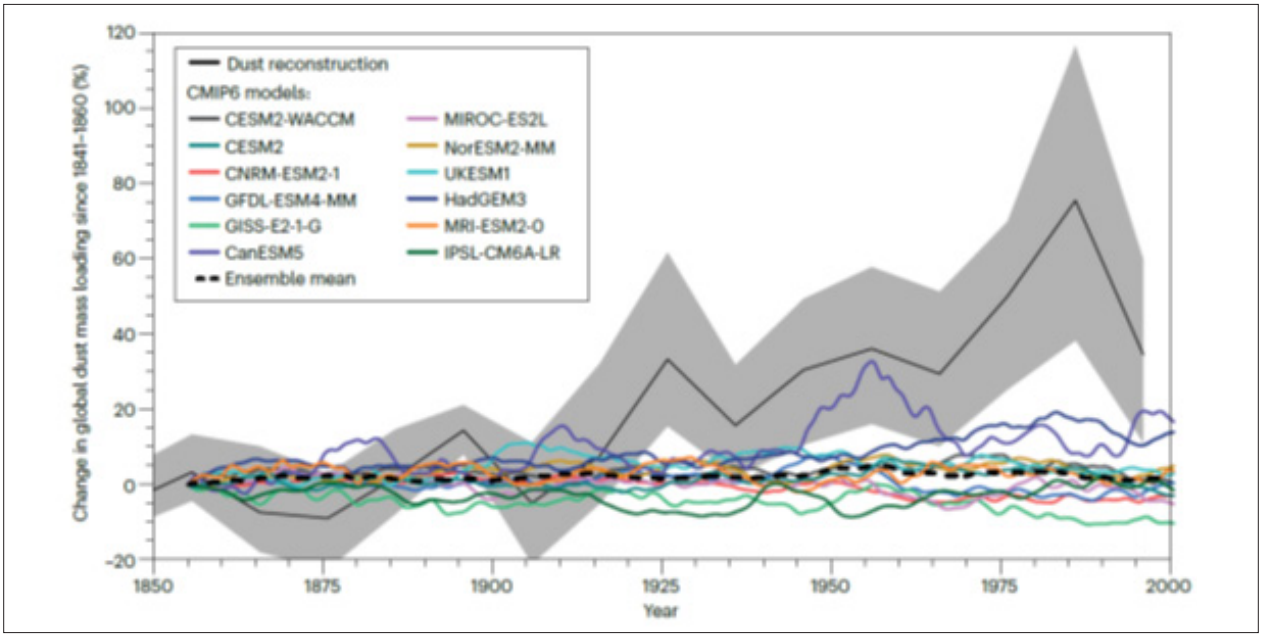

Figure 23. Figure from Kok et al. (2023). Climate model representations of historical changes in dust loading. Changes in global dust loading relative to 1841–1860 from the dust reconstruction (solid black line) and 12 CMIP6 models with prognostic dust aerosol cycles (coloured lines, and dashed black line for the ensemble mean). CMIP6 data are 10-year running means from historical runs. Grey shading denotes the 90% confidence interval for the dust reconstruction. All models and the ensemble mean fail to reproduce the large historical increase in dust loading. Reproduced under the Creative Commons 4.0 (CC 4.0) license.

Task 5.2 och 5.3: Implementation of revised parameterizations and their effects in ESMs

Table 1 outlines the process improvements that were implemented to the ESMs participating in FORCeS. While the publication of many of these results is still in progress, in the following, we highlight some studies that give some preliminary implications of the importance of these updates.

Milousis et al. (2024) implemented ISORROPIA-lite (see Sect. 5.1) into EMAC with separate treatments for both fine and coarse aerosol modes, and evaluated the model against surface measurements from three regional

Table 1. Process improvements implemented to FORCeS ESMs. The last row refers to the simplifications proposed by Proske et al. (2022, 2023).

Process	FORCeS models		
	EC-Earth3-AerChem	NorESM2-LM	MPI-ESM1.2-HAM
Inorganic aerosol partitioning	x	–	–
Droplet activation	x	x	–
New particle formation (NPF) and improved size distribution	–	x	–
Black (BC) and brown carbon (BrC) (a) implementation of complex BC morphology (b) BrC and BC absorption	a) – b) x	–	a) x b) –
Dust mineral composition and its optical properties	x	–	–
Ice Nucleation from dust	x	–	–
Secondary ice production (SIP)	x	x	x
Prognostic cloud fraction scheme	–	–	x
Sea spray	x	x	–
Cloud microphysics	–	–	x

observational networks in the polluted Northern Hemisphere (Interagency Monitoring of Protected Visual Environments (IMPROVE), European Monitoring and Evaluation Programme (EMEP), and Acid Deposition Monitoring Network of East Asia (EANET). ISORROPIA-lite was shown to agree well with the more sophisticated versions of ISORROPIA (see also Kakavas et al., 2022). The differences between ISORROPIA II v2.3 and ISORROPIA-lite were minimal in all comparisons with the normalized mean absolute difference in concentrations of major aerosol components being less than 11%. The most notable differences were lower aerosol concentrations predicted by ISORROPIA-lite in regions with relative humidity in the range of 20% to 60% compared to the predictions of ISORROPIA II v2.3. The use of ISORROPIA-lite accelerated EMAC by nearly 5% compared to the use of ISORROPIA II v2.3. The agreement between the model predictions and observations were deemed satisfactory especially over the United states while nitrate was overestimated by the model over East Asia (see Fig. 24).

One of the outcomes from WP1 in terms of improvements in the description of absorbing aerosols, with relevance for also ice nucleation, was the development of dust mineral composition description. Gonçalves Ageitos et al. (2023) introduced the explicit mineralogy representation within the state-of-the-art Multiscale Online Nonhydrostatic AtmospheRe Chemistry (MONARCH) model. They compared two existing soil mineralogy datasets, which remain a source of uncertainty for dust mineralogy modeling and provided an evaluation of multiannual simulations against available mineralogy observations. The simulations broadly reproduced the most abundant mineral fractions independently of the soil composition data used. Feldspars and calcite were highly sensitive to the soil mineralogy map, mainly due to the different assumptions made in each soil dataset to extrapolate a handful of soil measurements to arid and semi-arid regions worldwide. In terms of climate-related variables, the changes in underlying soil mineralogy affected in particular the regional variability of the single-scattering albedo at solar wavelengths or the total iron deposited over oceans (see Fig. 25).

As described above, the studies by Proske et al. (2022 and 2023) focused on the systematic simplification of cloud microphysics and aerosol processes. Proske et al. (2023) continued the work started by Proske et al. (2022) and used PPEs to explore potential simplifications, finding e.g., heterogeneous freezing or secondary ice production to be potentially drastically simplifiable. The simplifications were implemented in ECHAM-HAM and the results compared to the more complex model variants (see Fig. 26 for an example). Depending on one's modeling vision one may interpret this study's findings as pointing to simplification potential in the cloud microphysics scheme or the need for process representation improvements where the model behavior does not tally with our physical understanding – given that the simplification suggestions were made based on present models with potential structural uncertainties.

5.6 Progress within WP6 "Constraining climate sensitivity and near-term climate response"

WP6 identified and evaluated observable quantities that govern the transient climate response (TCR), which is the standard measure of transient climate sensitivity (TCS) in ESMs. WP6 also combined this work with statistical and simple/idealized modelling to arrive at a new central estimate and narrower uncertainty range for TCR/TCS, as well as a re-evaluation of the emission reductions needed to meet the PA. Another important task of WP6 was to use existing and develop new emergent constraints to evaluate the FORCeS models.

WP6 has analyzed TCR and ECS in CMIP6 models, developed new emergent constraints using e.g. network analysis, and conducted studies providing insights into what can be learned from simulations from models with different strengths, weaknesses and technical implementation. Finally, simple models have been used to address and communicate key new insights about the role of aerosols in the time evolution of climate response and its implications for policy.

Task 6.1: Evaluate FORCeS ESMs at the beginning of the project (transient climate response and emergent constraints)

In first half of the project, the TCR of FORCeS ESMs as well as their performance with respect to established emergent constraints was evaluated and shared with the consortium through D6.1 (see also Schlund et al., 2020; van Noije et al., 2021). Of relevance for this task was also work following up on studies using previous generation models (CMIP5, as in Grose et al. 2018) by investigating the relationship between different measures of climate sensitivity, primarily Equilibrium Climate Sensitivity (ECS) and TCR, in CMIP6 models, and their respective "predictive power" of future temperature projection. As in CMIP5, the sensitivity measures are

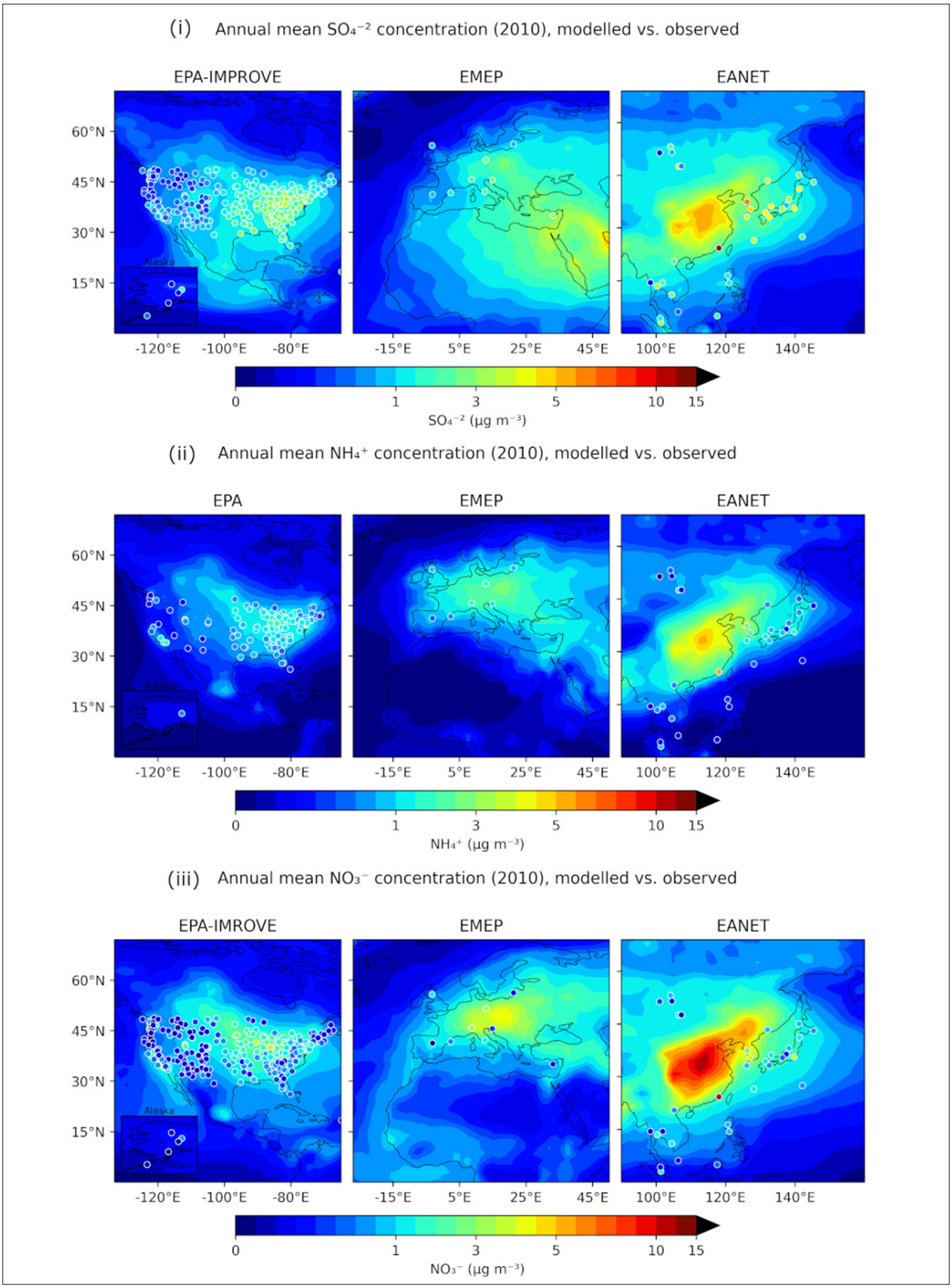

Figure 24. Figure from Milousis et al. (2024). Annual mean surface concentrations of PM2.5 for (i) SO4 (ii) NH3 and (iii) NO3 as simulated by EMAC using ISORROPIA-lite (shaded contours) versus observations of the same species from the IMPROVE, EMEP and EANET networks (colored circles). Reproduced under the Creative Commons 4.0 (CC 4.0) license.

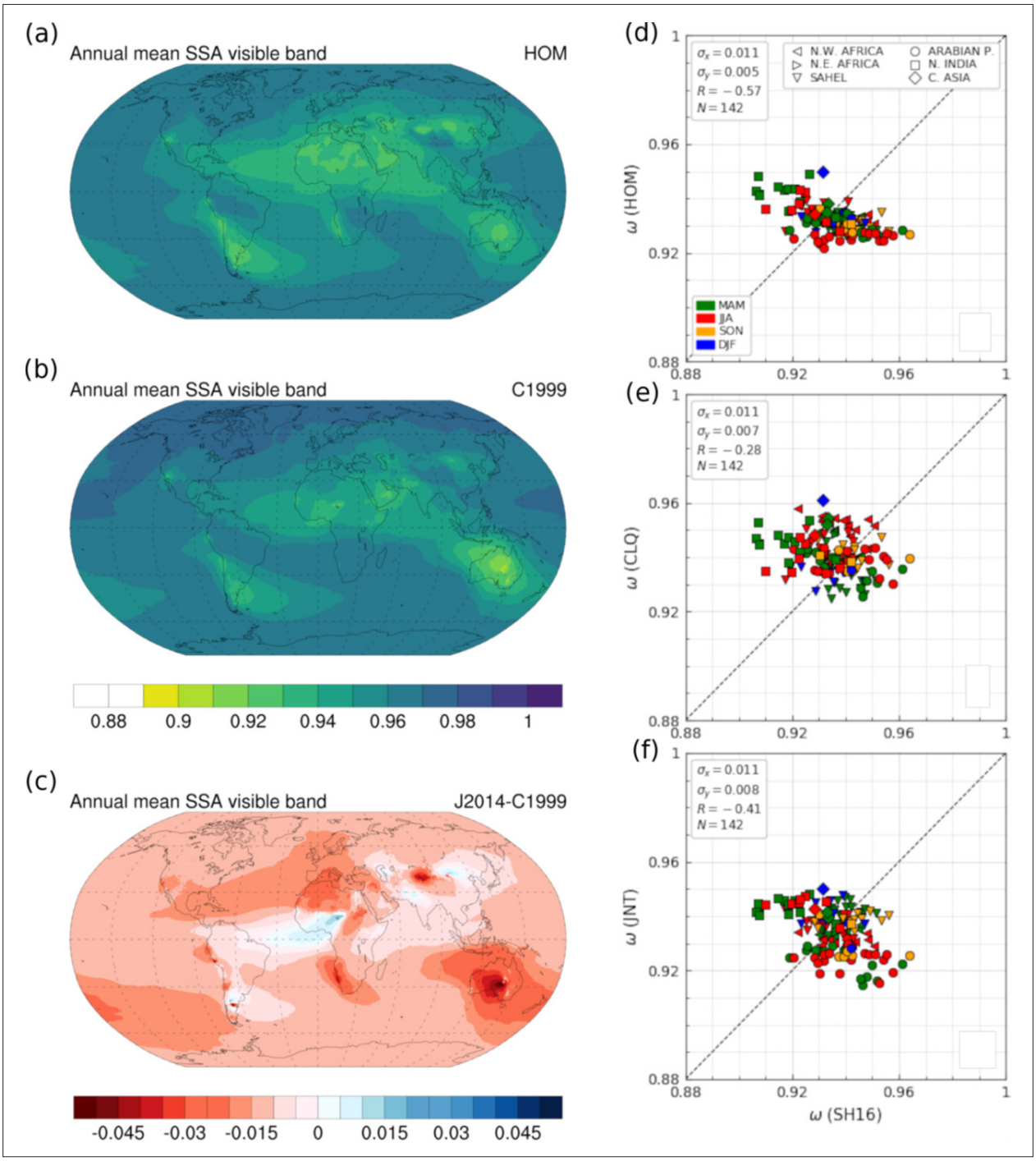

Figure 25. Figure from Gonçalves et al. (2023). Annual mean single-scattering albedo (SSA), averaged in the UV-VIS band (0.3–0.77 µm), considering dust to be an optically homogeneous species (a), as the sum of three optically different species using (b) C1999-modeled mineralogy. Differences between the latter and (c) J2014-modeled mineralogy. Comparison of monthly mean UV-VIS SSA, calculated considering dust to be a homogeneous species (d), and the mineralogy provided by C1999 (e) and J2014 (f) against dust-filtered SSA (averaged in the UV-VIS band) from AERONET version-3 level-2.0 Almucantar retrievals at the selected AERONET stations and months, labeled by region and season. Reproduced under the Creative Commons 4.0 (CC 4.0) license.

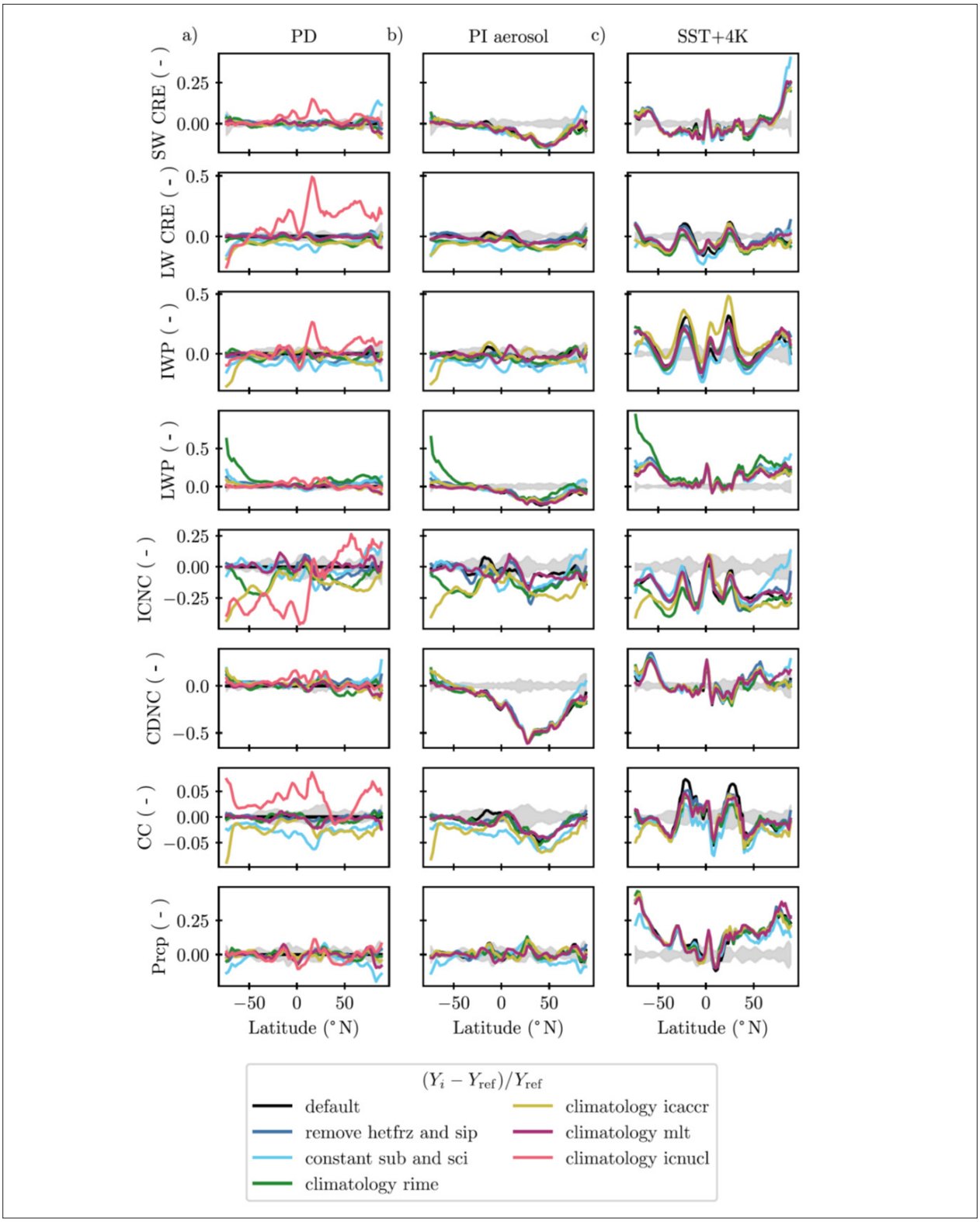

Figure 26. Figure from Proske et al. (2023). Relative deviations of the simplified model versions from the default in terms of the zonal 5 years mean (variables vertically integrated where applicable) for (a) Present day (PD), (b) Pre-industrial (PI) conditions (PI aerosol emissions), and (c) possible future conditions (realized with a 4 K increased sea surface temperatures). The gray shading indicates the inter-annual variability of the PD default simulation. Process labels are explained in Table 1, and variables in B1 in Appendix B of Proske et al. (2023). Note that the southernmost latitudes are excluded in this Figure as their small absolute values cause deceptively large relative deviations. Reproduced under the Creative Commons 4.0 (CC 4.0) license.

correlated, and they correlate with the projected temperature anomaly, but for CMIP6 models the transient measure TCR is a better predictor of the model projected temperature change from the pre-industrial state, not only on decadal timescale but throughout much of the 21st century. For strong mitigation scenarios, the difference persists until the end of the century. Regional analysis shows a superior predictive power of ECS over TCR during the latter half of the 21st century in areas with slow warming, illustrating that although TCR is a better predictor of warming on a global scale, it does not capture delayed regional feedbacks, or pattern effects. The transient warming at CO_2 quadrupling (T140) was consequently found to be correlated with temperature anomaly for a longer time than TCR. T140 also best describes the pattern of regional temperature anomaly at the end of the century. These results were of use in the continued work on emergent constraints on climate sensitivity, as a guide to what measure of sensitivity is actually the most meaningful to constrain, depending on the time period in focus. The findings were summarized in Huusko et al. (2021).

Task 6.2: Develop new metrics for ESM evaluation with the goal of "getting the right answer for the right reason"

In a step towards new ways of evaluating, and constraining models and their cloud feedback and thereby sensitivity, Task 6.2 has partly focused on the "too-few-too-bright" problem, i.e. that models tend to produce clouds that cover less area, and are more reflective than suggested by observations, and by compensating errors arrive at a reasonable TOA radiative effect. Using a compilation of several historical satellite data sets (CLARA-2A, Cloud_cci, PATMOS-x, MODIS and CERES) (Kuma et al., 2023a) found that this bias is present for clouds over the ocean across latitudes, and persists in both CMIP5 and CMIP6 models. The results indicate that models with smaller combined biases in cloud fraction, and cloud brightness, and distributions therein, are at the higher end of the sensitivity range (Fig. 27, Kuma et al., 2023a).

Kuma et al. (2023b) presented a full reconstruction of CMIP3, CMIP5, and CMIP6 code genealogy of 167 atmospheric models, GCMs, and ESMs (of which 114 participated in CMIP) based on the available literature, with a focus on the atmospheric component and atmospheric physics. They identified 12 main model families and proposed family and ancestry weighting methods designed to reduce the effect of model structural dependence in multi-model ensembles (MMEs). They further analyzed weighted ECS, (see Fig. 28), climate feedbacks, forcing, and global mean near-surface air temperature, and how they differ by model family. Models in the same family often had similar climate properties. Weighting could partially reconcile differences in ECS and cloud feedbacks between CMIP5 and CMIP6.

Another part of Task 6.2 has been dedicated to optimizing the usage of network analysis, specifically the δ-Maps method, as a "workhorse" to build climate networks from aerosol-cloud interaction and climate model simulations and evaluate them using a series of network metrics. The method has been used to evaluate the CMIP5/CMIP6 historical runs simulated by the three FORCeS ESMs in order to get the "past performance" of the simulated sea surface temperatures (SST) against the "ground truth" from reanalysis. The purpose was to quantify model biases and to characterize the internal variability of simulations, by representing different metrics of simulated and observed networks in metric spaces (Ricard et al., manuscript in review).

Task 6.3: Re-evaluate FORCeS ESMs with respect to climate sensitivity – what are the implications for near-term climate evolution?

As described above, several new and complementary approaches to constraining ECS and TCR have emerged from FORCeS (see e.g. the work by Kuma et al., 2023a, 2023b and Ricard et al. *manuscript in review* described in the previous section). Besides the studies described above, there are at least three independent assessments of ECS and TCR currently ongoing (Yuan et al. *to be presented in EGU GA 2024*; Skeie et al., *manuscript in preparation* and Che and Storelvmo, *manuscript in preparation*), but not yet published, using slightly different approaches for constraining them. Preliminary results from these studies have been summarized in a deliverable report shared with the consortium. An overall assessment of the selection of these studies and their implications for climate sensitivity is ongoing and will be summarized in an extra policy brief that will appear slightly after the formal project end of FORCeS. The preliminary results tend to suggest that even the higher end of the plausible climate sensitivity range provided by IPCC AR6 cannot be ruled out.

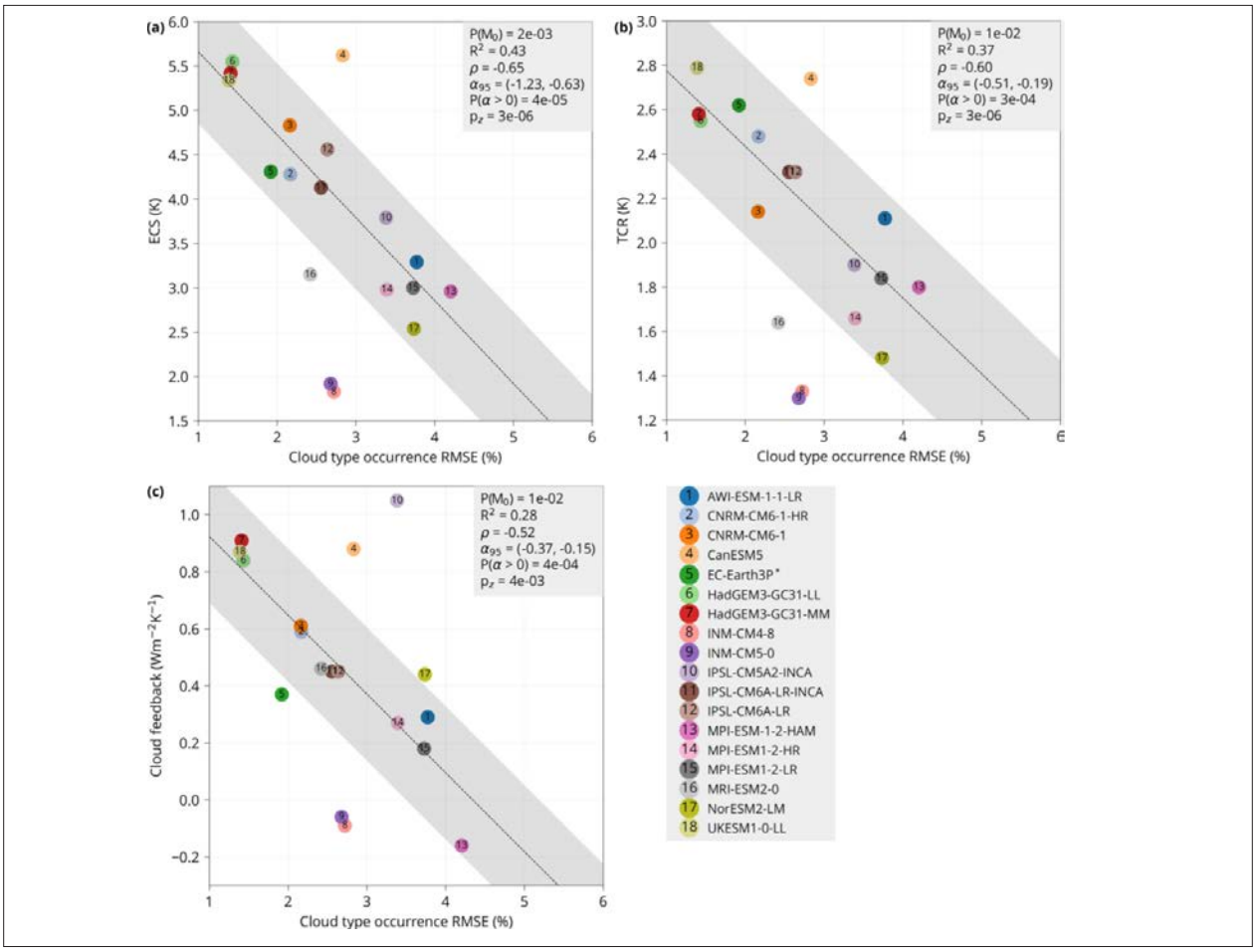

Figure 27. Figure from Kuma et al. (2023a). (a) Dependence of ECS, (b) transient climate response (TCR) and (c) climate feedback of CMIP6 models on the model total cloud type root mean square error (RMSE) relative to CERES, calculated from the geographical distribution (as in Fig. 6). The points are calculated from the ANN for 27 cloud types. Confidence bands represent the 68% range. Linear regression is calculated using Bayesian simulation assuming a Cauchy error distribution (Appendix A). Shown is also the probability of the null hypothesis model P(M0) (explained in Sect. 4.6), the coefficient of determination (R2), the correlation coefficient (ρ), the 95% confidence interval of the slope (α_{95}) of the linear regression, the probability that the slope is greater than zero $P(\alpha > 0)$ and the p value of a z test (pz) for the difference in the means of two groups of models in the bottom 50% and top 50% of ECS (a), TCR (b) and cloud feedback (c). For some models, marked with "*", ECS was not available and was taken from a related available model (see Table 1). Reproduced under the Creative Commons 4.0 (CC 4.0) license.

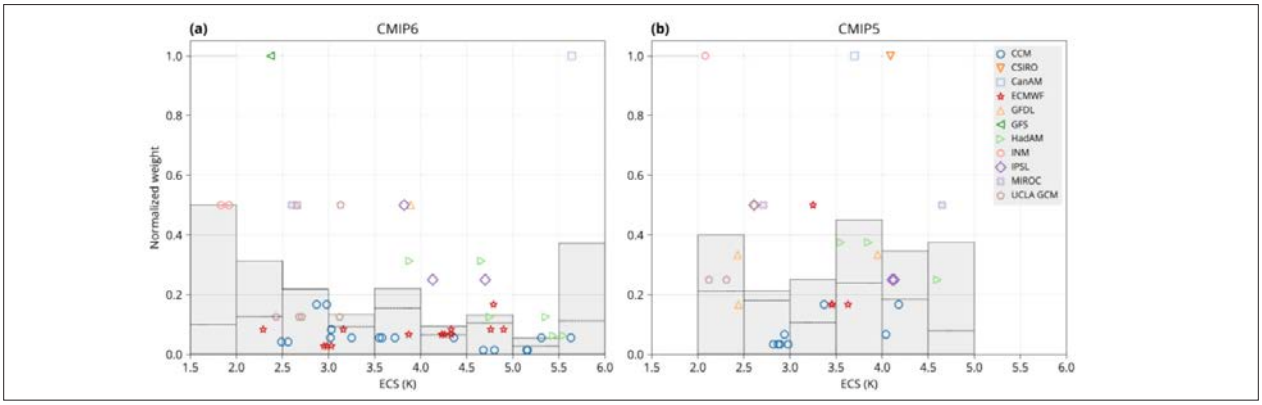

Figure 28. Figure from Kuma et al. (2023b). Statistical weights and effective climate sensitivity (ECS) of models in the Coupled Model Intercomparison Project (CMIP) phases 6 (a) and 5 (b) under the ancestry weighting. The model weights are normalized so that the maximum value is 1.0. The models are classified by their family, indicated by symbols. The shaded bars show a simple mean of model weights in the corresponding range of ECS. The dashed lines show the same as the bars, but multiplied by the number of models in the ECS range and normalized to sum to one. Reproduced under the Creative Commons 4.0 (CC 4.0) license.

Task 6.4: Link aerosol forcing to peak warming by using statistical methods/simplified models

This Task focuses on understanding the consequences of the special features of aerosol-driven radiative forcing as compared with the well-mixed GHGs for the time-dependent evolution of the climate system and the policy measures required for reaching the targets of PA. The key methodologies used were simplified representations of the policy-climate system, using statistical models, climate model outputs and simple climate models – particularly the FaIRv2.0 model (Jenkins et al., 2023a, 2023b). In the first half of the project, the Task piloted with studies that applied the simplified methodologies for analysing the usefulness, costs and relevant metrics for a "two-basket" approach in emission climate change mitigation – where cumulative and long-lived climate pollutants could be accounted for separately in policy discourse and global stocktake (Allen et al., 2021; Cain et al., 2021). During the second half of the project, studies that were more focused on the time evolution of aerosol emissions, their radiative effects and the associated interlinkages to policy were conducted in the context of this task.

Jenkins et al. (2022) used a large ERF ensemble from the IPCC's AR6 to attribute the anthropogenic contributions to global mean surface temperature (GMST), and top-of-atmosphere radiative flux. They used aerosol optical depth observations and concluded the GMST trend having increased between 2000-2009 and 2010–19, coinciding with the anthropogenic warming trend. This, as well as observed trends in top-of-atmosphere radiative fluxes and aerosol optical depths, supports the claim of an aerosol-induced temporary acceleration in the rate of warming. However, all three observation datasets additionally suggest that smaller aerosol ERF trend changes are compatible with observations since 2000, since radiative flux and GMST trends are significantly influenced by internal variability over this period (see also Quaas et al., 2022).

Jenkins et al. (2023b) studied the impact of the Hunga-Tonga H'aapai (HHTH) volcanic eruption on short-term climate evolution using the SOCRATES radiative transfer model together with ERA5 meteorology. Temperature response was calculated with the FaIR v2.0 simple climate model. This study found that the eruption had a notable impact on the short-term probability of the exceedance of 1.5°C, but ambition of emission reduction dominated on the long-term (Fig. 29).

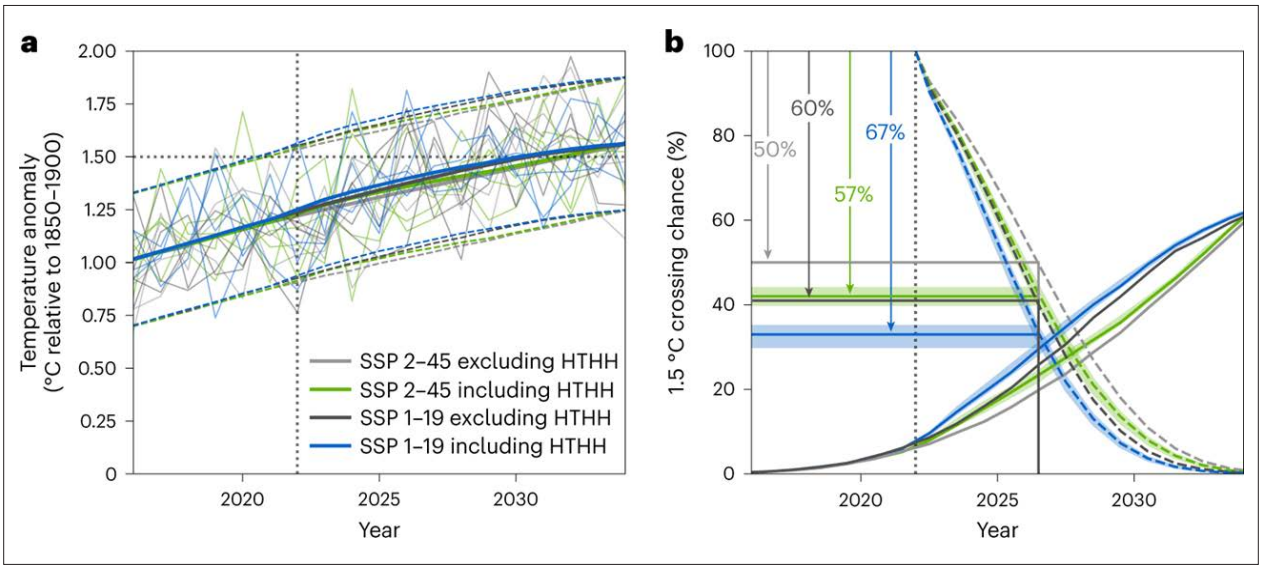

Figure 29. Figure from Jenkins et al. (2023b). Impact of the 2022 HTHH eruption on projected global average surface temperature anomaly between 2015 and 2035. HTHH eruption occurs in 2022 (vertical dotted lines). **a)** The temperature anomaly relative to 1850–1900 calculated with FaIR v.2.0 and best-estimate climate response parameters for two SSP scenarios (SSP 2–45, current policy trajectory; and SSP 1–19, ambitious mitigation pathway), both including (green/blue for SSP 2–45/SSP 1–19) and excluding (light/dark grey for SSP 2–45/SSP 1–19) the estimated forcing response to the HTHH eruption. Dashed lines show the 5th–95th percentile range; best-estimate responses are shown with thick coloured lines; thin lines show interannual variability. **b)** The likelihood of global surface temperature anomaly exceeding 1.5 °C between 2015 and 2035 (solid lines) and the cumulative probability that no year has yet exceeded 1.5 °C (dashed lines). Cumulative risks of 1.5 °C exceedance for the 5 years period 2022–2026 are marked with arrows in the top left corner of b. The shaded ranges show the uncertainty in the 2022–2026 1.5 °C exceedance risk. Reproduced under the Creative Commons 4.0 (CC 4.0) license.

To improve future projections of the interactions between air quality and climate policies, Jia and Quaas (2023) used satellite observations to show that the aerosol–Nd relation (in log–log space) is not linear as commonly assumed. Instead, the Nd sensitivity decreases at large aerosol concentrations due to the transition from aerosol-limited to updraft-limited regime, making the widely used linear method problematic. A sigmoidal transition was shown to adequately fit the data. When using this revised relationship, the additional warming that arises from air pollution mitigation was projected to be delayed by two to three decades in heavily polluted locations, compared to the linear relationship. This cloud-mediated climate penalty would manifest markedly starting around 2025 in China and 2050 in India after applying the strongest air quality policy, underlining the urgency of mitigating greenhouse gas emissions (Fig. 30).

Finally, Jenkins et al. (2023a) discussed means for addressing the triple challenge of energy policy: increasing resilience and guaranteeing the security of supply of both fossil and non-fossil energy, minimising the impact on consumer energy prices, and retaining consistency with Paris Agreement climate goals. They suggest opening to a conversation about applying the principle of extended producer responsibility (EPR) to fossil fuels could deconflict energy security and climate policy at an affordable cost by stopping fossil fuels from causing further global warming. Implementing EPR through a combination of geological CO_2 storage and nature-based solutions can deliver net zero at comparable or lower costs than conventional scenarios driven with a global carbon price and subject to constraints on CO_2 storage deployment. It would also mean that the principal beneficiary of high fossil fuel prices, the fossil fuel industry itself, plays its part in addressing the climate challenge while reducing the risk of asset stranding.

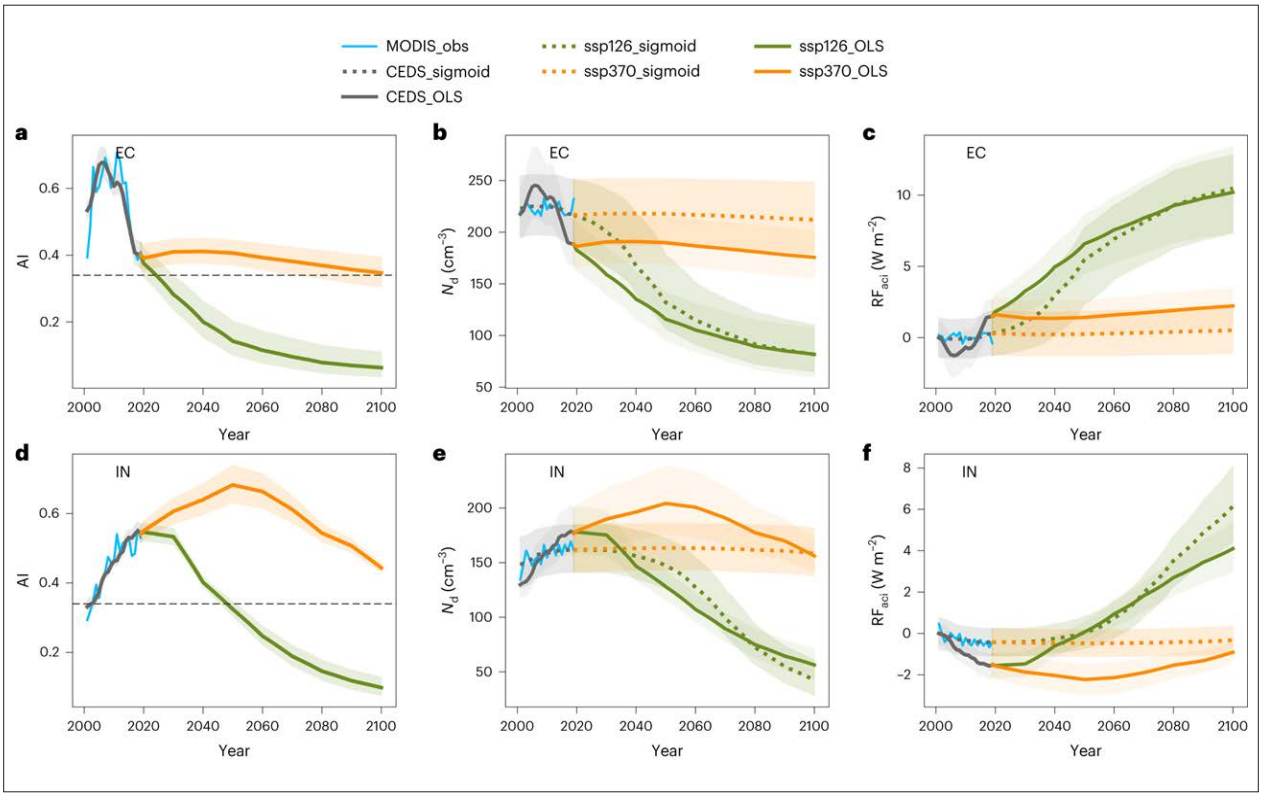

Figure 30. Figure from Jia and Quaas (2023). Observed and predicted aerosol index, cloud droplet number concentration and radiative forcing during 2000–2100. a–f, Past and future mean regional changes in AI (a,d), Nd (b,e) and RFaci (c,f) over EC (top) and IN (bottom) diagnosed from past (grey) and future aerosol emissions under strongmitigation (SSP1–2.6; green) and high-emissions (SSP3–7.0; orange) scenarios. To enhance the conciseness and readability, the results for mid-emissions (SSP2–4.5) are not displayed here and instead are shown in Extended Data Fig. 1. Historical observations of AI and Nd from MODIS Level 3 1° × 1° products (2001–2020) are shown in cyan. Solid and dashed lines indicate the predictions using OLS and sigmoid methods, respectively, for Nd and RFaci, with the shaded areas representing the 95% confidence interval (according to a Student's t test) that represents the regression uncertainty. The horizontal dashed lines in a and d denote the critical AI (0.35) from the sigmoidal fit in Fig. 2b, below which the updraft-limited regime is transiting towards the aerosol-limited regime, that is, the aerosol effect starts to appear. Here the critical AI is defined as the AI value when SAI equals to 0.2, in which case the aerosol effect on Nd is assumed to be negligible. Reproduced under the Creative Commons 4.0 (CC 4.0) license.

5.7 Scientific progress contributing to the FORCeS objectives and outcomes achieved

The three objectives specified in the DoA and in Sect. 3 above have been guiding the work within FORCeS. Overall, we are satisfied with the progress towards the objectives as outlined below (see also Fig. 1).

Scientific progress towards Objective 1 and the related outcomes: FORCeS has consolidated and re-evaluated the key processes and aerosol components identified in the DoA, and made targeted improvements of these aspects within the FORCeS ESMs (see Sects. 5.1–5.3). In the case of aerosol (see Sect. 5.1), we have chosen to focus particularly on organic aerosol, aerosol nitrate, ultrafine aerosol dynamics and emissions, and absorbing aerosol. For clouds (see Sect. 5.2), the consortium targeted all the relevant processes governing the evolution of a cloud: from the formation of cloud droplets or ice crystals to precipitation formation – including aerosol and precursor processing and scavenging by clouds. In parallel with the targeted improvements of the aforementioned processes, analysis of model sensitivities, performance and observational constraints helped simplify the process descriptions where possible (see Sects. 5.3 and 5.4) and rule out implausible model variants. To set the scene for evaluating the FORCeS ESMs after the process improvements, we benchmarked various aspects of these models as it was within their contribution to the CMIP6 project, implemented the new parameterizations and evaluated the outcomes (see Sects. 5.5 and 5.6). As a result, our understanding of the global aerosol populations, cloud microphysics and their descriptions ESMs has increased substantially, and the ESMs participating in the FORCeS activities, along with their reliability when it comes to future projections e.g. as part of the CMIP7 initiative, have correspondingly improved.

Scientific progress towards Objective 2: We have analysed the budgets of key aerosol components and radiative forcing as simulated by the FORCeS ESMs during the past decade, and identified the most important factors causing uncertainty in these estimates (see Sect. 5.3). We have collected and identified the data sets to be utilized for finding new constraints for the anthropogenic aerosol forcing, and developed new observational constraints for the key processes targeted that span over all the relevant scales – from the molecular to the global scale (see Sect. 5.4). We have set constraints on the aerosol radiative forcing and identified critical structural uncertainties in ESMs that need to be improved through further work on the key processes and their simplification. As a result, we have a substantially improved our understanding of the components of this uncertainty and the aspects that could be improved. We did not deem a multi-model assessment of the aerosol forcing and its uncertainty meaningful by the end of the project because of the large structural differences between the participating models. However, the study by Regayre et al. (2023) showed, focusing on the UKESM model, that through fixing the current structural uncertainties in models using relevant observational constraints, an about 50% reduction of the aerosol forcing uncertainty could be achieved.

Scientific progress towards Objective 3: We have analysed the budgets of key aerosol components and radiative forcing as simulated by the FORCeS ESMs during the past decade, and identified the most important factors causing uncertainty in these estimates (see Sect. 5.3). We have collected and identified the data sets to be utilized for finding new constraints for the anthropogenic aerosol forcing, and developed new observational constraints for the key processes targeted that span over all the relevant scales – from the molecular to the global scale (see Sect. 5.4). We have set constraints on the aerosol radiative forcing and identified critical structural uncertainties in ESMs that need to be improved through further work on the key processes and their simplification. As a result, we have a substantially improved our understanding of the components of this uncertainty and the aspects that could be improved. We did not deem a multi-model assessment of the aerosol forcing and its uncertainty meaningful by the end of the project because of the large structural differences between the participating models. However, the study by Regayre et al. (2023) showed, focusing on the UKESM model, that through fixing the current structural uncertainties in models using relevant observational constraints, an about 50% reduction of the aerosol forcing uncertainty could be achieved.

6. Summary

Overall, FORCeS progressed according to the plan laid out in the DoA, with some relatively minor deviations caused primarily by the COVID-19 pandemic. Progress was made towards understanding and reducing the uncertainty in estimates of the radiative forcing associated with anthropogenic aerosol. Specifically, we have consolidated key aerosol components (organics, nitrate, absorbing components) and processes (ultrafine aerosol dynamics, interactions with clouds) as well as cloud processes (interaction with aerosol particles, microphysics of precipitation formation, ice formation and updrafts) to target in the FORCeS Earth System Models (ESMs, i.e. EC-Earth, ECHAM/ICON and NorESM). We have updated and evaluated the descriptions of these key processes within the FORCeS ESMs based on a wealth of observational data over various scales, as well as to smaller-scale theoretical considerations, to ensure physical and chemical robustness of the climate-scale representation of these processes. We used the observational constraints together with sophisticated multidimensional analysis of the model response to narrow down the plausible range of aerosol and cloud evolution, as well as radiative forcing estimates. To fill key gaps in observational constraints, novel laboratory experiments and field campaigns were within FORCeS, and detailed models were used to develop new and more process-based metrics and constraints for climate model evaluation. Finally, multiple lines of evidence were used to provide better constrained estimates of aerosol, cloud and radiative forcing trends, providing also an assessment of plausible values climate sensitivity and transient climate response in the context of the improved knowledge on aerosol and cloud processes in the climate system.

References

Ahola, J., Raatikainen, T., Alper, M. E., Keskinen, J.-P., Kokkola, H., Kukkurainen, A., et al. (2022). Technical note: Parameterising cloud base updraft velocity of marine stratocumuli. Atmospheric Chemistry and Physics 22, 4523–4537. doi: 10.5194/acp-22-4523-2022

Ahsan, H., Wang, H., Wu, J., Wu, M., Smith, S. J., Bauer, S., et al. (2023). The Emissions Model Intercomparison Project (Emissions-MIP): quantifying model sensitivity to emission characteristics. Atmospheric Chemistry and Physics 23, 14779–14799. doi: 10.5194/acp-23-14779-2023

Allen, M., Tanaka, K., Macey, A., Cain, M., Jenkins, S., Lynch, J., et al. (2021). Ensuring that offsets and other internationally transferred mitigation outcomes contribute effectively to limiting global warming. Environ. Res. Lett. 16, 074009. doi: 10.1088/1748-9326/abfcf9

Allen, R. J., Turnock, S., Nabat, P., Neubauer, D., Lohmann, U., Olivié, D., et al. (2020). Climate and air quality impacts due to mitigation of non-methane near-term climate forcers. Atmospheric Chemistry and Physics 20, 9641–9663. doi: 10.5194/acp-20-9641-2020

Andersen, H., Cermak, J., Douglas, A., Myers, T. A., Nowack, P., Stier, P., et al. (2023). Sensitivities of cloud radiative effects to large-scale meteorology and aerosols from global observations. Atmospheric Chemistry and Physics 23, 10775–10794. doi: 10.5194/acp-23-10775-2023

Andersen, H., Cermak, J., Zipfel, L., and Myers, T. A. (2022). Attribution of Observed Recent Decrease in Low Clouds Over the Northeastern Pacific to Cloud-Controlling Factors. Geophysical Research Letters 49, e2021GL096498. doi: 10.1029/2021GL096498

Arola, A., Lipponen, A., Kolmonen, P., Virtanen, T. H., Bellouin, N., Grosvenor, D. P., et al. (2022). Aerosol effects on clouds are concealed by natural cloud heterogeneity and satellite retrieval errors. Nat Commun 13, 7357. doi: 10.1038/s41467-022-34948-5

Artaxo, P., Hansson, H.-C., Andreae, M. O., Bäck, J., Alves, E. G., Barbosa, H. M. J., et al. (2022). Tropical and Boreal Forest – Atmosphere Interactions: A Review. Tellus B: Chemical and Physical Meteorology 74, 24–163. doi: 10.16993/tellusb.34

Baker, A. R., Kanakidou, M., Nenes, A., Myriokefalitakis, S., Croot, P. L., Duce, R. A., et al. (2021). Changing atmospheric acidity as a modulator of nutrient deposition and ocean biogeochemistry. Science Advances 7, eabd8800. doi: 10.1126/sciadv.abd8800

Bardakov, R., Krejci, R., Riipinen, I., and Ekman, A. M. L. (2022). The Role of Convective Up- and Downdrafts in the Transport of Trace Gases in the Amazon. Journal of Geophysical Research: Atmospheres 127, e2022JD037265. doi: 10.1029/2022JD037265

Bardakov, R., Riipinen, I., Krejci, R., Savre, J., Thornton, J. A., and Ekman, A. M. L. (2020). A Novel Framework to Study Trace Gas Transport in Deep Convective Clouds. Journal of Advances in Modeling Earth Systems 12, e2019MS001931. doi: 10.1029/2019MS001931

Bardakov, R., Thornton, J. A., Riipinen, I., Krejci, R., and Ekman, A. M. L. (2021). Transport and chemistry of isoprene and its oxidation products in deep convective clouds. Tellus B: Chemical and Physical Meteorology 73, 1–21. doi: 10.1080/16000889.2021.1979856

Bell, D. M., Wu, C., Bertrand, A., Graham, E., Schoonbaert, J., Giannoukos, S., et al. (2022). Particle-phase processing of α-pinene NO_3 secondary organic aerosol in the dark. Atmospheric Chemistry and Physics 22, 13167–13182. doi: 10.5194/acp-22-13167-2022

Bergas-Massó, E., Gonçalves Ageitos, M., Myriokefalitakis, S., Miller, R. L., van Noije, T., Le Sager, P., et al. (2023). Pre-Industrial, Present and Future Atmospheric Soluble Iron Deposition and the Role of Aerosol Acidity and Oxalate Under CMIP6 Emissions. Earth's Future 11, e2022EF003353. doi: 10.1029/2022EF003353

Bergman, T., Makkonen, R., Schrödner, R., Swietlicki, E., Phillips, V. T. J., Le Sager, P., et al. (2022). Description and evaluation of a secondary organic aerosol and new particle formation scheme within TM5-MP v1.2. Geoscientific Model Development 15, 683–713. doi: 10.5194/gmd-15-683-2022

Blichner, S. M., Yli-Juuti, T., Mielonen, T., Pöhlker, C., Holopainen, E., Heikkinen, L., et al. (2024). Process-evaluation of forest aerosol-cloud-climate feedback shows clear evidence from observations and large uncertainty in models. Nat Commun 15, 969. doi: 10.1038/s41467-024-45001-y

Boutle, I., Angevine, W., Bao, J.-W., Bergot, T., Bhattacharya, R., Bott, A., et al. (2022). Demistify: a large-eddy simulation (LES) and single-column model (SCM) intercomparison of radiation fog. Atmospheric Chemistry and Physics 22, 319–333. doi: 10.5194/acp-22-319-2022

Braun, C., Voigt, A., Hoose, C., Ekman, A. M. L., and Pinto, J. G. (2022). Controls on Subtropical Cloud Reflectivity during a Waterbelt Scenario for the Cryogenian Glaciations. Journal of Climate 35, 7057–7076. doi: 10.1175/JCLI-D-22-0241.1

Bulatovic, I., Igel, A. L., Leck, C., Heintzenberg, J., Riipinen, I., and Ekman, A. M. L. (2021). The importance of Aitken mode aerosol particles for cloud sustenance in the summertime high Arctic – a simulation study supported by observational data. Atmospheric Chemistry and Physics 21, 3871–3897. doi: 10.5194/acp-21-3871-2021

Bulatovic, I., Savre, J., Tjernström, M., Leck, C., and Ekman, A. M. L. (2023). Large-eddy simulation of a two-layer boundary-layer cloud system from the Arctic Ocean 2018 expedition. Atmospheric Chemistry and Physics 23, 7033–7055. doi: 10.5194/acp-23-7033-2023

Cain, M., Shine, K., Frame, D., Lynch, J., Macey, A., Pierrehumbert, R., et al. (2021). Comment on 'Unintentional unfairness when applying new greenhouse gas emissions metrics at country level.' Environ. Res. Lett. 16, 068001. doi: 10.1088/1748-9326/ac02eb

Calderón, S. M., Tonttila, J., Buchholz, A., Joutsensaari, J., Komppula, M., Leskinen, A., et al. (2022). Aerosol–stratocumulus interactions: towards a better process understanding using closures between observations and large eddy simulations. Atmospheric Chemistry and Physics 22, 12417–12441. doi: 10.5194/acp-22-12417-2022

Carlsson, P. T. M., Vereecken, L., Novelli, A., Bernard, F., Brown, S. S., Brownwood, B., et al. (2023). Comparison of isoprene chemical mechanisms under atmospheric night-time conditions in chamber experiments: evidence of hydroperoxy aldehydes and epoxy products from NO3 oxidation. Atmospheric Chemistry and Physics 23, 3147–3180. doi: 10.5194/acp-23-3147-2023

Chatziparaschos, M., Daskalakis, N., Myriokefalitakis, S., Kalivitis, N., Nenes, A., Gonçalves Ageitos, M., et al. (2023). Role of K-feldspar and quartz in global ice nucleation by mineral dust in mixed-phase clouds. Atmospheric Chemistry and Physics 23, 1785–1801. doi: 10.5194/acp-23-1785-2023

Che, H., Stier, P., Watson-Parris, D., Gordon, H., and Deaconu, L. (2022). Source attribution of cloud condensation nuclei and their impact on stratocumulus clouds and radiation in the south-eastern Atlantic. Atmospheric Chemistry and Physics 22, 10789–10807. doi: 10.5194/acp-22-10789-2022

Cherian, R., and Quaas, J. (2020). Trends in AOD, Clouds, and Cloud Radiative Effects in Satellite Data and CMIP5 and CMIP6 Model Simulations Over Aerosol Source Regions. Geophysical Research Letters 47, e2020GL087132. doi: 10.1029/2020GL087132

Christensen, M. W., Gettelman, A., Cermak, J., Dagan, G., Diamond, M., Douglas, A., et al. (2022). Opportunistic experiments to constrain aerosol effective radiative forcing. Atmospheric Chemistry and Physics 22, 641–674. doi: 10.5194/acp-22-641-2022

Collins, J. W., Lamarque, J. F., Schulz, M., Boucher, O., Eyring, V., Hegglin, I. M., et al. (2017). AerChemMIP: Quantifying the effects of chemistry and aerosols in CMIP6. Geoscientific Model Development 10, 585–607. doi: 10.5194/gmd-10-585-2017

Dagan, G., Stier, P., Dingley, B., and Williams, A. I. L. (2022). Examining the Regional Co-Variability of the Atmospheric Water and Energy Imbalances in Different Model Configurations—Linking Clouds and Circulation. Journal of Advances in Modeling Earth Systems 14, e2021MS002951. doi: 10.1029/2021MS002951

Dagan, G., Stier, P., and Watson-Parris, D. (2020). Aerosol Forcing Masks and Delays the Formation of the North Atlantic Warming Hole by Three Decades. Geophysical Research Letters 47, e2020GL090778. doi: 10.1029/2020GL090778

Daskalakis, N., Gallardo, L., Kanakidou, M., Nüß, J. R., Menares, C., Rondanelli, R., et al. (2022). Impact of biomass burning and stratospheric intrusions in the remote South Pacific Ocean troposphere. Atmospheric Chemistry and Physics 22, 4075–4099. doi: 10.5194/acp-22-4075-2022

Decesari, S., Paglione, M., Mazzanti, A., and Tagliavini, E. (2024). NMR spectroscopic applications to atmospheric organic aerosol analysis – Part 1: A critical review of data source and analysis, potentialities and limitations. TrAC Trends in Analytical Chemistry 171, 117516. doi: 10.1016/j.trac.2023.117516

Dingley, B., Dagan, G., and Stier, P. (2021). Forcing Convection to Aggregate Using Diabatic Heating Perturbations. Journal of Advances in Modeling Earth Systems 13, e2021MS002579. doi: 10.1029/2021MS002579

Dingley, B., Dagan, G., Stier, P., and Herbert, R. (2023). The Impact of a Land-Sea Contrast on Convective Aggregation in Radiative-Convective Equilibrium. Journal of Advances in Modeling Earth Systems 15, e2022MS003249. doi: 10.1029/2022MS003249

Dinkelacker, B. T., Garcia Rivera, P., Skyllakou, K., Adams, P. J., and Pandis, S. N. (2024). Predicted and observed changes in summertime biogenic and total organic aerosol in the southeast United States from 2001 to 2010. Atmospheric Environment 316, 120186. doi: 10.1016/j.atmosenv.2023.120186

Donahue, N. M., Robinson, A. L., Stanier, C. O., and Pandis, S. N. (2006). Coupled partitioning, dilution, and chemical aging of semivolatile organics. Environmental Science and Technology 40, 2635–2643. doi: 10.1021/es052297c

Douglas, A., and Stier, P. (2021). Using the learnings of machine learning to distill cloud controlling environmental regimes from satellite observations. Copernicus Meetings. doi: 10.5194/egusphere-egu21-16443

Eyring, V., Bony, S., Meehl, G. A., Senior, C. A., Stevens, B., Stouffer, R. J., et al. (2016). Overview of the Coupled Model Intercomparison Project Phase 6 (CMIP6) experimental design and organization. Geoscientific Model Development 9, 1937–1958. doi: 10.5194/gmd-9-1937-2016

Fiedler, S., van Noije, T., Smith, C. J., Boucher, O., Dufresne, J.-L., Kirkevåg, A., et al. (2023). Historical Changes and Reasons for Model Differences in Anthropogenic Aerosol Forcing in CMIP6. Geophysical Research Letters 50, e2023GL104848. doi: 10.1029/2023GL104848

Fiedler, S., Wyser, K., Rogelj, J., and van Noije, T. (2021). Radiative effects of reduced aerosol emissions during the COVID-19 pandemic and the future recovery. Atmospheric Research 264, 105866. doi: 10.1016/j.atmosres.2021.105866

Foskinis, R., Nenes, A., Papayannis, A., Georgakaki, P., Eleftheriadis, K., Vratolis, S., et al. (2022). Towards reliable retrievals of cloud droplet number for non-precipitating planetary boundary layer clouds and their susceptibility to aerosol. Frontiers in Remote Sensing 3. Available at: https://www.frontiersin.org/articles/10.3389/frsen.2022.958207 (Accessed November 9, 2023).

Fountoukis, C., and Nenes, A. (2007). ISORROPIAII: A computationally efficient thermodynamic equilibrium model for K+-Ca2+-Mg2+-NH4+-Na+-SO42--NO3--Cl--H2O aerosols. Atmospheric Chemistry and Physics 7, 4639–4659. doi: 10.5194/acp-7-4639-2007

Frey, L., Höpner, F., Kirkevåg, A., and Bender, F. a.-M. (2021). Absorbing aerosols over Asia – an inter-model and model-observation comparison study using CAM5.3-Oslo. Tellus B: Chemical and Physical Meteorology 73, 1909815. doi: 10.1080/16000889.2021.1909815

Gliß, J., Mortier, A., Schulz, M., Andrews, E., Balkanski, Y., Bauer, S. E., et al. (2021). AeroCom phase III multi-model evaluation of the aerosol life cycle and optical properties using ground- And space-based remote sensing as well as surface in situ observations. Atmospheric Chemistry and Physics 21, 87–128. doi: 10.5194/acp-21-87-2021

Gonçalves Ageitos, M., Obiso, V., Miller, R. L., Jorba, O., Klose, M., Dawson, M., et al. (2023). Modeling dust mineralogical composition: sensitivity to soil mineralogy atlases and their expected climate impacts. Atmospheric Chemistry and Physics 23, 8623–8657. doi: 10.5194/acp-23-8623-2023

Graham, E. L., Wu, C., Bell, D. M., Bertrand, A., Haslett, S. L., Baltensperger, U., et al. (2023). Volatility of aerosol particles from NO3 oxidation of various biogenic organic precursors. Atmospheric Chemistry and Physics 23, 7347–7362. doi: 10.5194/acp-23-7347-2023

Graham, E. L., Zieger, P., Mohr, C., Wideqvist, U., Hennig, T., Ekman, A. M. L., et al. (2020). Physical and chemical properties of aerosol particles and cloud residuals on Mt. Åreskutan in Central Sweden during summer 2014. Tellus B: Chemical and Physical Meteorology 72, 1776080. doi: 10.1080/16000889.2020.1776080

Gramlich, Y., Siegel, K., Haslett, S. L., Freitas, G., Krejci, R., Zieger, P., et al. (2023). Revealing the chemical characteristics of Arctic low-level cloud residuals – in situ observations from a mountain site. Atmospheric Chemistry and Physics 23, 6813–6834. doi: 10.5194/acp-23-6813-2023

Grose, M. R., Gregory, J., Colman, R., and Andrews, T. (2018). What Climate Sensitivity Index Is Most Useful for Projections? Geophysical Research Letters 45, 1559–1566. doi: 10.1002/2017GL075742

Gryspeerdt, E., Goren, T., and Smith, T. W. P. (2021). Observing the timescales of aerosol–cloud interactions in snapshot satellite images. Atmospheric Chemistry and Physics 21, 6093–6109. doi: 10.5194/acp-21-6093-2021

Guo, Y., Shen, H., Pullinen, I., Luo, H., Kang, S., Vereecken, L., et al. (2022). Identification of highly oxygenated organic molecules and their role in aerosol formation in the reaction of limonene with nitrate radical. Atmospheric Chemistry and Physics 22, 11323–11346. doi: 10.5194/acp-22-11323-2022

Hakala, S., Vakkari, V., Bianchi, F., Dada, L., Deng, C., Dällenbach, K. R., et al. (2022). Observed coupling between air mass history, secondary growth of nucleation mode particles and aerosol pollution levels in Beijing. Environ. Sci.: Atmos. 2, 146–164. doi: 10.1039/D1EA00089F

Hakala, S., Vakkari, V., Lihavainen, H., Hyvärinen, A.-P., Neitola, K., Kontkanen, J., et al. (2023). Explaining apparent particle shrinkage related to new particle formation events in western Saudi Arabia does not require evaporation. Atmospheric Chemistry and Physics 23, 9287–9321. doi: 10.5194/acp-23-9287-2023

Hasekamp, O. P., Gryspeerdt, E., and Quaas, J. (2019). Analysis of polarimetric satellite measurements suggests stronger cooling due to aerosol-cloud interactions. Nat Commun 10, 5405. doi: 10.1038/s41467-019-13372-2

Heikkinen, L., Äijälä, M., Daellenbach, K. R., Chen, G., Garmash, O., Aliaga, D., et al. (2021). Eight years of sub-micrometre organic aerosol composition data from the boreal forest characterized using a machine-learning approach. Atmospheric Chemistry and Physics 21, 10081–10109. doi: 10.5194/acp-21-10081-2021

Herbert, R., Stier, P., and Dagan, G. (2021). Isolating Large-Scale Smoke Impacts on Cloud and Precipitation Processes Over the Amazon With Convection Permitting Resolution. Journal of Geophysical Research: Atmospheres 126, e2021JD034615. doi: 10.1029/2021JD034615

Heslin-Rees, D., Tunved, P., Ström, J., Cremer, R., Zieger, P., Riipinen, I., et al. (2024). Increase in precipitation scavenging contributes to long-term reductions of light-absorbing aerosol in the Arctic. Atmospheric Chemistry and Physics 24, 2059–2075. doi: 10.5194/acp-24-2059-2024

Hodzic, A., Mahowald, N., Dawson, M., Johnson, J., Bernardet, L., Bosler, P. A., et al. (2023). Generalized Aerosol/Chemistry Interface (GIANT): A Community Effort to Advance Collaborative Science across Weather and Climate Models. Bulletin of the American Meteorological Society 104, E2065–E2080. doi: 10.1175/BAMS-D-23-0013.1

Holopainen, E., Kokkola, H., Laakso, A., and Kühn, T. (2020). In-cloud scavenging scheme for sectional aerosol modules – implementation in the framework of the Sectional Aerosol module for Large Scale Applications version 2.0 (SALSA2.0) global aerosol module. Geoscientific Model Development 13, 6215–6235. doi: 10.5194/gmd-13-6215-2020

Hoose, C. (2022). Another Piece of Evidence for Important but Uncertain Ice Multiplication Processes. AGU Advances 3, e2022AV000669. doi: 10.1029/2022AV000669

Huusko, L. L., Bender, F. A.-M., Ekman, A. M. L., and Storelvmo, T. (2021). Climate sensitivity indices and their relation with projected temperature change in CMIP6 models. Environ. Res. Lett. 16, 064095. doi: 10.1088/1748-9326/ac0748

Hyttinen, N., Pullinen, I., Nissinen, A., Schobesberger, S., Virtanen, A., and Yli-Juuti, T. (2022). Comparison of saturation vapor pressures of α-pinene + O_3 oxidation products derived from COSMO-RS computations and thermal desorption experiments. Atmospheric Chemistry and Physics 22, 1195–1208. doi: 10.5194/acp-22-1195-2022

Isokääntä, S., Kim, P., Mikkonen, S., Kühn, T., Kokkola, H., Yli-Juuti, T., et al. (2022). The effect of clouds and precipitation on the aerosol concentrations and composition in a boreal forest environment. Atmospheric Chemistry and Physics 22, 11823–11843. doi: 10.5194/acp-22-11823-2022

Jenkins, S., Kuijper, M., Helferty, H., Girardin, C., and Allen, M. (2023a). Extended producer responsibility for fossil fuels. Environ. Res. Lett. 18, 011005. doi: 10.1088/1748-9326/aca4e8*

Jenkins, S., Povey, A., Gettelman, A., Grainger, R., Stier, P., and Allen, M. (2022). Is Anthropogenic Global Warming Accelerating? Journal of Climate 1, 1–43. doi: 10.1175/JCLI-D-22-0081.1

Jenkins, S., Smith, C., Allen, M., and Grainger, R. (2023b). Tonga eruption increases chance of temporary surface temperature anomaly above 1.5 °C. Nat. Clim. Chang. 13, 127–129. doi: 10.1038/s41558-022-01568-2

Jia, H., and Quaas, J. (2023). Nonlinearity of the cloud response postpones climate penalty of mitigating air pollution in polluted regions. Nat. Clim. Chang. 13, 943–950. doi: 10.1038/s41558-023-01775-5

Jia, H., Quaas, J., Gryspeerdt, E., Böhm, C., and Sourdeval, O. (2022). Addressing the difficulties in quantifying droplet number response to aerosol from satellite observations. Atmospheric Chemistry and Physics 22, 7353–7372. doi: 10.5194/acp-22-7353-2022

Jorga, S. D., Florou, K., Patoulias, D., and Pandis, S. N. (2023). New particle formation and growth during summer in an urban environment: a dual chamber study. Atmospheric Chemistry and Physics 23, 85–97. doi: 10.5194/acp-23-85-2023

Julsrud, I. R., Storelvmo, T., Schulz, M., Moseid, K. O., and Wild, M. (2022). Disentangling Aerosol and Cloud Effects on Dimming and Brightening in Observations and CMIP6. Journal of Geophysical Research: Atmospheres 127, e2021JD035476. doi: 10.1029/2021JD035476

Kakavas, S., and Pandis, S. N. (2021). Effects of urban dust emissions on fine and coarse PM levels and composition. Atmospheric Environment 246, 118006. doi: 10.1016/j.atmosenv.2020.118006

Kakavas, S., Pandis, S. N., and Nenes, A. (2022). ISORROPIA-Lite: A Comprehensive Atmospheric Aerosol Thermodynamics Module for Earth System Models. Tellus B: Chemical and Physical Meteorology 74, 1–23. doi: 10.16993/tellusb.33

Kakavas, S., Pandis, S. N., and Nenes, A. (2023). Effects of simulated secondary organic aerosol water on PM1 levels and composition over the US. Atmospheric Chemistry and Physics 23, 13555–13564. doi: 10.5194/acp-23-13555-2023

Karlsson, L., Baccarini, A., Duplessis, P., Baumgardner, D., Brooks, I. M., Chang, R. Y.-W., et al. (2022). Physical and Chemical Properties of Cloud Droplet Residuals and Aerosol Particles During the Arctic Ocean 2018 Expedition. Journal of Geophysical Research: Atmospheres 127, e2021JD036383. doi: 10.1029/2021JD036383

Karydis, V. A., Tsimpidi, A. P., Pozzer, A., and Lelieveld, J. (2021). How alkaline compounds control atmospheric aerosol particle acidity. Atmospheric Chemistry and Physics 21, 14983–15001. doi: 10.5194/acp-21-14983-2021

Kelesidis, G. A., Neubauer, D., Fan, L.-S., Lohmann, U., and Pratsinis, S. E. (2022). Enhanced Light Absorption and Radiative Forcing by Black Carbon Agglomerates. Environ. Sci. Technol. 56, 8610–8618. doi: 10.1021/acs.est.2c00428

Khadir, T., Riipinen, I., Talvinen, S., Heslin-Rees, D., Pöhlker, C., Rizzo, L., et al. (2023). Sink, Source or Something In-Between? Net Effects of Precipitation on Aerosol Particle Populations. Geophysical Research Letters 50, e2023GL104325. doi: 10.1029/2023GL104325

Kim, M., Cermak, J., Andersen, H., Fuchs, J., and Stirnberg, R. (2020). A New Satellite-Based Retrieval of Low-Cloud Liquid-Water Path Using Machine Learning and Meteosat SEVIRI Data. Remote Sensing 12, 3475. doi: 10.3390/rs12213475

Klose, M., Jorba, O., Gonçalves Ageitos, M., Escribano, J., Dawson, M. L., Obiso, V., et al. (2021). Mineral dust cycle in the Multiscale Online Nonhydrostatic AtmospheRe CHemistry model (MONARCH) Version 2.0. Geoscientific Model Development 14, 6403–6444. doi: 10.5194/gmd-14-6403-2021

Kok, J. F., Adebiyi, A. A., Albani, S., Balkanski, Y., Checa-Garcia, R., Chin, M., et al. (2021a). Contribution of the world's main dust source regions to the global cycle of desert dust. Atmospheric Chemistry and Physics 21, 8169–8193. doi: 10.5194/acp-21-8169-2021

Kok, J. F., Adebiyi, A. A., Albani, S., Balkanski, Y., Checa-Garcia, R., Chin, M., et al. (2021b). Improved representation of the global dust cycle using observational constraints on dust properties and abundance. Atmospheric Chemistry and Physics 21, 8127–8167. doi: 10.5194/acp-21-8127-2021

Kok, J. F., Storelvmo, T., Karydis, V. A., Adebiyi, A. A., Mahowald, N. M., Evan, A. T., et al. (2023). Mineral dust aerosol impacts on global climate and climate change. Nat Rev Earth Environ 4, 71–86. doi: 10.1038/s43017-022-00379-5

Kontkanen, J., Stolzenburg, D., Olenius, T., Yan, C., Dada, L., Ahonen, L., et al. (2022). What controls the observed size-dependency of the growth rates of sub-10 nm atmospheric particles? Environ. Sci.: Atmos. 2, 449–468. doi: 10.1039/D1EA00103E

Krishnan, S., Ekman, A. M. L., Hansson, H.-C., Riipinen, I., Lewinschal, A., Wilcox, L. J., et al. (2020). The Roles of the Atmosphere and Ocean in Driving Arctic Warming Due to European Aerosol Reductions. Geophysical Research Letters 47, e2019GL086681. doi: 10.1029/2019GL086681

Kuma, P., Bender, F. A.-M., and Jönsson, A. R. (2023a). Climate Model Code Genealogy and Its Relation to Climate Feedbacks and Sensitivity. Journal of Advances in Modeling Earth Systems 15, e2022MS003588. doi: 10.1029/2022MS003588

Kuma, P., Bender, F. A.-M., Schuddeboom, A., McDonald, A. J., and Seland, Ø. (2023b). Machine learning of cloud types in satellite observations and climate models. Atmospheric Chemistry and Physics 23, 523–549. doi: 10.5194/acp-23-523-2023

Laaksonen, A., Malila, J., and Nenes, A. (2020). Heterogeneous nucleation of water vapor on different types of black carbon particles. Atmospheric Chemistry and Physics 20, 13579–13589. doi: 10.5194/acp-20-13579-2020

Langton, T., Stier, P., Watson-Parris, D., and Mulcahy, J. P. (2021). Decomposing Effective Radiative Forcing Due to Aerosol Cloud Interactions by Global Cloud Regimes. Geophysical Research Letters 48, e2021GL093833. doi: 10.1029/2021GL093833

Lapere, R., Thomas, J. L., Marelle, L., Ekman, A. M. L., Frey, M. M., Lund, M. T., et al. (2023). The Representation of Sea Salt Aerosols and Their Role in Polar Climate Within CMIP6. Journal of Geophysical Research: Atmospheres 128, e2022JD038235. doi: 10.1029/2022JD038235

Lee, D. S., Fahey, D. W., Skowron, A., Allen, M. R., Burkhardt, U., Chen, Q., et al. (2021). The contribution of global aviation to anthropogenic climate forcing for 2000 to 2018. Atmospheric Environment 244, 117834. doi: 10.1016/j.atmosenv.2020.117834

Leinonen, V., Kokkola, H., Yli-Juuti, T., Mielonen, T., Kühn, T., Nieminen, T., et al. (2022). Comparison of particle number size distribution trends in ground measurements and climate models. Atmospheric Chemistry and Physics 22, 12873–12905. doi: 10.5194/acp-22-12873-2022

Li, G., Wieder, J., Pasquier, J. T., Henneberger, J., and Kanji, Z. A. (2022). Predicting atmospheric background number concentration of ice-nucleating particles in the Arctic. Atmospheric Chemistry and Physics 22, 14441–14454. doi: 10.5194/acp-22-14441-2022

Li, L., Mahowald, N. M., Miller, R. L., Pérez García-Pando, C., Klose, M., Hamilton, D. S., et al. (2021). Quantifying the range of the dust direct radiative effect due to source mineralogy uncertainty. Atmospheric Chemistry and Physics 21, 3973–4005. doi: 10.5194/acp-21-3973-2021

Lohmann, U., Friebel, F., Kanji, Z. A., Mahrt, F., Mensah, A. A., and Neubauer, D. (2020). Future warming exacerbated by aged-soot effect on cloud formation. Nat. Geosci. 13, 674–680. doi: 10.1038/s41561-020-0631-0

Luo, H., Vereecken, L., Shen, H., Kang, S., Pullinen, I., Hallquist, M., et al. (2023). Formation of highly oxygenated organic molecules from the oxidation of limonene by OH radical: significant contribution of H-abstraction pathway. Atmospheric Chemistry and Physics 23, 7297–7319. doi: 10.5194/acp-23-7297-2023

Maahn, M., Goren, T., Shupe, M. D., and de Boer, G. (2021). Liquid Containing Clouds at the North Slope of Alaska Demonstrate Sensitivity to Local Industrial Aerosol Emissions. Geophysical Research Letters 48, e2021GL094307. doi: 10.1029/2021GL094307

Manavi, S. E. I., and Pandis, S. N. (2022). A lumped species approach for the simulation of secondary organic aerosol production from intermediate-volatility organic compounds (IVOCs): application to road transport in PMCAMx-iv (v1.0). Geoscientific Model Development 15, 7731–7749. doi: 10.5194/gmd-15-7731-2022

Manshausen, P., Watson-Parris, D., Christensen, M. W., Jalkanen, J.-P., and Stier, P. (2022). Invisible ship tracks show large cloud sensitivity to aerosol. Nature 610, 101–106. doi: 10.1038/s41586-022-05122-0

Mansour, K., Decesari, S., Ceburnis, D., Ovadnevaite, J., and Rinaldi, M. (2023). Machine learning for prediction of daily sea surface dimethylsulfide concentration and emission flux over the North Atlantic Ocean (1998–2021). Science of The Total Environment 871, 162123. doi: 10.1016/j.scitotenv.2023.162123

Mansour, K., Rinaldi, M., Preißler, J., Decesari, S., Ovadnevaite, J., Ceburnis, D., et al. (2022). Phytoplankton Impact on Marine Cloud Microphysical Properties Over the Northeast Atlantic Ocean. Journal of Geophysical Research: Atmospheres 127, e2021JD036355. doi: 10.1029/2021JD036355

Milousis, A., Tsimpidi, A. P., Tost, H., Pandis, S. N., Nenes, A., Kiendler-Scharr, A., et al. (2024). Implementation of the ISORROPIA-lite aerosol thermodynamics model into the EMAC chemistry climate model (based on MESSy v2.55): implications for aerosol composition and acidity. Geoscientific Model Development 17, 1111–1131. doi: 10.5194/gmd-17-1111-2024

Mortier, A., Gliß, J., Schulz, M., Aas, W., Andrews, E., Bian, H., et al. (2020). Evaluation of climate model aerosol trends with ground-based observations over the last 2 decades - an AeroCom and CMIP6 analysis. Atmospheric Chemistry and Physics 20, 13355–13378. doi: 10.5194/acp-20-13355-2020

Moseid, K. O., Schulz, M., Eichler, A., Schwikowski, M., McConnell, J. R., Olivié, D., et al. (2022). Using Ice Cores to Evaluate CMIP6 Aerosol Concentrations Over the Historical Era. Journal of Geophysical Research: Atmospheres 127, e2021JD036105. doi: 10.1029/2021JD036105

Moseid, K. O., Schulz, M., Storelvmo, T., Julsrud, I. R., Olivié, D., Nabat, P., et al. (2020). Bias in CMIP6 models as compared to observed regional dimming and brightening. Atmospheric Chemistry and Physics 20, 16023–16040. doi: 10.5194/acp-20-16023-2020

Murphy, B. N., Julin, J., Riipinen, I., and Ekman, A. M. L. (2015). Organic aerosol processing in tropical deep convective clouds: Development of a new model (CRM-ORG) and implications for sources of particle number. Journal of Geophysical Research: Atmospheres 120, 10,441-10,464. doi: 10.1002/2015JD023551

Myriokefalitakis, S., Bergas-Massó, E., Gonçalves-Ageitos, M., Pérez García-Pando, C., van Noije, T., Le Sager, P., et al. (2022). Multiphase processes in the EC-Earth model and their relevance to the atmospheric oxalate, sulfate, and iron cycles. Geoscientific Model Development 15, 3079–3120. doi: 10.5194/gmd-15-3079-2022

Nenes, A., Pandis, S. N., Kanakidou, M., Russell, A. G., Song, S., Vasilakos, P., et al. (2021). Aerosol acidity and liquid water content regulate the dry deposition of inorganic reactive nitrogen. Atmospheric Chemistry and Physics 21, 6023–6033. doi: 10.5194/acp-21-6023-2021

Neubauer, D., Ferrachat, S., Siegenthaler-Le Drian, C., Stier, P., Partridge, D. G., Tegen, I., et al. (2019). The global aerosol-climate model ECHAM6.3-HAM2.3-Part 2: Cloud evaluation, aerosol radiative forcing, and climate sensitivity. Geoscientific Model Development 12, 3609–3639. doi: 10.5194/gmd-12-3609-2019

Nordling, K., Keskinen, J.-P., Romakkaniemi, S., Kokkola, H., Räisänen, P., Lipponen, A., et al. (2024). Technical note: Emulation of a large-eddy simulator for stratocumulus clouds in a general circulation model. Atmospheric Chemistry and Physics 24, 869–890. doi: 10.5194/acp-24-869-2024

Onsum Moseid, K., Schulz, M., Storelvmo, T., Rian Julsrud, I., Olivié, D., Nabat, P., et al. (2020). Bias in CMIP6 models as compared to observed regional dimming and brightening. Atmospheric Chemistry and Physics 20, 16023–16040. doi: 10.5194/acp-20-16023-2020

Paglione, M., Decesari, S., Rinaldi, M., Tarozzi, L., Manarini, F., Gilardoni, S., et al. (2021). Historical Changes in Seasonal Aerosol Acidity in the Po Valley (Italy) as Inferred from Fog Water and Aerosol Measurements. Environ. Sci. Technol. 55, 7307–7315. doi: 10.1021/acs.est.1c00651

Papakonstantinou-Presvelou, I., Sourdeval, O., and Quaas, J. (2022). Strong Ocean/Sea-Ice Contrasts Observed in Satellite-Derived Ice Crystal Number Concentrations in Arctic Ice Boundary-Layer Clouds. Geophysical Research Letters 49, e2022GL098207. doi: 10.1029/2022GL098207

Pasquier, J. T., David, R. O., Freitas, G., Gierens, R., Gramlich, Y., Haslett, S., et al. (2022a). The Ny-Ålesund Aerosol Cloud Experiment (NASCENT): Overview and First Results. Bulletin of the American Meteorological Society 103, E2533–E2558. doi: 10.1175/BAMS-D-21-0034.1

Pasquier, J. T., Henneberger, J., Korolev, A., Ramelli, F., Wieder, J., Lauber, A., et al. (2023). Understanding the History of Two Complex Ice Crystal Habits Deduced From a Holographic Imager. Geophysical Research Letters 50, e2022GL100247. doi: 10.1029/2022GL100247

Pasquier, J. T., Henneberger, J., Ramelli, F., Lauber, A., David, R. O., Wieder, J., et al. (2022b). Conditions favorable for secondary ice production in Arctic mixed-phase clouds. Atmospheric Chemistry and Physics Discussions, 1–33. doi: 10.5194/acp-2022-314

Patoulias, D., Florou, K., Pandis, S. N., and Nenes, A. (2024). New Particle Formation Events Can Reduce Cloud Droplets in Boundary Layer Clouds at the Continental Scale. Geophysical Research Letters 51, e2023GL106182. doi: 10.1029/2023GL106182

Patoulias, D., and Pandis, S. N. (2022). Simulation of the effects of low-volatility organic compounds on aerosol number concentrations in Europe. Atmospheric Chemistry and Physics 22, 1689–1706. doi: 10.5194/acp-22-1689-2022

Peace, A. H., Booth, B. B. B., Regayre, L. A., Carslaw, K. S., Sexton, D. M. H., Bonfils, C. J. W., et al. (2022). Evaluating uncertainty in aerosol forcing of tropical precipitation shifts. Earth System Dynamics 13, 1215–1232. doi: 10.5194/esd-13-1215-2022

Pereira Freitas, G., Adachi, K., Conen, F., Heslin-Rees, D., Krejci, R., Tobo, Y., et al. (2023). Regionally sourced bio-aerosols drive high-temperature ice nucleating particles in the Arctic. Nat Commun 14, 5997. doi: 10.1038/s41467-023-41696-7

Petäjä, T., Tabakova, K., Manninen, A., Ezhova, E., O'Connor, E., Moisseev, D., et al. (2022). Influence of biogenic emissions from boreal forests on aerosol–cloud interactions. Nat. Geosci. 15, 42–47. doi: 10.1038/s41561-021-00876-0

Prank, M., Tonttila, J., Ahola, J., Kokkola, H., Kühn, T., Romakkaniemi, S., et al. (2022). Impacts of marine organic emissions on low-level stratiform clouds – a large eddy simulator study. Atmospheric Chemistry and Physics 22, 10971–10992. doi: 10.5194/acp-22-10971-2022

Proske, U., Bessenbacher, V., Dedekind, Z., Lohmann, U., and Neubauer, D. (2021). How frequent is natural cloud seeding from ice cloud layers (< −35°C) over Switzerland? Atmospheric Chemistry and Physics 21, 5195–5216. doi: 10.5194/acp-21-5195-2021

Proske, U., Ferrachat, S., Klampt, S., Abeling, M., and Lohmann, U. (2023). Addressing Complexity in Global Aerosol Climate Model Cloud Microphysics. Journal of Advances in Modeling Earth Systems 15, e2022MS003571. doi: 10.1029/2022MS003571

Proske, U., Ferrachat, S., Neubauer, D., Staab, M., and Lohmann, U. (2022). Assessing the potential for simplification in global climate model cloud microphysics. Atmospheric Chemistry and Physics 22, 4737–4762. doi: 10.5194/acp-22-4737-2022

Quaas, J., Arola, A., Cairns, B., Christensen, M., Deneke, H., Ekman, A. M. L., et al. (2020). Constraining the Twomey effect from satellite observations: issues and perspectives. Atmos. Chem. Phys 20, 15079–15099. doi: 10.5194/acp-20-15079-2020

Quaas, J., Gryspeerdt, E., Vautard, R., and Boucher, O. (2021). Climate impact of aircraft-induced cirrus assessed from satellite observations before and during COVID-19. Environ. Res. Lett. 16, 064051. doi: 10.1088/1748-9326/abf686

Quaas, J., Jia, H., Smith, C., Albright, A. L., Aas, W., Bellouin, N., et al. (2022). Robust evidence for reversal of the trend in aerosol effective climate forcing. Atmospheric Chemistry and Physics 22, 12221–12239. doi: 10.5194/acp-22-12221-2022

Raatikainen, T., Prank, M., Ahola, J., Kokkola, H., Tonttila, J., and Romakkaniemi, S. (2022). The effect of marine ice-nucleating particles on mixed-phase clouds. Atmospheric Chemistry and Physics 22, 3763–3778. doi: 10.5194/acp-22-3763-2022

Räty, M., Sogacheva, L., Keskinen, H.-M., Kerminen, V.-M., Nieminen, T., Petäjä, T., et al. (2023). Dynamics of aerosol, humidity, and clouds in air masses travelling over Fennoscandian boreal forests. Atmospheric Chemistry and Physics 23, 3779–3798. doi: 10.5194/acp-23-3779-2023

Regayre, L. A., Deaconu, L., Grosvenor, D. P., Sexton, D. M. H., Symonds, C., Langton, T., et al. (2023). Identifying climate model structural inconsistencies allows for tight constraint of aerosol radiative forcing. Atmospheric Chemistry and Physics 23, 8749–8768. doi: 10.5194/acp-23-8749-2023

Rinaldi, M., Hiranuma, N., Santachiara, G., Mazzola, M., Mansour, K., Paglione, M., et al. (2021). Ice-nucleating particle concentration measurements from Ny-Ålesund during the Arctic spring–summer in 2018. Atmospheric Chemistry and Physics 21, 14725–14748. doi: 10.5194/acp-21-14725-2021

Roudsari, G., Lbadaoui-Darvas, M., Welti, A., Nenes, A., and Laaksonen, A. (2024). The molecular scale mechanism of deposition ice nucleation on silver iodide. Environ. Sci.: Atmos. 4, 243–251. doi: 10.1039/D3EA00140G

Ruuskanen, A., Romakkaniemi, S., Kokkola, H., Arola, A., Mikkonen, S., Portin, H., et al. (2021). Observations on aerosol optical properties and scavenging during cloud events. Atmospheric Chemistry and Physics 21, 1683–1695. doi: 10.5194/acp-21-1683-2021

Sand, M., Samset, B. H., Myhre, G., Gliß, J., Bauer, S. E., Bian, H., et al. (2021). Aerosol absorption in global models from AeroCom phase III. Atmospheric Chemistry and Physics 21, 15929–15947. doi: 10.5194/acp-21-15929-2021

Schlesinger, D., Riipinen, I., Lowe, S. J., Olenius, T., Kong, X., and Pettersson, J. B. C. (2020). Molecular perspective on water vapor accommodation into ice and its dependence on temperature. Journal of Physical Chemistry A 124, 10879–10889. doi: 10.1021/acs.jpca.0c09357

Schlund, M., Lauer, A., Gentine, P., Sherwood, S. C., and Eyring, V. (2020). Emergent constraints on equilibrium climate sensitivity in CMIP5: do they hold for CMIP6? Earth System Dynamics 11, 1233–1258. doi: 10.5194/esd-11-1233-2020

Schmale, J., Zieger, P., and Ekman, A. M. L. (2021). Aerosols in current and future Arctic climate. Nat. Clim. Chang. 11, 95–105. doi: 10.1038/s41558-020-00969-5

Seland, Ø., Bentsen, M., Olivié, D., Toniazzo, T., Gjermundsen, A., Graff, L. S., et al. (2020). Overview of the Norwegian Earth System Model (NorESM2) and key climate response of CMIP6 DECK, historical, and scenario simulations. Geoscientific Model Development 13, 6165–6200. doi: 10.5194/gmd-13-6165-2020

Shen, H., Vereecken, L., Kang, S., Pullinen, I., Fuchs, H., Zhao, D., et al. (2022). Unexpected significance of a minor reaction pathway in daytime formation of biogenic highly oxygenated organic compounds. Science Advances 8, eabp8702. doi: 10.1126/sciadv.abp8702

Siegel, K., Karlsson, L., Zieger, P., Baccarini, A., Schmale, J., Lawler, M., et al. (2021). Insights into the molecular composition of semi-volatile aerosols in the summertime central Arctic Ocean using FIGAERO-CIMS. Environmental Science: Atmospheres 1, 161–175. doi: 10.1039/D0EA00023J

Sippial, D. J., Uruci, P., Kostenidou, E., and Pandis, S. N. (2023). Formation of secondary organic aerosol during the dark-ozonolysis of α-humulene. Environ. Sci.: Atmos. 3, 1025–1033. doi: 10.1039/D2EA00181K

Slater, J., Coe, H., McFiggans, G., Tonttila, J., and Romakkaniemi, S. (2022). The effect of BC on aerosol–boundary layer feedback: potential implications for urban pollution episodes. Atmospheric Chemistry and Physics 22, 2937–2953. doi: 10.5194/acp-22-2937-2022

Sotiropoulou, G., Ickes, L., Nenes, A., and Ekman, A. M. L. (2021a). Ice multiplication from ice–ice collisions in the high Arctic: sensitivity to ice habit, rimed fraction, ice type and uncertainties in the numerical description of the process. Atmospheric Chemistry and Physics 21, 9741–9760. doi: 10.5194/acp-21-9741-2021

Sotiropoulou, G., Vignon, É., Young, G., Morrison, H., O'Shea, S. J., Lachlan-Cope, T., et al. (2021b). Secondary ice production in summer clouds over the Antarctic coast: an underappreciated process in atmospheric models. Atmospheric Chemistry and Physics 21, 755–771. doi: 10.5194/acp-21-755-2021

Spill, G., Stier, P., Field, P. R., and Dagan, G. (2021). Contrasting Responses of Idealised and Realistic Simulations of Shallow Cumuli to Aerosol Perturbations. Geophysical Research Letters 48, e2021GL094137. doi: 10.1029/2021GL094137

Stolzenburg, D., Cai, R., Blichner, S. M., Kontkanen, J., Zhou, P., Makkonen, R., et al. (2023). Atmospheric nanoparticle growth. Rev. Mod. Phys. 95, 045002. doi: 10.1103/RevModPhys.95.045002

Su, W., Liang, L., Myhre, G., Thorsen, T. J., Loeb, N. G., Schuster, G. L., et al. (2021). Understanding Top-of-Atmosphere Flux Bias in the AeroCom Phase III Models: A Clear-Sky Perspective. Journal of Advances in Modeling Earth Systems 13, e2021MS002584. doi: 10.1029/2021MS002584

Sudhakar, D., Schwarz, M., Ekman, A. M. L., Gryspeerdt, E., Goren, T., Sourdeval, O., et al. (2022). Exploring Satellite-Derived Relationships between Cloud Droplet Number Concentration and Liquid Water Path Using a Large-Domain Large-Eddy Simulation. Tellus B: Chemical and Physical Meteorology 74, 176–188. doi: 10.16993/tellusb.27

Theodoritsi, G. N., Ciarelli, G., and Pandis, S. N. (2021). Simulation of the evolution of biomass burning organic aerosol with different volatility basis set schemes in PMCAMx-SRv1.0. Geoscientific Model Development 14, 2041–2055. doi: 10.5194/gmd-14-2041-2021

Tiitta, P., Leskinen, A., Kaikkonen, V. A., Molkoselkä, E. O., Mäkynen, A. J., Joutsensaari, J., et al. (2022). Intercomparison of holographic imaging and single-particle forward light scattering in situ measurements of liquid clouds in changing atmospheric conditions. Atmospheric Measurement Techniques 15, 2993–3009. doi: 10.5194/amt-15-2993-2022

Tsiligiannis, E., Wu, R., Lee, B. H., Salvador, C. M., Priestley, M., Carlsson, P. T. M., et al. (2022). A Four Carbon Organonitrate as a Significant Product of Secondary Isoprene Chemistry. Geophysical Research Letters 49, e2021GL097366. doi: 10.1029/2021GL097366

Tsimpidi, A. P., Karydis, V. A., Pozzer, A., Pandis, S. N., and Lelieveld, J. (2014). ORACLE (v1.0): module to simulate the organic aerosol composition and evolution in the atmosphere. Geoscientific Model Development 7, 3153–3172. doi: 10.5194/gmd-7-3153-2014

Turnock, S. T., Allen, R. J., Andrews, M., Bauer, S. E., Deushi, M., Emmons, L., et al. (2020). Historical and future changes in air pollutants from CMIP6 models. Atmospheric Chemistry and Physics 20, 14547–14579. doi: 10.5194/acp-20-14547-2020

Väisänen, O., Hao, L., Virtanen, A., and Romakkaniemi, S. (2020). Trajectory-based analysis on the source areas and transportation pathways of atmospheric particulate matter over Eastern Finland. Tellus B: Chemical and Physical Meteorology 72, 1799687. doi: 10.1080/16000889.2020.1799687

van Noije, T., Bergman, T., Le Sager, P., O'Donnell, D., Makkonen, R., Gonçalves-Ageitos, M., et al. (2021). EC-Earth3-AerChem: a global climate model with interactive aerosols and atmospheric chemistry participating in CMIP6. Geoscientific Model Development 14, 5637–5668. doi: 10.5194/gmd-14-5637-2021

Villanueva, D., Neubauer, D., Gasparini, B., Ickes, L., and Tegen, I. (2021). Constraining the Impact of Dust-Driven Droplet Freezing on Climate Using Cloud-Top-Phase Observations. Geophysical Research Letters 48, e2021GL092687. doi: 10.1029/2021GL092687

Wang, M., Xiao, M., Bertozzi, B., Marie, G., Rörup, B., Schulze, B., et al. (2022). Synergistic HNO3–H2SO4–NH3 upper tropospheric particle formation. Nature 605, 483–489. doi: 10.1038/s41586-022-04605-4

Watson-Parris, D., Christensen, M. W., Laurenson, A., Clewley, D., Gryspeerdt, E., and Stier, P. (2022a). Shipping regulations lead to large reduction in cloud perturbations. Proceedings of the National Academy of Sciences 119, e2206885119. doi: 10.1073/pnas.2206885119

Watson-Parris, D., Rao, Y., Olivié, D., Seland, Ø., Nowack, P., Camps-Valls, G., et al. (2022b). ClimateBench v1.0: A Benchmark for Data-Driven Climate Projections. Journal of Advances in Modeling Earth Systems 14, e2021MS002954. doi: 10.1029/2021MS002954

Watson-Parris, D., Williams, A., Deaconu, L., and Stier, P. (2021). Model calibration using ESEm v1.1.0 – an open, scalable Earth system emulator. Geoscientific Model Development 14, 7659–7672. doi: 10.5194/gmd-14-7659-2021

Williams, A. I. L., Stier, P., Dagan, G., and Watson-Parris, D. (2022). Strong control of effective radiative forcing by the spatial pattern of absorbing aerosol. Nat. Clim. Chang. 12, 735–742. doi: 10.1038/s41558-022-01415-4

Wu, C., Bell, D. M., Graham, E. L., Haslett, S., Riipinen, I., Baltensperger, U., et al. (2021a). Photolytically induced changes in composition and volatility of biogenic secondary organic aerosol from nitrate radical oxidation during night-to-day transition. Atmospheric Chemistry and Physics 21, 14907–14925. doi: 10.5194/acp-21-14907-2021

Wu, R., Vereecken, L., Tsiligiannis, E., Kang, S., Albrecht, S. R., Hantschke, L., et al. (2021b). Molecular composition and volatility of multi-generation products formed from isoprene oxidation by nitrate radical. Atmospheric Chemistry and Physics 21, 10799–10824. doi: 10.5194/acp-21-10799-2021

Wyser, K., Kjellström, E., Koenigk, T., Martins, H., and Döscher, R. (2020). Warmer climate projections in EC-Earth3-Veg: the role of changes in the greenhouse gas concentrations from CMIP5 to CMIP6. Environ. Res. Lett. 15, 054020. doi: 10.1088/1748-9326/ab81c2

Yli-Juuti, T., Mielonen, T., Heikkinen, L., Arola, A., Ehn, M., Isokääntä, S., et al. (2021). Significance of the organic aerosol driven climate feedback in the boreal area. Nat Commun 12, 5637. doi: 10.1038/s41467-021-25850-7

Zhang, C., Guo, Y., Shen, H., Luo, H., Pullinen, I., Schmitt, S. H., et al. (2023). Contrasting Influence of Nitrogen Oxides on the Cloud Condensation Nuclei Activity of Monoterpene-Derived Secondary Organic Aerosol in Daytime and Nighttime Oxidation. Geophysical Research Letters 50, e2022GL102110. doi: 10.1029/2022GL102110

Zhang, S., Stier, P., and Watson-Parris, D. (2021). On the contribution of fast and slow responses to precipitation changes caused by aerosol perturbations. Atmospheric Chemistry and Physics 21, 10179–10197. doi: 10.5194/acp-21-10179-2021

Zipfel, L., Andersen, H., and Cermak, J. (2022). Machine-Learning Based Analysis of Liquid Water Path Adjustments to Aerosol Perturbations in Marine Boundary Layer Clouds Using Satellite Observations. Atmosphere 13, 586. doi: 10.3390/atmos13040586

FORCeS contact information

Project manager Ana Cordeiro | *ana.cordeiro@su.se*
Office for Research, Engagement and Innovation Services (REIS)
Stockholm University, SE-106 91 Stockholm, Sweden